

The Institute of Paper Chemistry

Appleton, Wisconsin

Doctor's Dissertation

Polymer Adsorption and Fractionation
in the Polystyrene-Dichloroethane-
Carbon Black System

Philip H. Emery, Jr.

June, 1965

POLYMER ADSORPTION AND FRACTIONATION
IN THE POLYSTYRENE-DICHLOROETHANE-
CARBON BLACK SYSTEM

A thesis submitted by

Philip H. Emery, Jr.

B.S. 1957, University of Maine
M.S. 1960, Lawrence College

in partial fulfillment of the requirements
of The Institute of Paper Chemistry
for the degree of Doctor of Philosophy
from Lawrence University,
Appleton, Wisconsin

June, 1965

TABLE OF CONTENTS

	Page
SUMMARY	1
INTRODUCTION	4
Literature Review	4
Scope and Approach	8
SELECTION OF THE ADSORPTION SYSTEM	10
Adsorbate	10
Solvent	10
Adsorbent	11
EXPERIMENTAL EQUIPMENT, MATERIALS, AND PROCEDURES	13
Description, Purification, and Characterization of Materials	13
Polystyrene	13
Samples	13
Purification	14
Characterization	14
1,2-Dichloroethane	15
Purification	15
Solvent Quality	16
Cyclohexane	17
Graphitized Carbon Black	18
Samples	18
Purification	20
Characterization	23
Electron Microscopy	23
Nitrogen Gas Adsorption Measurements	26
Determination of Solution Concentrations	28
Gravimetric Analysis	28

Spectrophotometric Analysis	29
Intrinsic Viscosity Determinations	31
General Method	31
One-Point Method	35
Conversion of Gravimetric Concentration to Volumetric Concentration	35
Adsorption Runs	37
Cleaning Procedure	37
Apparatus	37
Procedure	38
Preliminary Preparations	38
Initiation of the Adsorption Run	38
Equilibration Period	38
Separation of Adsorbent and Solution	40
Analysis	41
Determination of Sedimentation Coefficient Distributions from Sedimentation Velocity Experiments with an Ultracentrifuge	42
Introduction	42
Experimental	43
Choice of Solvent	43
Preparation of Samples	43
Equipment and Procedures	44
Calculation of Apparent Distribution	46
Location of Original Boundary	47
Diffusion Correction	48
Concentration Correction	52
EXPERIMENTAL DATA AND DISCUSSION OF RESULTS	56

Equilibrium Adsorption and Fractionation of Polystyrenes of Broad Molecular Weight Distribution	56
Intrinsic Viscosity and Related Studies	56
Experimental	56
Langmuir Behavior	57
Fractionation Behavior in the Bulk Phase	64
Perfect Fractionation	72
Behavior in the Surface Phase	75
Degree of Fractionation	79
Intrinsic Viscosity as a Measure of Fractionation	83
Summary	86
Sedimentation Velocity Studies	91
Experimental	91
Sedimentation Coefficient Distributions	92
Concentration Dependence of the Fractionation Process	101
Partitioning of Polymer Homologs Between the Bulk and Surface Phases	101
Comparison of Partitioning Relationship with Recent Theoretical Developments	112
Degree of Fractionation	118
Summary	119
Adsorption and Fractionation of Polystyrenes of Broad Molecular Weight Distribution During the Approach to Equilibrium	121
Experimental	121
Results	122
Exchange Phenomena	131
Importance of Diffusional Transport in the Adsorption Process	133
Summary	138

Exchange Experiments Using Polystyrenes of Narrow Molecular Weight Distribution	140
Experimental	140
Results and Discussion	141
Summary	147
Replacement Experiments Using Polystyrenes of Narrow Molecular Weight Distribution	149
Experimental	149
Results and Discussion	150
Summary	156
GENERAL DISCUSSION	158
Polymer Degradation	158
Structure of the Surface Layer	158
Behavior of the Surface Layer	160
SUMMARY AND CONCLUSIONS	163
SUGGESTIONS FOR FUTURE RESEARCH	171
ACKNOWLEDGMENTS	173
LITERATURE CITED	174
APPENDIX I. INTRINSIC VISCOSITY DETERMINATIONS AND RELATED PARAMETERS	179
APPENDIX II. CLEANING PROCEDURES	182
APPENDIX III. EMPIRICAL CONSTANTS USED IN CONVERSION OF SEDIMENTATION COEFFICIENT DISTRIBUTIONS TO INTRINSIC VISCOSITY QUANTITIES	183

SUMMARY

Conflicting reports occur about the role of adsorbate polymolecularity in the adsorption of high polymers at the liquid-solid interface. The object of the present investigation was to make a critical examination of this molecular weight inhomogeneity under carefully selected conditions.

To avoid unnecessary complications, a system was selected which is believed to involve only molecular interactions of the van der Waals type, i.e., physical adsorption. In addition, a nonporous adsorbent was chosen so that each of the solute components had essentially equal access to the interfacial region.

Polystyrene, 1,2-dichloroethane, and a graphitized carbon black were selected as the adsorbate, solvent, and adsorbent, respectively. Polystyrene samples of broad and narrow molecular weight distribution were employed. The adsorbent had a specific surface area of 12.4 sq. m./g., determined by nitrogen gas adsorption.

Solutions of polystyrene were mixed with the adsorbent for specified periods of time, and the resulting supernatant solutions were isolated and analyzed for changes in intrinsic viscosity and concentration. The weight of adsorbed polymer was determined from the change in solution concentration. Fractionation and preferential adsorption of the polymer were adjudged by the change in intrinsic viscosity. The system required approximately three days to reach equilibrium.

For selected equilibrium adsorption experiments, the distribution of sedimentation coefficient was determined for the polymer in each of the supernatant solutions. The distributions were obtained from sedimentation velocity experiments with an ultracentrifuge and were corrected for the effects of diffusion and concentration.

At equilibrium, the system exhibited Langmuir behavior over a wide range of surface coverage and nearly four decades of solution concentration. The polymer was very strongly adsorbed, nearly saturating the adsorbent surfaces at equilibrium concentrations as low as 0.05% by weight.

The polymer samples were fractionated significantly by the adsorption process, the higher molecular weight species being adsorbed preferentially for all the equilibrium conditions investigated. For polystyrene samples of broad molecular weight distribution, the equilibrium fractionation depended only on the percentage of polymer adsorbed, irrespective of the ratio of adsorbent to solution or concentration employed. The observed fractionation was not complete, and the equilibrium adsorption process could not be used to predict the molecular weight distribution or its equivalent by the methods employed.

Knowing the sedimentation coefficient distributions of the polymer before and after adsorption, the distribution of polymer in the surface phase was calculated. In each case, the equilibrium distributions for the bulk and surface phases were related by a partitioning expression which differed substantially from that describing phase separation. Although a strong fractionation was obtained, the equilibrium adsorption process was not an efficient analytical tool for molecular separations — the polymer in either phase was distributed broadly with respect to molecular weight.

For a polystyrene sample of broad molecular weight distribution, the smaller molecules were preferentially adsorbed initially and were displaced gradually by larger ones as equilibrium was approached. The exchange of different molecular weight species was verified with narrow fractions of polystyrene — previously adsorbed small molecules were displaced by larger ones and vice versa.

The length of time spent by adsorbed molecules in contact with the adsorbent did not alter the ability of these molecules to be displaced, indicating that the adsorptive forces in the system were only physical in nature.

From the exchange and partitioning phenomena encountered, it is believed that the exchange process made it possible for the adsorption system to attain a distinct partitioning condition at equilibrium - one which conceivably minimized the Gibbs free energy of the system.

INTRODUCTION

The adsorption of polymeric adsorbates on solid substrates is a phenomenon of widespread importance in biological systems, for example, as well as in industrial applications such as rubber reinforcement, papermaking, and protective coatings. Comprehension of this phenomenon, however, has progressed slowly due to the number and complexity of the variables involved and the lack of experimental techniques. Recently, important information pertaining to the structure of the surface layer was obtained with infrared spectrometry (1), ellipsometry (2), and surface potential measurements (3). These investigations served to complement the present study.

LITERATURE REVIEW

Although an exhaustive review of the literature is not included here, an attempt is made to present the background information pertinent to the present study whose object is to investigate the importance of adsorbate polymolecularity in the adsorption of high polymers at the liquid-solid interface.

Hughes and von Frankenberg (4) have reviewed the literature related to the physical adsorption of macromolecules at the liquid-solid interface. Silberberg (5) made an extensive tabulation of experimental observations reported for polymeric adsorbates at the gas-liquid and liquid-solid interfaces.

Extensive studies of polymer adsorption at the liquid-solid interface were made by Koral (6), Perkel (7), and Ellerstein (8). (I am indebted to Prof. R. Ullman of the Polytechnic Institute of Brooklyn for providing a copy of the dissertation by Ellerstein.) These investigators examined the importance of adsorbent characteristics, chemical and physical structures of the polymer, adsorbate molecular weight, nature of the solvent, and temperature.

Mark and Saito (9) were first to apply chromatographic adsorption to fractionation of a high polymer. They found that the low molecular weight species of cellulose acetate were preferentially adsorbed on blood carbon. Levi and Giera (10) confirmed this result but were unsuccessful in fractionating elastomers by that method.

Goldfinger and co-workers (11-13) investigated the adsorption of butadiene-styrene copolymers (GR-S) from xylene solution onto carbon blacks and found that the low molecular weight species were preferentially adsorbed. They detected no preferential retention correlated with the chemical composition of the copolymer. Landler (14) also found synthetic elastomers to be fractionated by adsorption chromatography, the lower molecular weight species being preferentially retained.

Claesson and co-workers (15, 16) fractionated a variety of polymers, including polyvinyl acetate, nitrocellulose, and synthetic rubber by chromatographic adsorption and found the lower molecular weight species to be preferentially adsorbed.

Kolthoff and co-workers (17-19) concluded from intrinsic viscosity data that the low molecular weight species of GR-S were preferentially adsorbed initially on carbon blacks and were replaced gradually by species of higher molecular weight. At equilibrium, the higher molecular weight species were strongly preferentially adsorbed. Gilliland and Gutoff (20) found the adsorption of polyisobutylene - isoprene copolymer and polyisobutylene on various carbon blacks to be so preferential with respect to molecular weight that the fractionation curves compared favorably with the most probable distributions for those polymers.

Frisch and co-workers (21) cited additional molecular weight effects on polymer adsorption and suggested that sufficient time was not allowed in many earlier investigations for the establishment of equilibrium. For the adsorption of polystyrene from toluene onto carbon black, they found that the intrinsic viscosity of the solution increased initially over that of the original solution and gradually decreased, thereafter, until equilibrium was attained. They, like Kolthoff, suggested that the low molecular weight species were preferentially adsorbed initially and were displaced gradually by larger molecules over a period of several days.

Using charcoal and relatively short adsorption times, Swenson (22) found that the lower molecular weight species of cellulose acetate were selectively adsorbed. This preferential adsorption was attributed to differences in the ability of the various species to diffuse into the porous charcoal. Miller and Pacsu (23), using a similar adsorption system, concluded that the process depended primarily on the diffusion of polymer molecules into the carbon matrix and that no displacement of previously adsorbed molecules was effected by other species.

Gilliland and Gutoff (24) derived an equilibrium expression for the partitioning of solute components between the bulk and surface phases. Using Flory's lattice treatment, they obtained equations for the partial free energy of solute species in either phase. By equating the partial free energies of dissolved and adsorbed solutes, they found that

$$N'_x/N_x = \left\{ N_s/(N_o p) \right\} \left\{ (1 - \phi)(j_a/j_u)^p \exp[(H_p/kT) + \chi'_1 - \chi'_1(1 - 2\phi)] \right\}^x \quad (1)$$

*Exp is used in this thesis to denote the power of e, the base of Napierian logarithms, i.e., $\exp(x) = e^x$.

where

$\frac{N'_x}{x}$ = number of molecules of degree of polymerization (D.P.) = \underline{x} in the surface phase

$\frac{N_x}{x}$ = number of molecules of D.P. = \underline{x} in the bulk phase

$\frac{N_s}{s}$ = number of adsorption sites (each site being large enough to accommodate one segment)

$\frac{N_o}{o}$ = number of solvent molecules in the bulk phase

\underline{p} = probability that a given segment of an adsorbed molecule is itself adsorbed at the interface

ϕ = fraction of adsorption sites occupied by polymer

\underline{j}_a = partition function (vibrational, rotational, and translational motions) per mer for the adsorbed molecule

\underline{j}_u = partition function per mer for the dissolved molecule

\underline{H} = heat of adsorption in energy per segment

\underline{k} = Boltzmann's constant

\underline{T} = absolute temperature

χ_1 = interaction parameter for the bulk phase

χ'_1 = interaction parameter for the surface phase.

The above relationship is limited to adsorption from dilute solutions at their theta temperatures. Furthermore, the relationship was derived under the assumptions (a) that the same lattice treatment holds for the polymer, the solvent, and the adsorption sites, (b) that the adsorbed segments are not mobile, (c) that the adsorbed layer may be represented by a lattice of such a thickness that the average polymer density is equal to the density on the surface, and (d) that the polymer distribution is uniform within this lattice. The treatment assumes, of course, that equilibrium thermodynamics can be applied to polymer adsorption.

Since Equation (1) describes the fractionation or partitioning of the solute species at equilibrium, it will be possible to apply this relationship to the experimental results obtained in the present study.

SCOPE AND APPROACH

It is evident that the object of the present study, i.e., the role of adsorbate polymolecularity in the adsorption of high polymers at liquid-solid interfaces, is not well established. Many of the discrepancies found in reported adsorption data can be explained because of differences in adsorption times, adsorbent porosities, and specific adsorbate-adsorbent interactions. To avoid unnecessary complications, the present investigation was limited to adsorbate-adsorbent interactions of the van der Waals type and the use of nonporous adsorbents.

Since one of the prime requisites was to make a quantitative evaluation of the fractionation effect, techniques which provided information concerning molecular weight effects were used wherever possible, and emphasis was placed on a quantitative interpretation of that information. The requirement that the adsorbent be nonporous is particularly important, since fractionation resulting from differences in surface accessibility would be difficult to evaluate.

Since polymer adsorption is a surface-chemical phenomenon, precautions were taken to minimize contaminating influences.

A single adsorbate-solvent-adsorbent system which is believed to be representative of the physical adsorption process was employed. Only the quantity of system components, adsorption time, and molecular weight characteristics of the adsorbate were varied in order to minimize the variables encountered.

The adsorption experiments were of the batch type. Alternative chromatographic techniques are difficult to control and involve variables which must be treated as distributions.

SELECTION OF THE ADSORPTION SYSTEM

ADSORBATE

Polystyrene was particularly suitable as the polymeric adsorbate because it satisfied the following requirements: (a) it is chemically stable over a wide range of temperature, (b) it has a linear chain structure, (c) it is soluble and stable in a variety of organic solvents, (d) it is available in a wide range of average molecular weights and in a variety of molecular weight distributions, (e) it can be easily purified, (f) it has no chemical groups likely to form chemical or hydrogen bonds with adsorbent surfaces. Published data on solution properties and on sedimentation velocity analysis of polystyrene also favored its selection.

The requirement concerning the stability of the polymer is essential in order to (a) maintain uniform adsorptive properties, (b) prevent changes in the molecular weight distribution from degradation, and (c) permit accurate determination of solution concentrations by gravimetric analysis.

SOLVENT

It was demonstrated (6) that strong interactions between solvent and adsorbent or between solvent and polymer seriously retard the adsorption process, particularly if the interactions between polymer and adsorbent are limited to van der Waals' forces. However, the solvent-polymer interactions must be sufficient to prevent phase separation in the solution for any experimental conditions employed.

1,2-Dichloroethane (DCE) was selected as the solvent because it fulfilled the following requirements: (a) it is easy to obtain consistent and adequate

purification, (b) it has no chemical groups likely to promote strong interactions or the formation of chemical or hydrogen bonds with adsorbent surfaces, (c) it is not such a strong solvent for polystyrene that interactions between solvent and polymer seriously limit the amount of adsorption, (d) it has sufficient affinity for polystyrene to prevent phase separation (25) under any conditions likely to be encountered, and (e) it is a favorable solvent for use in ultraviolet absorption spectrophotometry. Information available from the literature for the polystyrene - DCE system also favored the selection of DCE.

ADSORBENT

A graphitized carbon black was selected as the adsorbent after a number of materials had been tested experimentally. The following requirements were met by this adsorbent: (a) it is a solid, nonporous material with surfaces accessible to polymer molecules, (b) it is inert and exhibits no appreciable swelling in solvent, (c) it has adequate specific surface area, (d) it is readily dispersed in solvent by mild agitation, and (e) it is stable and is easily and reproducibly purified. The above requirements are not easily fulfilled. The irregular and porous nature of most commercial adsorbents would conceivably favor adsorption of low molecular weight materials in areas completely inaccessible to larger molecules. Several materials which satisfied the nonporous requirement were tested experimentally and found to be entirely unsuitable. In some cases the material could not be adequately dispersed in the solvent by agitation. In many cases where the dispersion was adequate, the amount of adsorption was too limited.

These problems were not encountered with graphitized carbon blacks obtained from the Cabot Corporation, Boston, Massachusetts. Two grades were tested

experimentally: Spheron 6 and Sterling FT, possessing high and low specific surface areas, respectively. The latter, Sterling FT, chosen in the present study appeared to have several advantages which will be discussed later.

EXPERIMENTAL EQUIPMENT, MATERIALS, AND PROCEDURES

DESCRIPTION, PURIFICATION, AND CHARACTERIZATION OF MATERIALS

POLYSTYRENE

Samples

The polystyrene samples were purified prior to use with the exception of Sample B6. This material, of very broad molecular weight distribution, was provided by Dr. H. W. McCormick of the Dow Chemical Company, Midland, Michigan. Only a portion of this sample was purified, and both the purified and original materials were employed.

A commercial sample of broad molecular weight distribution, Dylene Polystyrene type 8, was furnished by the Koppers Company, Pittsburgh, Pennsylvania.

Two samples of narrow molecular weight distribution, Polystyrene S26 and S34, were kindly provided by Dr. J. F. Rudd of the Dow Chemical Company, Midland, Michigan.

The molecular weight characteristics of the polymer samples are given in Table I. The number- and weight-average molecular weights, \overline{M}_n and \overline{M}_w , respectively, were determined by the suppliers (26, 27) using an ultracentrifugal technique. Considerable information regarding physical characteristics of the Dow samples has been reported (26-29).

TABLE I
ORIGINAL POLYSTYRENE SAMPLES

Sample	Method of Preparation	$\overline{M}_w \times 10^{-5}$	$\overline{M}_w/\overline{M}_n$
B6	Isothermal	4.47	2.85
S34	Anionic	3.62	1.06
S26	Anionic	1.59	1.08
Dylene Type 8	(Commercial)	--	--

Purification

Reagent grades of benzene and methanol, employed in the polymer purification as solvent and nonsolvent, respectively, were filtered through type 27B (0.25 μ) Polypore membrane filters prior to use. (Only solvent-resistant Polypore filters, manufactured by the Gelman Instrument Company, Chelsea, Michigan, were utilized in this work.)

Benzene was added to the polystyrene sample to yield a solution concentration of approximately 0.5% (on a weight basis). The solvent was allowed to swell the polymer overnight, after which very mild agitation was employed for a few hours.

The solution was filtered successively through type 27A (0.45 μ) and type 27B (0.25 μ) membrane filters under a slight positive pressure. The resulting solution was precipitated by dropwise addition into two volumes of ice-cold methanol. At least one day was allowed for the polymer residue to settle before the liquid was decanted.

The polymer was redissolved in benzene, filtered, and precipitated as before. This dissolution-precipitation procedure was repeated a minimum of three times before the residue was allowed to air dry. The sample was then dried to the minimum pressure attainable on an N.R.C. type 3505-2 dehydration unit (NRC Equipment Corporation, Newton Highlands, Massachusetts). From the appearance and behavior of the purified samples, it is believed that they were essentially free of occluded solvents.

Characterization

Intrinsic viscosities, $[\eta]$, were determined (see Table II) in 1,2-dichloroethane at 30.0°C., and the viscosity-average molecular weights, \overline{M}_v , were calculated from Equation (42).

TABLE II
CHARACTERIZATION OF POLYSTYRENE SAMPLES

Sample	Description	$[\eta]$, dl./g.	$\overline{M}_v \times 10^{-5}$	$\overline{M}_w \times 10^{-5}$	$\overline{M}_w/\overline{M}_n$
B6	Original	1.090	4.26	4.47	2.85
PB6	Purified B6	1.078	4.19	5.12	2.43
PS34	Purified S34	0.892	3.14	3.62 ^a	1.06 ^a
PS26	Purified S26	0.501	1.31	1.59 ^a	1.08 ^a
DRT8	Purified Dylene Type 8	0.760	2.46	--	--

^aValues reported (26) for original samples.

McCormick (27) and Taylor (29) independently determined the molecular weight distribution of the original B6 sample, using sedimentation velocity methods. A similar procedure was used in the present work to determine the distribution of sedimentation coefficient for Sample PB6, i.e., purified B6.

Knowing the distribution function, molecular weight averages can be calculated from their defining equations. Such calculations have been reported by Rudd (26) for Samples B6, S26, and S34. The molecular weight averages for Sample PB6 were calculated with Equations (71) and (72). The results of these calculations are shown in Table II.

1,2-DICHLOROETHANE

Purification

The procedure used to purify 1,2-dichloroethane is a modification of that employed by Barton and Howlett (30). Reagent-grade solvent (Matheson, Coleman, and Bell Company, b.p. 84-85°C.) was shaken thoroughly with concentrated sulfuric acid. Following decantation, the solvent was washed successively with one volume

of 1N sodium hydroxide and approximately 3 volumes of a saturated aqueous solution of sodium bicarbonate. The solvent was then rinsed thoroughly with approximately 6 volumes of distilled water and dried over anhydrous calcium chloride.

Extracted solvent was refluxed with reagent-grade phosphorus pentoxide for several hours in an atmosphere of dry nitrogen. Following refluxing, the solvent was twice fractionally distilled from phosphorus pentoxide in a 3-ft. column packed with 6 by 6 mm. Raschig rings. The initial reflux ratio was maintained at approximately 20:1. The desired fraction, constituting the middle 80% of the starting material, was collected at a reflux ratio of approximately 3:1.

Solvent Quality

Maclean, et al. (31) demonstrated that ultraviolet spectrophotometry is widely applicable as a criterion of solvent uniformity and is sometimes a more sensitive method than determinations of density, refractive index, or other physical quantities. This technique was used in the present study for detection of impurities originally present and for evaluating the effectiveness of purification procedures.

A substantial reduction in the ultraviolet absorbance* of the solvent was obtained with the purification procedure. Reagent-grade 1,2-dichloroethane could be reproducibly purified to a level superior to spectroquality grade, as adjudged by spectrophotometric methods. Typical absorbance values are given in Table III for reagent and spectroquality grades (Matheson, Coleman, and Bell Company) and purified material. The absorbance measurements were obtained with a Beckman model DU spectrophotometer, using distilled water as a reference.

*The term, absorbance, is used in accordance with the recommended definition of the American Society of Testing and Materials (32) as follows:

$$A = \log(1/T)$$

where A and T are the absorbance and relative transmittance, respectively.

TABLE III

ULTRAVIOLET ABSORBANCE OF 1,2-DICHLOROETHANE
SAMPLES AGAINST DISTILLED WATER

Wavelength, mμ	Absorbance		
	Reagent	Spectroquality	Purified
225	--	1.08	0.962
226	1.07	0.909	0.794
228	0.778	0.620	0.533
230	0.569	0.431	0.348
235	0.286	0.193	0.117
240	0.150	0.109	0.039
245	0.072	0.066	0.011
250	0.023	0.041	0.004
255	0.004	0.028	0.000
260	0.003	0.019	0.000

The density of a typical sample of purified solvent was determined by a pycnometric technique. The average of six determinations at 30.0°C. was 1.23903 g./ml. (All determinations were within ± 0.00023 g./ml.) This value is in excellent agreement with the value of 1.2383 g./ml. reported by Timmermans and Martin (33).

CYCLOHEXANE

Reagent-grade cyclohexane, obtained from the Matheson, Coleman, and Bell Company (m.p. 5-6°C.), was treated with an acidic solution of potassium permanganate and passed through a column of activated silica gel, as described elsewhere (34). The purification procedure was selected for its ability to remove any unsaturated or oxygenated impurities.

A substantial improvement in the optical properties of the solvent was obtained with this treatment, presumably due to the removal of unsaturated impurities. The ultraviolet absorption characteristics of the resulting solvent are compared with the original solvent in Table IV, using distilled water as a reference.

TABLE IV
ULTRAVIOLET ABSORPTION CHARACTERISTICS
OF CYCLOHEXANE SAMPLES AGAINST DISTILLED WATER

Wavelength, mμ	Absorbance	
	Original	Purified
220	2+	0.302
225	2+	0.176
230	2+	0.100
235	1.70	0.057
240	0.651	0.032
245	0.419	0.017
250	0.386	0.010
255	0.391	0.007
260	0.363	0.006
270	0.240	0.004

Just prior to use, the treated solvent was further purified by distillation in which the middle 40% of the starting material was collected.

GRAPHITIZED CARBON BLACK

Samples

Samples of graphitized carbon black, known as Spheron 6 (commonly referred to as graphon) and Sterling FT, were kindly provided by Mr. W. J. McNeil of the

Cabot Corporation, Boston, Massachusetts. Some of the properties of these materials were provided by the supplier and are shown in Table V.

TABLE V
PROPERTIES OF GRAPHITIZED CARBON BLACKS^a

	Spheron 6	Sterling FT
Surface area, sq. m./g. (electron microscope)	117.0	13.3
Surface area, sq. m./g. (nitrogen adsorption)	89.4	10.3
Average particle diameter, μ (nitrogen adsorption)	36.1	322
Moisture, %	0.00	0.00
Volatile content ^b , %	0.085	0.066
Ash, %	0.01	0.02

^aPertain to blacks from lot D3.

^bDetermined by loss of weight on heating at 1000°C. in vacuo.

Graphitized carbon blacks are prepared by heating regular blacks in an inert atmosphere for 2-hr. periods at temperatures ranging from 2700 to 3100°C. (35). Spheron 6 and Sterling FT are prepared from a medium processing channel black and a fine thermal black, respectively.

All carbon blacks yield the same general x-ray powder pattern, consisting of two rather diffuse bands corresponding to the 002 and 100 (Miller indices) reflections of graphite (35). Upon heating at temperatures in excess of 1000°C. these diffuse bands sharpen and additional reflections appear. The nature of these reflections led Biscoe and Warren (36) to conclude that carbon black is made up of individual graphite layers stacked roughly parallel to one another but in random orientation about the layer normal. The dimensions of these

parallel layer groups have frequently been estimated from the breadth of appropriate diffraction bands, indicating that they are generally less than a tenth the diameter of a carbon black particle (35). Changes in the x-ray diffraction pattern during heating (graphitization) indicate that these quasicrystallites become more ordered and increase in size.

Beebe and co-workers (37) found that the differential heats of adsorption of reinforcing blacks exhibited large variations as successive fractions of surface were covered. Partial "graphitization" of the blacks greatly reduced the activity of the more active sites, yielding a much more homogeneous surface. Considerable evidence (38-45) has established that graphitized carbon blacks consist of nonporous particles with exceptionally uniform surface characteristics.

Purification

Although the graphitized carbon blacks were able to adsorb sufficient quantities of polymer for the present study, it was found that polymer solutions were contaminated during exposure to these adsorbents. To investigate this difficulty, quantities of solvent and adsorbent were mixed for a 24-hr. period. The solvents were then decanted and analyzed for changes in optical characteristics. Absorbance measurements were obtained with a Beckman model DU spectrophotometer, using distilled water as a reference. As shown in Table VI, solvent absorbances were substantially increased by exposure to the adsorbents.

Believing that the blacks had adsorbed contaminating impurities during storage or upon shipment, samples were heated in a muffle furnace at 1200°F. for 24 hours. [This temperature was too low to modify the structure of the

blacks (35, 46) but sufficient to remove contaminating organic constituents.] The results of this furnace treatment are evident from Table VII. Note that absorbance values for the exposed solvents are nearly identical to those of the control solvent. Apparently, the furnace treatment eliminated most of the contaminating materials. Consequently, this treatment (24 hr. at 1200°F.) was employed for purification of the adsorbents.

TABLE VI
ULTRAVIOLET ABSORBANCE OF SOLVENT BEFORE AND AFTER EXPOSURE
TO GRAPHITIZED CARBON BLACKS FROM LOT D3

Wavelength, mμ	Ultraviolet Absorbance ^a			
	A	B	C	D
230	0.362	1.06	1.01	1.02
232	0.237	0.958	0.900	0.870
234	0.154	0.852	0.812	0.749
240	0.046	0.577	0.567	0.462
242	0.030	0.497	0.488	0.396
245	0.018	0.421	0.406	--
250	0.011	0.375	0.353	0.291
255	0.009	0.371	0.352	0.273
260	0.009	0.342	0.323	0.252
265	0.009	0.277	0.266	0.226
270	0.010	0.227	0.215	0.200
280	--	0.174	0.165	0.157
290	--	0.142	0.133	0.127
300	--	0.106	0.098	0.099
320	--	0.046	0.041	0.055

^aCode

- A - control solvent.
- B - 15 ml. of solvent exposed to 5 g. of Sterling FT-D3 black.
- C - 25 ml. of solvent exposed to 2 g. of Sterling FT-D3 black.
- D - 15 ml. of solvent exposed to 5 g. of Spheron 6-D3 black.

TABLE VII

ULTRAVIOLET ABSORBANCE OF SOLVENT BEFORE
AND AFTER EXPOSURE TO FURNACE-TREATED
GRAPHITIZED CARBON BLACKS FROM LOT D3

Wavelength, mμ	Ultraviolet Absorbance ^a		
	A	B	C
225	1.04	1.03	1.01
226	0.852	0.845	0.838
227	0.694	0.694	0.681
228	0.566	0.571	0.559
229	0.452	0.462	0.451
230	0.369	0.379	0.367
232	0.240	0.254	0.243
236	0.104	0.119	0.108
240	0.046	0.049	0.059
244	0.022	0.023	0.034
250	0.009	0.011	0.023
260	0.008	0.009	0.024
270	0.009	0.009	0.023
280	0.010	0.011	0.017
300	0.007	0.010	0.012

^aCode

A - Control solvent.

B - 20 ml. of solvent exposed to 2 g. of furnace-treated FT-D3 graphitized carbon black.

C - 25 ml. of solvent exposed to 2 g. of furnace-treated S6-D3 graphitized carbon black.

Upon removal from the furnace, the adsorbent was placed (over P_2O_5) in a vacuum desiccator which was immediately evacuated and refilled with prepurified nitrogen (Matheson, Coleman, and Bell Company). Adsorbents were stored in this manner until needed.

It should be noted that different lots of Sterling FT graphitized carbon black were involved in this study. Because the supplier's stock from lot D3 was depleted, it was necessary to obtain material from lot D4. According to

the supplier, these materials are prepared in the same manner but vary slightly from one lot to another, presumably because of small differences in the starting materials and the time-temperature cycle during graphitization.

Enough Sterling FT-D4 graphitized carbon black was obtained for the entire experimental program. Preliminary tests revealed that this material also contaminated the solvent upon exposure (although not as severely as the previous samples). Consequently, the furnace treatment was used on this material also.

Characterization

Electron Microscopy

Several electron micrographs were obtained at various degrees of magnification on the following samples of graphitized carbon black:

1. Sterling FT-D4, as received from the supplier.
2. Sterling FT-D4, furnace treated for 24 hours at 1200°F.
3. Spheron 6-D3, furnace treated for 24 hours at 1200°F.

Specimens were prepared for electron microscopy by dusting the adsorbent onto collodion film. Each specimen was shadowed by directing palladium vapor at an angle of 30° with respect to the specimen plane. Sterling FT-D4 samples were dispersed by dusting directly onto the film, but the S6-D3 material was in a pelletized form and could not be suitably dispersed in that manner. It was necessary to grind the S6-D3 sample in order to obtain any separation of individual particles.

Electron micrographs of the carbon black samples are shown in Fig. 1-3. As seen in the figures, Sterling FT-D4 particles resembled nearly symmetrical polyhedra as frequently noted in the literature. There was no perceptible change in the Sterling FT-D4 material from the furnace treatment. Apparently,

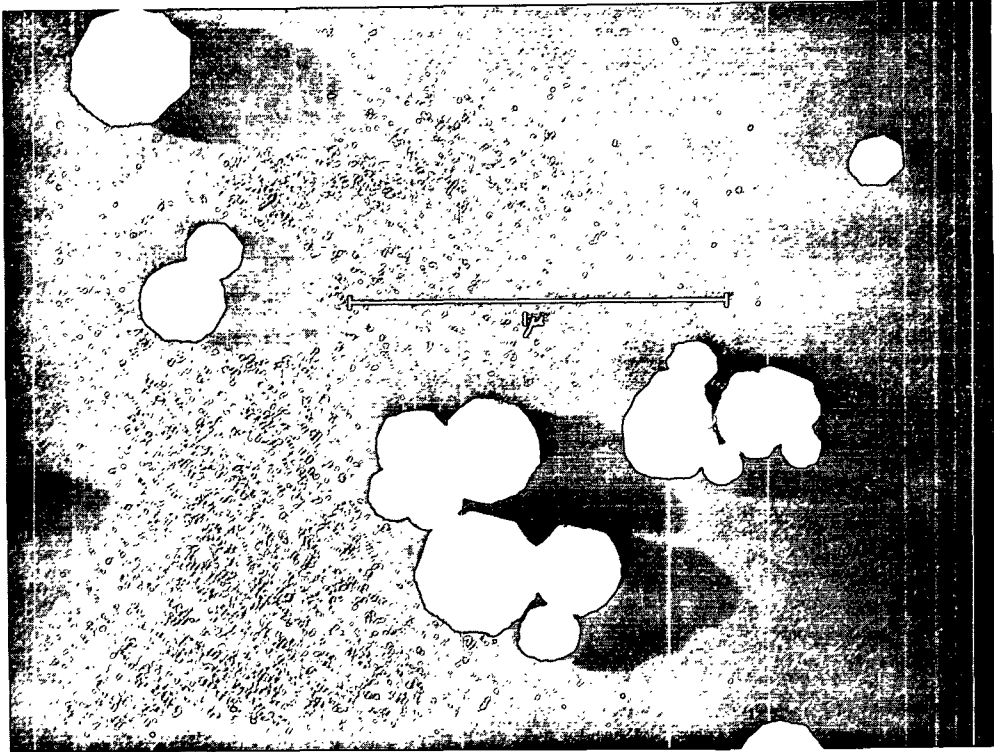


Figure 1. Electron Micrograph of Sterling FT-D4
Graphitized Carbon Black as Received

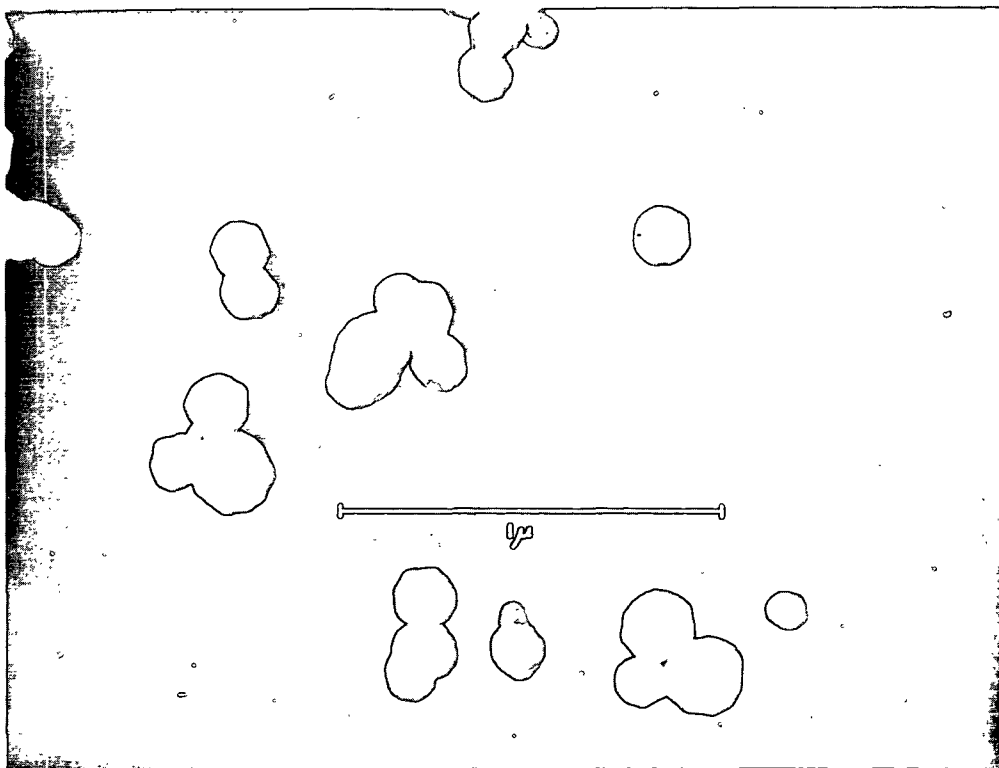


Figure 2. Electron Micrograph of Sterling FT-D4 Graphitized
Carbon Black After Furnace Treatment

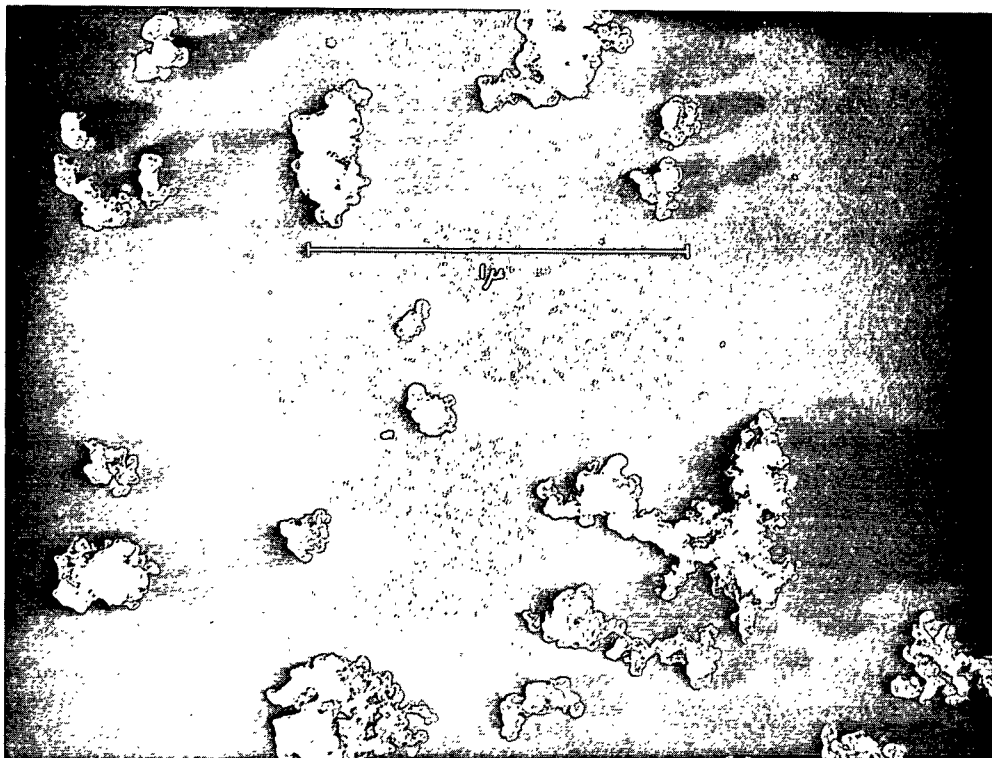


Figure 3. Electron Micrograph of Spheron 6-D3 Graphitized Carbon Black After Furnace Treatment

these samples were easily dispersed as individual particles, and there is no reason to suspect that the specific surface area presented to polymer molecules in solution was significantly lower than that determined by the gas adsorption method.

On the other hand, the S6-D3 sample was entirely unsuited for the present study. Even after substantial grinding, this pelletized material was highly aggregated as shown in Fig. 3, and the surface area available for polymer adsorption was indefinite. The "structure" of such an adsorbent would likely result in an undesirable contribution to polymer fractionation. Consequently, the use of this material was considered no further.

Nitrogen Gas Adsorption Measurements

Surface area determinations were made by the nitrogen gas adsorption technique on both the furnace-treated and untreated Sterling FT-D4 samples. The nitrogen adsorption measurements were performed at the temperature of liquid nitrogen ($-195.8^{\circ}\text{C}.$). The dead space determinations were carried out with helium at the same temperature.

The data obtained from different runs were combined for each sample and plotted in accordance with the theory of Brunauer, Emmett, and Teller (B.E.T.) for multilayer adsorption (47), as shown in Fig. 4. The quantities indicated in the figure are defined as follows: \underline{P} = equilibrium pressure, \underline{P}_0 = saturation pressure (liquefaction pressure of the adsorbate), and \underline{V} = total volume of adsorbed nitrogen corrected to S.T.P.

The slope and intercept of each B.E.T. plot were evaluated statistically (least sum of the squares) using only data below relative pressures of 0.18 and 0.23 for the furnace-treated and untreated samples, respectively. The volume of gas adsorbed (corrected to S.T.P.) when the entire adsorbent is covered with a complete unimolecular layer is given by the reciprocal sum of the slope and intercept from the B.E.T. plot. Knowing the unimolecular volumes and adsorbent weights, specific surface areas were calculated by assuming that an adsorbed nitrogen molecule occupies a cross-sectional area of 16.2 \AA^2 at $-195.8^{\circ}\text{C}.$ (48, 49). Values of 12.44 and 11.91 sq. m./g. were obtained for the furnace-treated and untreated samples, respectively.

The difference in specific surface area for the furnace-treated and untreated samples is rather small but may be significant. Oxidation of the carbon black surfaces probably occurred during the furnace treatment (50, 51).

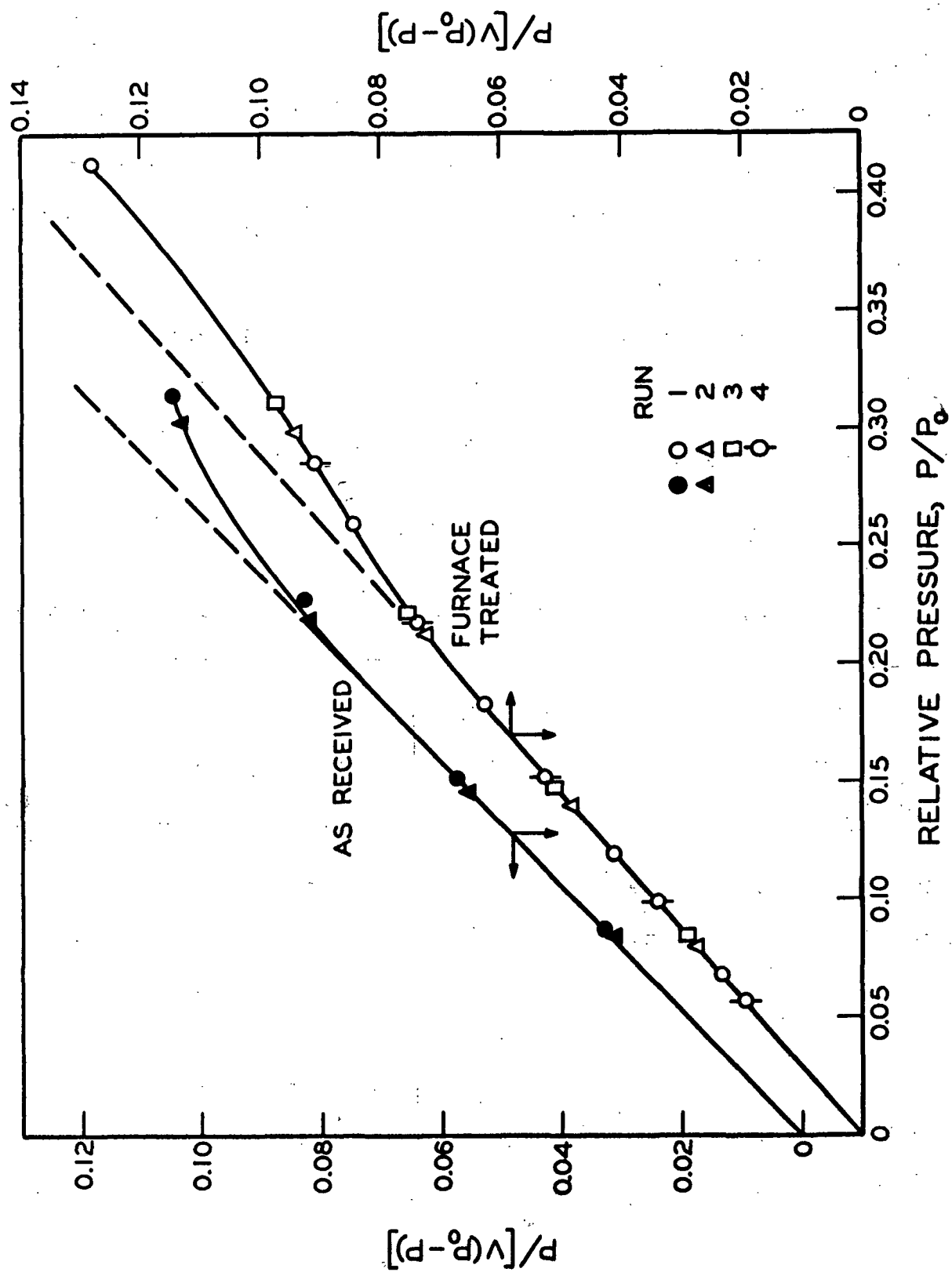


Figure 4. B.E.T. Plots of Nitrogen Gas Adsorption on Sterling FT-D4 Graphitized Carbon Black

Smith and Polley (39) found that specific surface areas of graphitized carbon blacks can be increased substantially by oxidation, the increase being related to a decrease in particle size as a result of carbon burned away. These investigators demonstrated that oxidation occurs uniformly over the surfaces with no development of porosity. This appeared to be true in the present study - electron micrographs indicated that the adsorbent particles retained their polyhedral shape following the furnace treatment.

Since polystyrene should have little tendency to form hydrogen bonds with oxygen, the presence of a surface oxide was not regarded as detrimental.

DETERMINATION OF SOLUTION CONCENTRATIONS

GRAVIMETRIC ANALYSIS

To evaluate the drying procedure used in gravimetric concentration determinations, two quantitative solutions were prepared with Polystyrene PB6. Three known weights of solution were employed from each of the solutions. Following solvent evaporation, the weight of residue was obtained (with an Ainsworth semimicro balance) for successive periods of drying in vacuo at 106°C.

For the more concentrated solution (0.58055%), deviations between the apparent and actual concentrations did not exceed 0.16% for any of the determinations between 37 and 103.8 hours of drying, as shown in Table VIII. Deviations between the apparent and actual concentrations for the less concentrated solution (0.23773%) were less than 0.3% over this same drying period. From these findings, drying times between 80 and 105 hours in vacuo at 106°C. were employed for gravimetric concentration determinations.

TABLE VIII

EVALUATION OF DRYING PROCEDURE FOR CONCENTRATION
DETERMINATIONS BY GRAVIMETRIC METHOD^a

Total Drying Time, ^b hr.	Apparent Concentration, %		
	Sample 59	Sample 94	Sample 43
0	0.61791	0.61590	0.62152
1.25	0.59076	0.59019	0.59370
3.42	0.58597	0.58519	0.58634
7.08	0.58428	0.58326	0.58349
10.2	0.58155	0.58229	0.58151
37.0	0.58079	0.58148	0.58086
60.0	0.58079	0.58089	0.58070
82.0	0.57997	0.58024	0.58006
103.8	0.58068	0.58078	0.58091

^aConcentration of starting solution: 0.58055% by weight polystyrene
PB6 in 1,2-dichloroethane.

^bDrying time in vacuo at 106°C.

SPECTROPHOTOMETRIC ANALYSIS

Ultraviolet absorption spectrophotometry provides a sensitive means of determining concentrations in the dilute solution region. Typical absorption spectra of polystyrene in 1,2-dichloroethane are shown in Fig. 5 for various concentrations of polymer. These spectra were obtained with a Beckman model DK-2 spectrophotometer using purified solvent as a reference.

The absorption spectra for two purified polymer preparations, obtained from solutions of nearly identical concentration, are compared in Fig. 5. Note that the spectra for these different preparations are essentially identical.

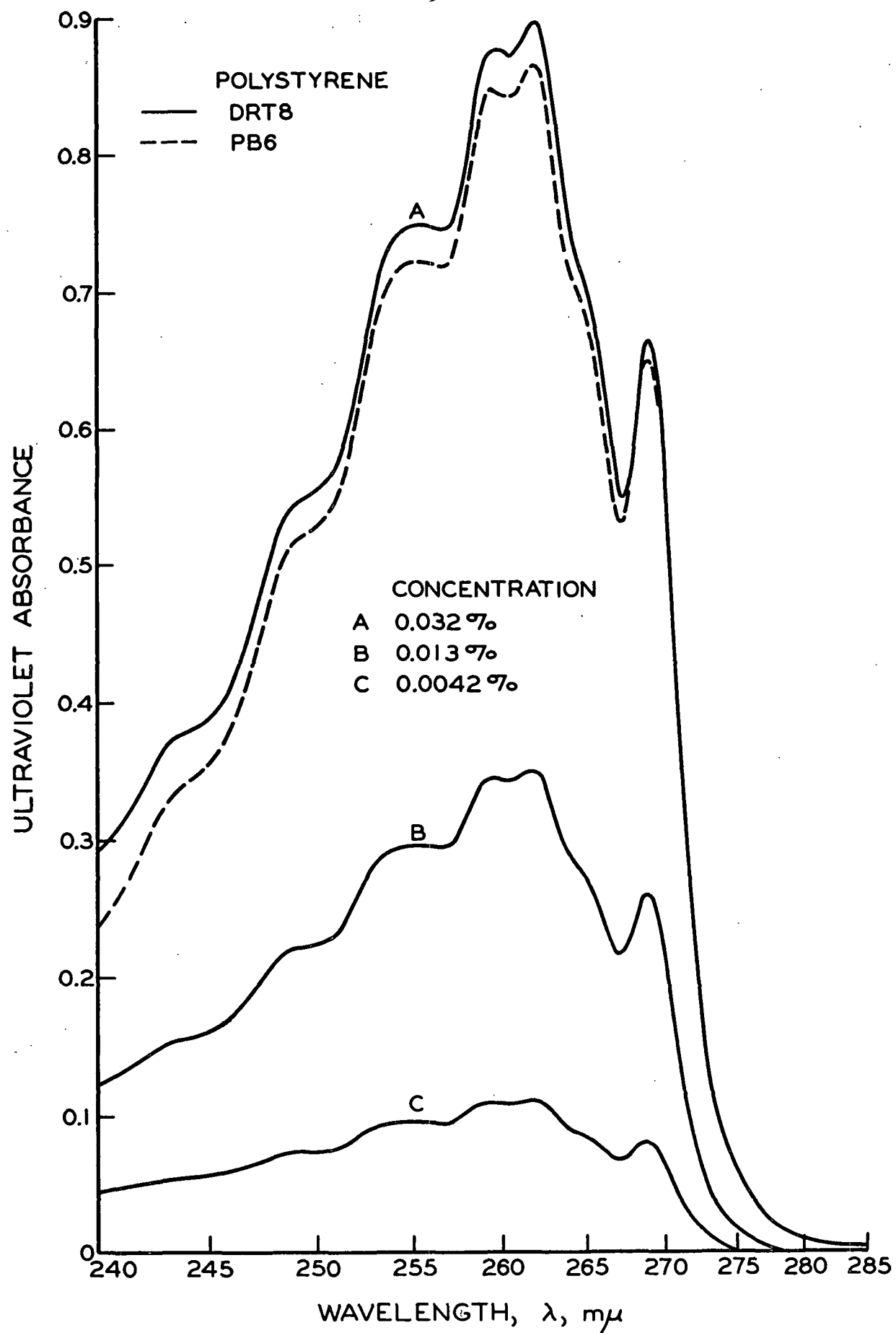


Figure 5. Ultraviolet Absorption Spectra of Polystyrene in 1,2-Dichloroethane

(The spectra for these samples prior to purification were vastly different from those shown in the figure.)

Several quantitative solutions of Polystyrene DRT8 in 1,2-dichloroethane were employed for obtaining concentration-absorbance calibration curves. Using a Beckman model DU spectrophotometer and purified solvent as a reference, absorbance measurements were made on the solutions at selected wavelengths, as shown in Fig. 6.

Whenever the spectrophotometric method was employed, every precaution was taken to insure that the absorption characteristics of the reference solvent matched those of the solvent in the solution.

INTRINSIC VISCOSITY DETERMINATIONS

GENERAL METHOD

Intrinsic viscosities were determined in 1,2-dichloroethane with a Cannon-Ubbelohde semimicro viscometer (size 25) having a solvent efflux time of 255 sec. Cannon, et al. (52) demonstrated that the kinetic energy correction for this type of viscometer is less than 0.05% for the conditions employed. The effect of rate of shear on the observed specific viscosity, η_{sp} , is negligible for polymers having intrinsic viscosities in the range of those employed (25, 53). Consequently, no corrections for kinetic energy or rate of shear effects were applied to the viscosity measurements.

When kinetic energy effects are negligible, the solution viscosity is directly proportional to efflux time. In this case, the specific viscosity, η_{sp} , is given by

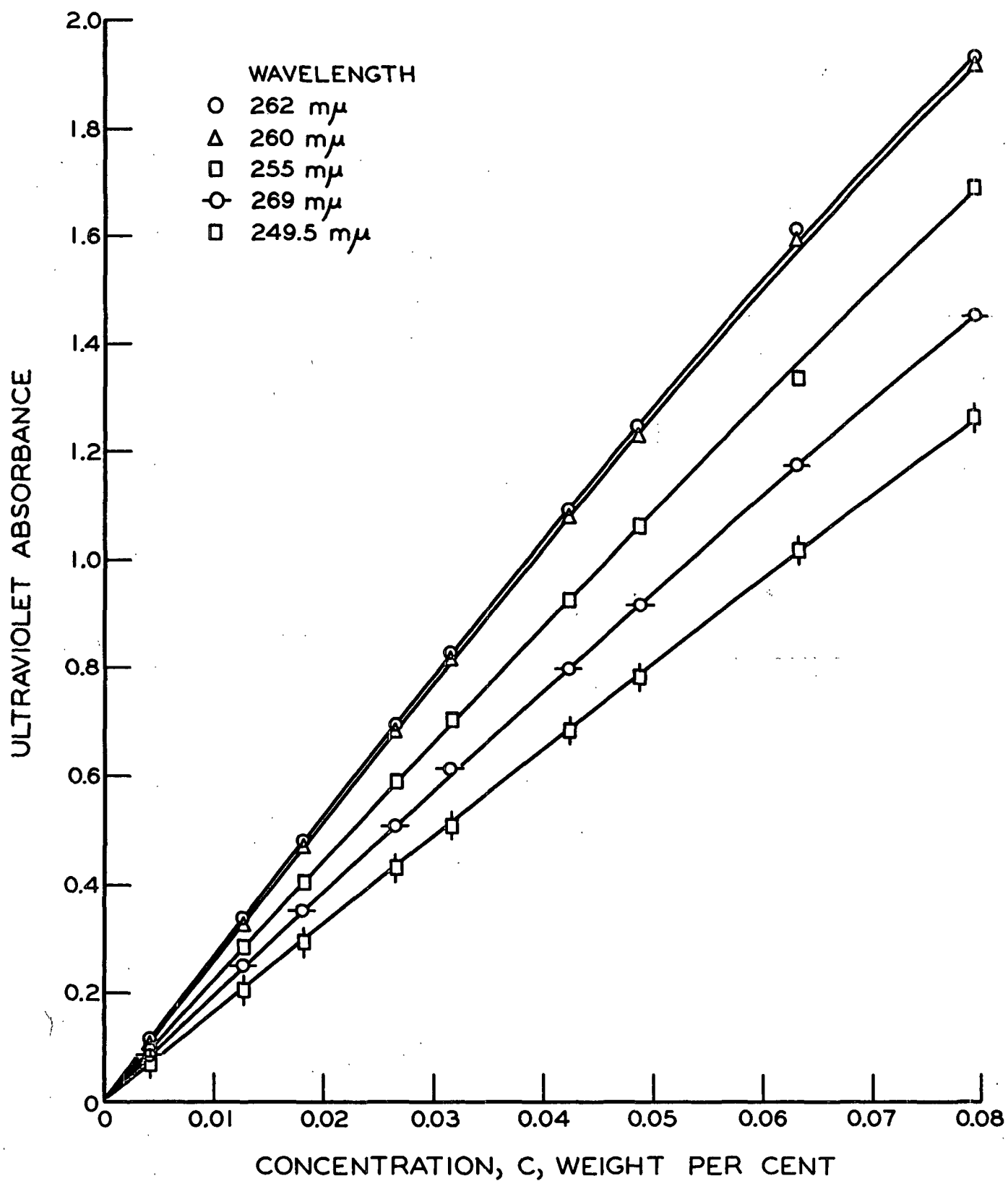


Figure 6. Spectrophotometric Calibration Curves for Determination of Dilute Solution Concentrations

$$\eta_{sp} = (t - t_o)/t_o \quad (2)$$

where \underline{t} and \underline{t}_o are the respective solution and solvent efflux times. The relative viscosity, $\underline{\eta}_r$, is given by

$$\eta_r = t/t_o \quad (3).$$

The viscometric data were plotted as η_{sp}/\underline{C} and $[\ln(\eta_r)]/\underline{C}$ (where \underline{C} is the volumetric concentration) against concentration, as shown in Fig. 7 for Polystyrene B6. The intrinsic viscosity, $[\eta]$, was taken as the common ordinate intercept (intercepts averaged when not identical) in accordance with the mutually related equations (54, 55):

$$\eta_{sp}/\underline{C} = [\eta] + k_\alpha [\eta]^2 \underline{C}, \text{ and} \quad (4)$$

$$[\ln(\eta_r)]/\underline{C} = [\eta] - k_\beta [\eta]^2 \underline{C} \quad (5),$$

where \underline{k}_α and \underline{k}_β are constants characteristic of a given solvent-polymer pair and temperature. These constants are independent of the molecular weight of the polymer and are related as follows:

$$\underline{k}_\alpha + \underline{k}_\beta = 0.5 \quad (6).$$

In actual practice, the determination of efflux times demand considerable care. Cleanliness was of the utmost importance. Each solution was filtered through a type AA (0.8 μ) Millipore filter (Millipore Filter Corporation, Bedford, Massachusetts) directly into the viscometer. Efflux times were recorded to the nearest tenth of a second, and a minimum of four readings were taken. In all cases, dilution techniques were avoided; each solution was prepared on a weight basis and measured individually.

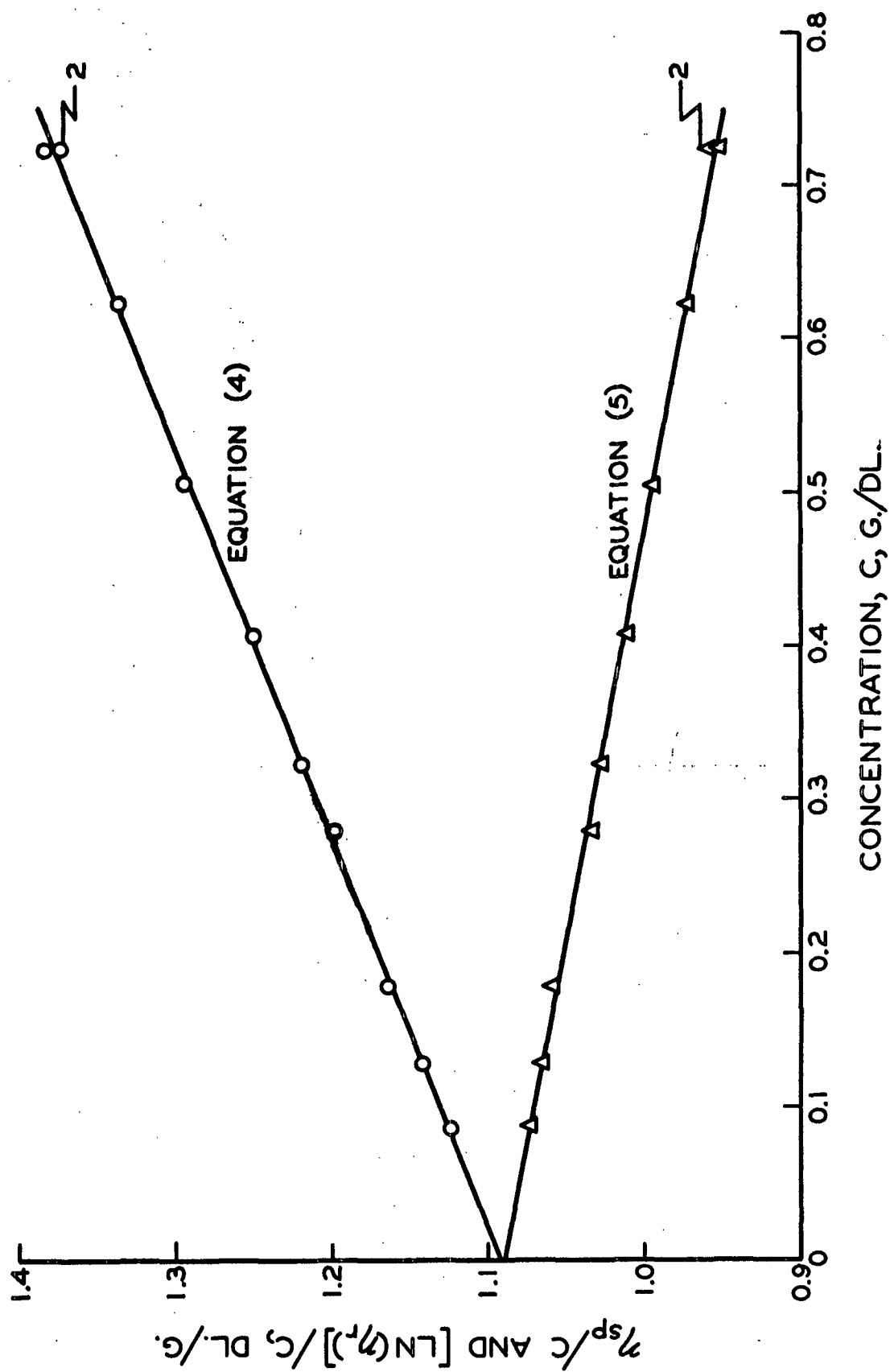


Figure 7. Concentration Extrapolations of Intrinsic Viscosity Data for Polystyrene B6 in 1,2-Dichloroethane at 30.0°C.

The intrinsic viscosity of each polymer sample was determined in 1,2-dichloroethane at 30.0 ± 0.01 and 25.0 ± 0.03 . The data from these determinations are shown in Fig. 42 and 43 of Appendix I.

ONE-POINT METHOD

Because of the time and quantity of solution required by the above method, it was necessary to employ a one-point method for solutions obtained from adsorption experiments. It has been demonstrated (56, 25) for a variety of solvents and a wide range of molecular weights that polystyrene solutions behave in accordance with Equations (4) and (5). Maron (57) combined these equations to obtain the following expression for direct calculation of intrinsic viscosity:

$$[\eta] = \{ \eta_{sp} + \gamma [\ln(\eta_r)] \} / [(1 + \gamma)C] \quad (7)$$

where $\gamma = k_{\alpha}/k_{\beta}$ (8).

The constants, k_{α} and k_{β} , were determined for each polymer sample and were found to be in good agreement (see Appendix I) with the values obtained for Polystyrene B6 (Fig. 7), i.e., $k_{\alpha} = 0.330$ and $k_{\beta} = 0.157$. Because of the extensive data obtained with Sample B6, these latter values were employed in Equations (7) and (8) to calculate intrinsic viscosity from efflux time determinations at a single concentration. The resulting one-point relationship for polystyrene in 1,2-dichloroethane at 30.0°C . is given as follows:

$$[\eta] = 0.321(\eta_{sp}/C) + 0.679[\ln(\eta_r)]/C \quad (9).$$

CONVERSION OF GRAVIMETRIC CONCENTRATION TO VOLUMETRIC CONCENTRATION

Because of need for accurate volumetric concentrations in viscometry, a means of converting concentrations from gravimetric to volumetric quantities

was developed. The apparent specific volume of polymer in solution, ϕ , can be obtained from the following:

$$\phi = (1/\rho_o) + (100/C_w)[(1/\rho) - (1/\rho_o)] \quad (10)$$

where ρ and ρ_o are the respective densities of solution and solvent, and C_w is the solution concentration in weight per cent. The above equation is equivalent to similar relationships of other investigators (58-60).

Solution ($C_w = 0.585\%$) and solvent densities were determined at 30.0°C., yielding respective averages of 1.23824 and 1.23903 g./ml. Employing these quantities in Equation (10), a value of 0.89 ml./g. was obtained for ϕ , which is in excellent agreement with those reported (61) for polystyrene in a variety of solvents at 25°C.

Assuming that ϕ is independent of concentration, solution densities at 30.0°C. can be obtained from Equation (10). With the solution density available, gravimetric concentrations can be accurately converted to volumetric terms with the following relationship:

$$C_v = (1.239 C_w)/[1 + (1.05 \times 10^{-3})C_w] \quad (11)$$

where C_v is the volumetric concentration at 30.0°C. in g./dl. Equation (11) was employed for conversions needed at 30°C. At other temperatures, solution and solvent densities were assumed to be equal. At 25°C., the solvent or solution density was taken as 1.246 g./ml., obtained from interpolation of reported results (33).

ADSORPTION RUNS

CLEANING PROCEDURE

Because of the importance of contaminating impurities in adsorption phenomena, considerable care was taken to clean equipment coming into direct contact with system components. Cleaning procedures are described in Appendix II.

APPARATUS

Adsorption experiments were conducted in 50-ml. centrifuge tubes provided with screw caps which had an inner cushion of rubber and a teflon liner.

During an adsorption run, tubes were mounted on an apparatus designed to control the degree of agitation and temperature. The apparatus was provided with several disks (12 inches in diameter) which were centrally mounted on a shaft (perpendicular to the plane of the disk). V-shaped cutouts were located at regular intervals along the periphery of each disk. An adsorption tube was mounted by locating the tube in appropriate cutouts of adjacent disks.

The disks could be radially displaced on the shaft, making it possible to set the angle between the adsorption tubes and the shaft at any desired interval. The apparatus was provided with a variable speed control so that the shaft speed could be maintained at any level below 120 r.p.m. Control of the angle and speed made it possible to vary the nature and degree of agitation over a wide range. On the other hand, by maintaining a constant rotational speed and fixed angle, the agitation was readily controlled.

The shaker apparatus was mounted in a constant temperature bath which provided control within $\pm 0.03^{\circ}\text{C}$.

PROCEDURE

Preliminary Preparations

Enough solvent was purified before each adsorption run to satisfy the solvent needs for an entire run, thereby keeping solvent quality constant. A portion of the purified solvent was used to prepare a stock solution whose concentration was determined gravimetrically. Solutions of lower concentration were made up on a weight basis from the stock solution and purified solvent.

Furnace-treated adsorbent was weighed to the nearest 0.3 mg. on an analytical balance and added to previously cleaned and tared adsorption tubes. The tubes containing adsorbent were heated in an oven overnight at 118°C . and subsequently stored in a vacuum desiccator filled with prepurified nitrogen.

Initiation of the Adsorption Run

Prior to each run, the adsorption tubes (containing adsorbent) and polymer solutions were thermostated at $25.0 \pm 0.03^{\circ}\text{C}$., the temperature used in all adsorption work. Solution additions were made subsequently from volumetric pipets, and the tubes were sealed by stretching teflon film across the mouth of each tube. The loaded tubes were sealed further with paraffin wax before mounting on the shaker apparatus.

Equilibration Period

Frequently, investigators have judged the time required for equilibration by observing the weight of polymer adsorbed as a function of time. In the present study, both the weight of adsorbed polymer and the intrinsic viscosity

of the bulk phase, $[\eta]_{\underline{B}}$, were observed as a function of time. (The term bulk phase is used throughout this thesis to indicate the solution phase or region containing dissolved solute as differentiated from the surface phase or region containing adsorbed polymer.) Data for Polystyrene PB6 and a mixture of Polystyrenes PS26 and PS34 are shown in Tables IX and X, respectively. Note that very little change was observed in the weight of adsorbed polymer after 13 or 14 hours; however, $[\eta]_{\underline{B}}$ continued to decrease sharply. Since there were no significant changes in $[\eta]_{\underline{B}}$ for either run after 3 days, that period was regarded as the minimum requirement for equilibration. (In most cases, equilibrium runs were continued for 4 days.)

TABLE IX

ADSORPTION OF POLYSTYRENE PB6 AS A FUNCTION OF TIME^a

Contact Time, hr.	$[\eta]_{\underline{B}}$, dl./g.	Weight Adsorbed Polymer, mg.
1.28	0.995	43.2
6.18	0.861	46.4
13.0	0.798	47.0
23.4	0.775	47.3
48.1	0.747	47.8
72.3	0.731	47.6
96.4	0.731	47.6

^aData from adsorption run No. 4S1-TCB.

The fact that $[\eta]_{\underline{B}}$ remained constant for 24 hours in one case and essentially constant for 47 hours in the other indicates that the rate of polymer degradation from agitation was negligible. (Other evidence will be presented later indicating that polymer degradation was negligible.)

TABLE X
ADSORPTION OF POLYSTYRENE MIXTURE
AS A FUNCTION OF TIME^a

Contact Time, hr.	$[\eta]_{\underline{B}}$, dl./g.	Weight Adsorbed Polymer, mg.
1.03	0.596	27.5
4.15	0.571	28.1
14.1	0.567	29.0
25.4	0.559	29.0
49.9	0.554	29.1
74.1	0.551	29.1
87.2	0.551	28.9
120.8	0.550	29.0

^aData from adsorption run No. 5S2-TCB.

Separation of Adsorbent and Solution

In adsorption experiments of long contact time, i.e., > 12 hr., the adsorbent and solution were separated by centrifuging the adsorption tubes, intact, under a force of approximately 3000 g for 20 min. The supernatant liquid was decanted, transferred to a clean centrifuge tube, and centrifuged as before. The resulting solution was filtered through a type AA (0.8 μ) Millipore membrane to remove any suspended carbon black.

For adsorption experiments of short duration, the initial separation of adsorbent and solution was obtained by filtration through a combined glass fiber prefilter and a type AM-3 (2.0 μ) Polypore membrane. The resulting filtrate was passed through a type AA (0.8 μ) Millipore filter.

Using the spectrophotometric method for concentration determinations, it was found that filtration of polymer solutions through membranes with average pore sizes as low as $0.45\ \mu$ (type HA, Millipore filter) did not remove any measurable quantities of polymer from solution.

Solvent which had been mixed with furnace-treated adsorbent for several days was tested for a possible increase in viscometric efflux time. The solvent was separated from the adsorbent by centrifugation and filtered through a type AA ($0.8\ \mu$) Millipore filter. The observed efflux time was identical to that of purified solvent (to the nearest tenth of a second), indicating that the final filtration removed suspended carbon black particles to the degree where there was no interference with viscosity determinations. There was no detectable residue obtained from evaporation of the exposed solvent.

ANALYSIS

A one-point intrinsic viscosity determination generally was made on each of the solutions obtained from adsorption experiments. Immediately following the efflux time determination, solution concentration was evaluated gravimetrically and converted to volumetric terms.

The weight of adsorbed polymer was calculated from the original solution volume and the concentration decrease resulting from adsorption. This method of calculation assumes that the bulk phase volume is equal to the original volume of solution employed. The error involved in that assumption is not likely to be serious. If all the solvent within 200 A. of the adsorbent surfaces is regarded as part of the surface phase, the total volume of solvent therein for each gram of adsorbent is only about 1.6% of the original volume usually employed (15.0 ml.).

DETERMINATION OF SEDIMENTATION COEFFICIENT DISTRIBUTIONS FROM
SEDIMENTATION VELOCITY EXPERIMENTS WITH AN ULTRACENTRIFUGE

INTRODUCTION

In cases where it was necessary to know the molecular weight distribution of polymer or its equivalent, sedimentation velocity experiments were conducted with an ultracentrifuge. Determination of polymer heterogeneity, specifically distributions of sedimentation coefficient, has been thoroughly reviewed (62-65). Recent studies (27, 29) with polystyrene contributed heavily to procedures employed in the present work.

The sedimentation velocity method used in the present work involves the transport of an initially sharp boundary between solvent and solution. Broadening or spreading of the boundary, which occurs during sedimentation, is influenced mainly by four factors: (1) polymolecularity, (2) diffusion, (3) concentration effects, and (4) pressure dependence of the sedimentation coefficient. Under appropriate conditions, the effect of polymolecularity is large in comparison to other factors. In that case, differential distribution functions can be calculated directly from sedimentation velocity data, as suggested by Baldwin and Williams (66), by assuming that observed behavior is only the result of differences in solute sedimentation rates (polymolecularity). Such determinations are regarded only as apparent distributions and are corrected subsequently for other influences.

The solvent employed in sedimentation velocity runs was selected because it minimized corrections needed. Corrections for diffusional transport were made by an appropriate extrapolation procedure. The effects of concentration were eliminated by using an analytical expression describing the dependence of

sedimentation coefficient, \underline{S} , on concentration. Corrections for the dependence of \underline{S} on pressure were neglected.

EXPERIMENTAL

Choice of Solvent

The ultracentrifuge work was conducted in cyclohexane just above the theta temperature. The Flory or theta temperature implies a temperature characteristic of a particular solvent-polymer system at which second virial coefficients in osmotic virial expansions (or in light-scattering expansions) become zero (67). At that temperature solute-solute and solvent-solute interactions are essentially balanced, and by working at sufficiently dilute concentrations, only interactions of a hydrodynamic nature are significant. The importance of using a theta system in sedimentation velocity experiments was discussed by Fujita (64) and demonstrated by McCormick (27) and Cantow (68). The theta temperature for the polystyrene - cyclohexane system has been determined by several experimental methods (69-71) which yielded temperatures in the range of 34.0 to 34.5°C.

Preparation of Samples

Since the adsorption experiments were conducted in 1,2-dichloroethane, a standard procedure was adopted for preparing ultracentrifuge samples in cyclohexane. Initially, dichloroethane solutions of polystyrene were placed in aluminum weighing dishes, and solvent was evaporated at room temperature. The resulting residues were dried in vacuo at 60°C. for at least 24 hours. The weighing dishes, containing the residues as thin films, were cut into strips and transferred to volumetric flasks. Every effort was made to keep the transfers quantitative, thereby preventing any possibility of fractionation. The flasks were then filled with purified cyclohexane and thermostated overnight at 37°C.

At temperatures below the theta point, polymeric species precipitate from solution. Consequently, at each point involving a transfer of solution or reduction in sample size, care was taken to insure that all species present were in solution. This was accomplished by thermostating the solution at a temperature slightly above the theta point for several hours.

Equipment and Procedures

Sedimentation velocity experiments were conducted in a Spinco Model E ultracentrifuge equipped with a temperature-controlling unit. Schlieren optics and a single-sector synthetic-boundary cell were employed. Prior to the cell loading, the cell components and loading accessories were thermostated at 50°C. for approximately one hour to prevent phase separation in the solution during the loading operation. The rotor, an ordinary An-D analytical head, was pre-heated to approximately 35°C.

Following the loading operation, the rotor and contents were allowed to equilibrate in the chamber at 35°C. for two hours before the run was started. Centrifugations were conducted at the maximum speed permitted for the cell components, i.e., 56,100 r.p.m., in order to minimize the contribution of diffusion to the boundary spreading. Speed-time data were recorded during the period of angular acceleration to permit an accurate calculation of the equivalent time at top speed. Schlieren photos were recorded automatically at two-minute intervals. The temperature of the rotor was maintained at $35 \pm 0.1^\circ\text{C}$. The equipment and typical operating conditions are summarized in Table XI.

A modified Wilder microcomparator providing an optically projected image of 20X magnification was used in the plate measurements. That instrument was provided with micrometers which were read to the nearest 0.0001 inch. Further experimental details are given elsewhere (65).

TABLE XI

SUMMARY OF EQUIPMENT AND TYPICAL OPERATING CONDITIONS

Ultracentrifuge: Spinco Analytical Model E

Rotor: type An-D

Cell: single-sector synthetic-boundary capillary type

Cell windows: sapphire

Light source: type A-H6 mercury arc lamp

Wavelength: 546 mμ (mercury green line)

Optics: schlieren with phase plate

Schlieren blade angle range: 60 to 70°

Rotor and cell temperature: 35°C.

High range heater voltage: 20

Refrigerant temperature: 10°F. (35°F. during angular acceleration period)

Top speed: 56,100 r.p.m.

Maximum angular acceleration: 13.5 rad./sec.²

Elapsed time to top speed: 12 min.

Duration of run: 30 min.

Volume of solution: 0.3 ml.

Volume of solvent: 0.1 ml.

Photographic plates: Kodak Spectroscopic II-G (2 x 10 in.)

Exposure time: 5 sec.

Automatic photo interval: 2 min.

CALCULATION OF APPARENT DISTRIBUTION

To account for sedimentational transport during the period of angular acceleration, an equivalent time of sedimentation, $\underline{t_e}$, at the final angular velocity, $\underline{\omega_f}$, was employed (63). The equivalent time can be accurately evaluated from the following:

$$t_e = (1/\omega_f^2) \int_0^t \omega^2 dt \quad (12)$$

where ω is the angular velocity at time, \underline{t} .

The sedimentation coefficient, \underline{S} , is readily given by (65):

$$S_i = (1/\omega_f^2 t_e) \ln(r_i/r_o) \quad (13)$$

where $\underline{r_i}$ and $\underline{r_o}$ are the distances from the center of rotation to the sedimenting species and the original boundary location, respectively. The apparent differential weight distribution function of \underline{S} , i.e., $\underline{g^*(S)}$, is given by the well-known relationship (62-64):

$$g^*(S_i) = \omega_f^2 t_e^3 r_i^3 (\partial \overline{\Delta n} / \partial r)_i / (\overline{\Delta n})_o r_o^2 \quad (14)$$

where $\overline{\Delta n}$ is the refractive index increment at time, \underline{t} , and position, $\underline{r_i}$, and $(\overline{\Delta n})_o$ is the refractive index increment of the original solution.

Equation (14) can be used to calculate the apparent differential weight distribution function of \underline{S} if (1) the refractive index of the solution is a linear function of concentration, and (2) the specific refractive index increment is the same for all solute components. Regarding the first condition, it has been reported (2) for the polystyrene - cyclohexane system that the refractive index of solution (at $\lambda = 546 \text{ m}\mu$) is a linear function of concentration

up to concentrations as high as 9% by weight. The second condition generally is regarded as an excellent assumption for polymers that are heterogeneous with respect to chain length only.

Trautman and Schumaker (72) demonstrated that the initial solution concentration, \underline{C}_0 , can be calculated from the following relationship:

$$C_0 = \int_0^{\infty} (r/r_0)^2 (\partial C / \partial r) dr \quad (15)$$

where \underline{C} is the solution concentration at time, \underline{t} , and position, \underline{r} . From the linear relationship between refractive index and solution concentration, it is evident that

$$(\overline{\Delta n})_0 = R C_0 \quad (16)$$

where \underline{R} is the specific refractive index increment.

By combining Equations (14), (15), and (16), the following is readily obtained:

$$g^*(S_i) = \omega_F^2 t_e r_i^3 (\partial \overline{\Delta n} / \partial r)_i / \int_0^{\infty} r^2 (\partial \overline{\Delta n} / \partial r) dr \quad (17).$$

The above relationship is in a form which facilitates direct use of the plate measurements. The gradient term, $\partial \overline{\Delta n} / \partial r$, is directly proportional to the height of the boundary curve (after subtraction for a reference base line) (73).

Equations (13) and (17) were used to calculate the apparent distributions.

Location of Original Boundary

Immediately following the boundary formation, the refractive index gradient at the boundary was so high that light was deviated completely out of the optical

system. This behavior appeared on the photographic plates as a sharp vertical line which could be located with considerable accuracy. These early photos were used to determine the original boundary location. Employing the micro-comparator technique, the distance between a known reference edge and the vertical line, ΔX_L , was determined for several photos. These quantities were extrapolated against equivalent time, as shown in Fig. 8. The resulting intercept was employed to calculate the original boundary location, r_0 , by an appropriate conversion from optical to actual radial distance.

DIFFUSION CORRECTION

As previously indicated, distributions obtained from Equations (13) and (17) are regarded only as apparent distribution curves. By extrapolating the distributions to infinite time, the contribution from diffusion spreading becomes vanishingly small compared to the effect of polymolecularity (64, 74, 75).

Several methods for performing the extrapolation to infinite time have been suggested. A method suggested by Baldwin (76) although not recommended strongly by him was found quite satisfactory for the present work. This method involves the extrapolation of \underline{S} against a reciprocal time function $[\underline{t}_e \exp(\bar{S}_1^* \frac{t}{t_e})]^{-1}$, for fixed values of $\underline{g}^*(\underline{S})/\underline{g}^*(\underline{S})_{\max}$. The mean sedimentation coefficient for an apparent distribution, \bar{S}_1^* , is appropriately defined by (64):

$$\bar{S}_1^* = \int_0^{\infty} S \underline{g}^*(S) dS / \int_0^{\infty} \underline{g}^*(S) dS \quad (18).$$

The term, $\underline{g}^*(\underline{S})_{\max}$, is used to designate the maximum value of $\underline{g}^*(\underline{S})$.

Typical extrapolation curves are shown in Fig. 9 and 10 for the trailing and leading sides of the boundary, respectively. Note that the extrapolations

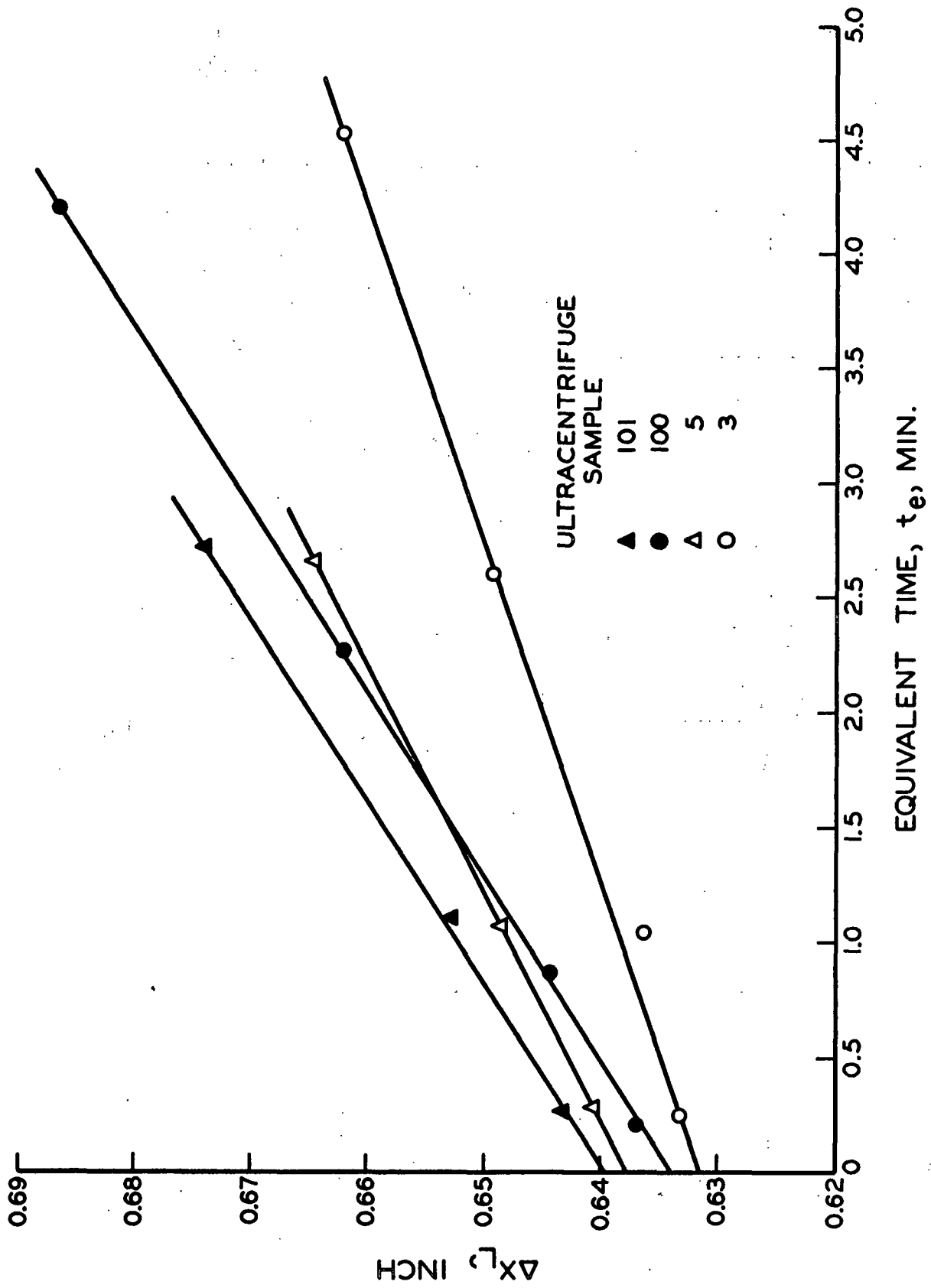


Figure 8. Location of Original Boundary Position

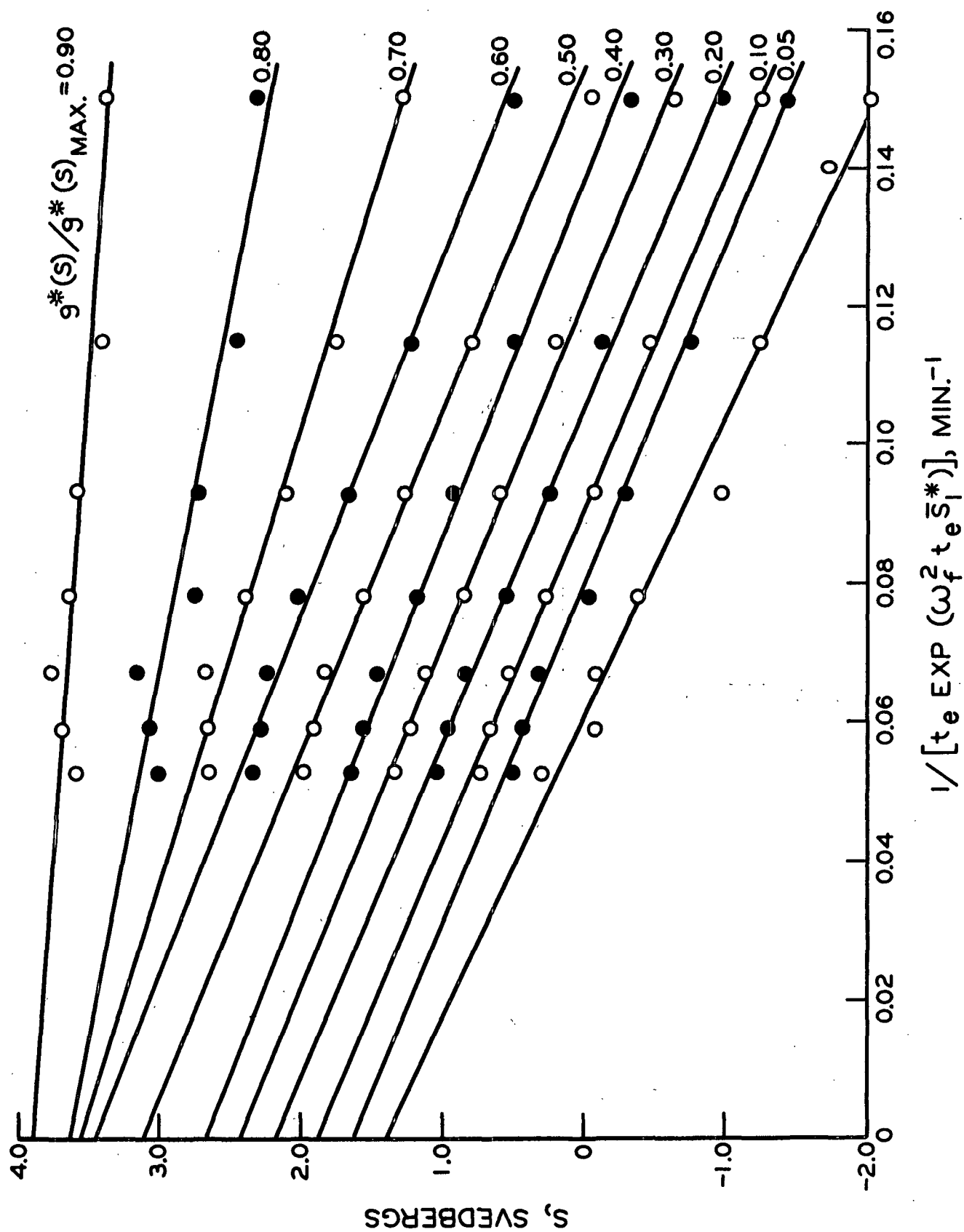


Figure 9. Diffusion Corrections Applied to Trailing Side of Boundary for Ultracentrifuge Sample 5

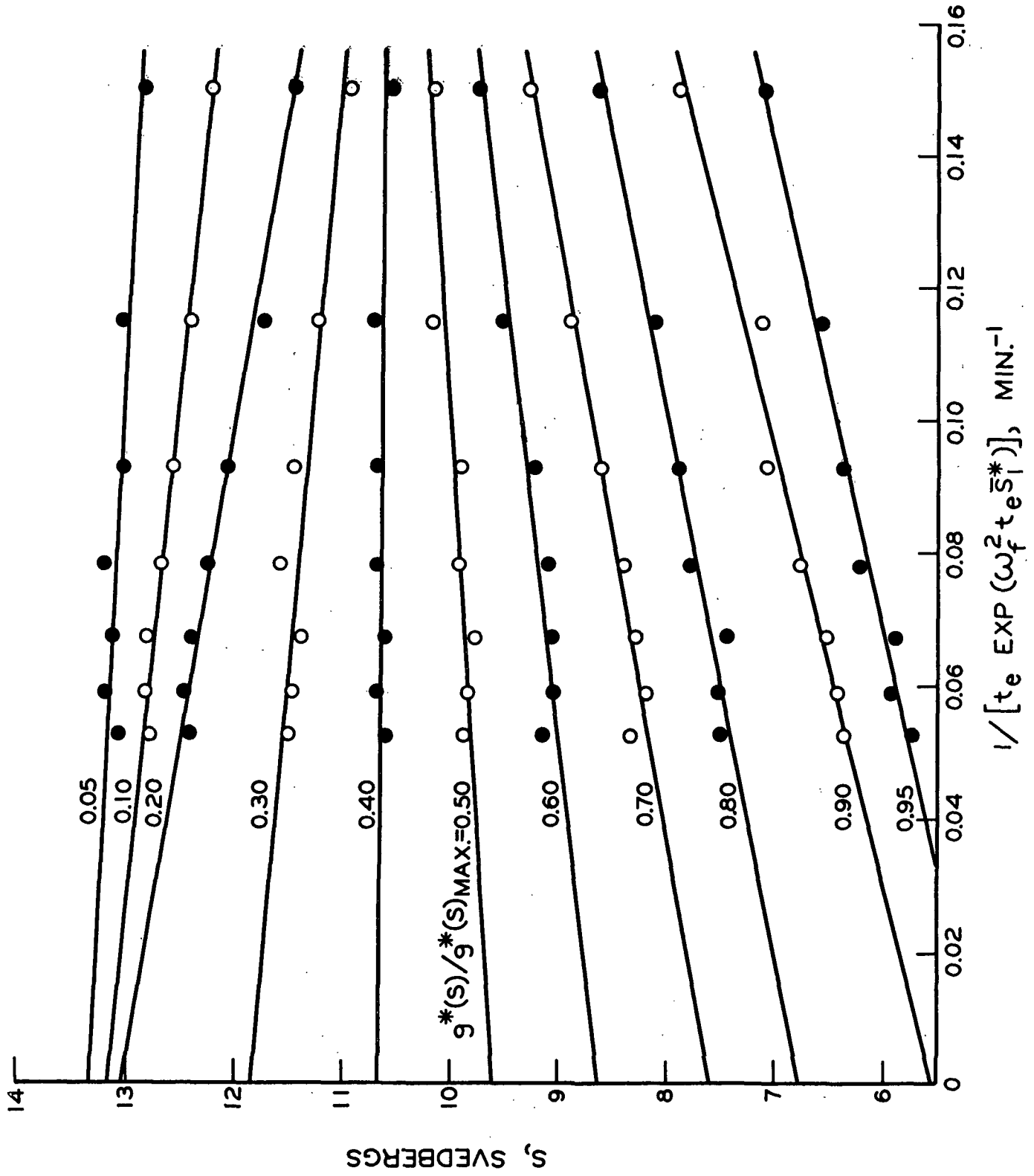


Figure 10. Diffusion Corrections Applied to Leading Side of Boundary for Ultracentrifuge Sample 5

are essentially linear over the entire range of \underline{S} , which is particularly desirable for quantitative evaluation. The extrapolations yield the diffusion-free distribution of $\underline{g}(\underline{S})/\underline{g}(\underline{S})_{\max}$ versus \underline{S} . The ordinate of the distribution, i.e., $\underline{g}(\underline{S})/\underline{g}(\underline{S})_{\max}$, is then multiplied by $\underline{g}(\underline{S})_{\max}$ to obtain the diffusion-free distribution of $\underline{g}(\underline{S})$ versus \underline{S} . The value of $\underline{g}(\underline{S})_{\max}$ can be accurately evaluated from the following:

$$\underline{g}(\underline{S})_{\max} = \left[\int_0^{\infty} \{ \underline{g}(\underline{S})/\underline{g}(\underline{S})_{\max} \} d\underline{S} \right]^{-1} \quad (19).$$

This extrapolation procedure is actually a modification of a method employed successfully by Eriksson (77) for diffusion corrections for polymethyl methacrylate.

CONCENTRATION CORRECTION

Because of the extensive work (both experimental and computational) required for concentration corrections by extrapolation techniques, it is desirable to use an analytical concentration correction whenever possible. The method of correcting the \underline{S} - $\underline{g}(\underline{S})$ distribution to infinite dilution from a single experiment at concentration \underline{C}_0 requires knowledge of the concentration dependence of \underline{S} . The method also involves certain assumptions, the most serious being that sedimentation coefficient depends only on the total concentration of the mixture (73).

The Johnston-Ogston and boundary sharpening effects both disappear at infinite dilution and, thereby, are eliminated simultaneously by extrapolating the diffusion-free distributions to infinite dilution (64). However, when the condition, $(\underline{S}/\underline{S}^0) > 0.9$, is satisfied (where \underline{S} is the sedimentation coefficient at some finite concentration and \underline{S}^0 is the corresponding value at

infinite dilution), there is very little difference in distributions obtained with and without correction for the Johnston-Ogston effect (73). Hence, concentration effects can be adequately accounted for by an analytical correction when the above condition is satisfied.

A photo taken near the middle of the run is used for the necessary correction information. The quantity, $\underline{dC/dS}$, is calculated from the following equation due to Baldwin (78):

$$(\underline{dC/dS})_i = g^*(S_i)C_o[\exp(-2\omega_{fe}^2 S_i)] \quad (20)$$

The above relationship facilitates determination of the actual concentration, \underline{C}_{si} , at the level in the cell where the sedimentation coefficient (uncorrected for concentration) is given as \underline{S}_i . This concentration is readily obtained from the following:

$$\underline{C}_{si} = \int_{-\infty}^{\underline{S}_i} (\underline{dC/dS}) dS \quad (21).$$

The dependence of \underline{S} on concentration in the polystyrene - cyclohexane system at 35°C. was reported by Cantow (68) for the concentration range from 0.2 to 1.5 g./dl.:

$$S = S^o / (1 + 0.006S^{o2}C^2) \quad (22)$$

where

- \underline{S} = concentration dependent sedimentation coefficient in svedbergs
- \underline{S}^o = sedimentation coefficient at infinite dilution in svedbergs
- \underline{C} = concentration in g./dl.

Knowing the relationship between \underline{C}_{si} and \underline{S}_i , i.e., Equation (21), values of \underline{S}_i^o corresponding to \underline{S}_i can be obtained from Equation (22) by a trial and

error method. A plot of corresponding \underline{S}_i and \underline{S}_i^0 values yields the slope, $(\underline{dS}/\underline{dS}^0)_i$, at each value of \underline{S}_i . The differential weight distribution function, already corrected for diffusion, i.e., $\underline{g}(\underline{S})$, can now be corrected to infinite dilution according to:

$$\underline{g}(\underline{S}_i^0) = \underline{g}(\underline{S}_i)(\underline{dS}/\underline{dS}^0)_i \quad (23).$$

The fully corrected distribution is given as $\underline{g}(\underline{S}^0)$ versus \underline{S}^0 .

The magnitude of the boundary sharpening correction is demonstrated in Fig. 11 with ultracentrifuge Sample 101. Since that sample possessed the highest average molecular weights and was the most concentrated of any employed, the correction shown represents a maximum.

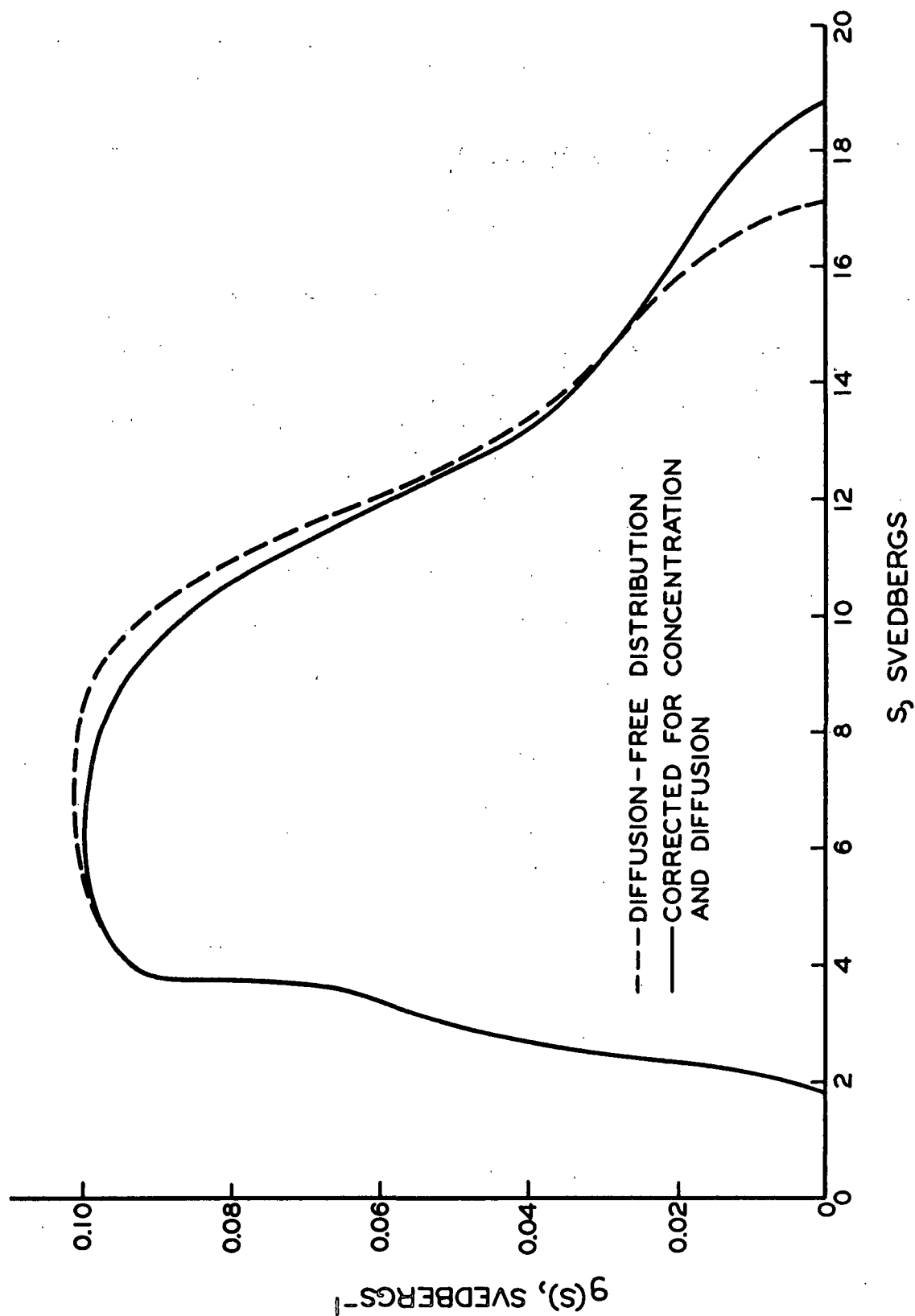


Figure 11. . . Concentration Correction Applied to Diffusion-Free Distribution for Ultracentrifuge Sample 101

EXPERIMENTAL DATA AND DISCUSSION OF RESULTS

EQUILIBRIUM ADSORPTION AND FRACTIONATION OF POLYSTYRENES OF BROAD MOLECULAR WEIGHT DISTRIBUTION

INTRINSIC VISCOSITY AND RELATED STUDIES

Experimental

Equilibrium adsorption experiments were conducted for different ratios of adsorbent weight to solution volume over a wide range of solution concentration. Polystyrene B6 was used both as received and purified. Solution volumes of 15.0 ml. were employed in each adsorption tube, and the weight of furnace-treated FT-D4 graphitized carbon black was varied from 0.5 to 6.0 g. The adsorption tubes were agitated for several days at $25.0 \pm 0.03^\circ\text{C}$. Following equilibration, the tubes were centrifuged, and the resulting supernatant solutions were filtered to remove any suspended carbon black. The experimental conditions employed in these equilibrium runs are summarized in Table XII.

TABLE XII
SUMMARY OF EXPERIMENTAL CONDITIONS FOR
EQUILIBRIUM ADSORPTION RUNS

Adsorption Run No.	Polystyrene Sample	Equilibration Period, days	Shaker Speed, r.p.m.	Shaker Angle
3S-ECB	B6	3	24.0	15°
4S4-ECB	PB6	4	24.0	15°

One-point intrinsic viscosity determinations were made on supernatant solutions having concentrations sufficiently high for accurate efflux time determinations.

Langmuir Behavior

Silberberg (5, 79) has demonstrated theoretically that polymer adsorption should conform to the Langmuir isotherm, although not for the reasons usually associated with such behavior. Langmuir behavior also has been observed experimentally (1, 80).

The Langmuir isotherm can be written as follows:

$$\Gamma = K_L \Gamma_m C / (1 + K_L C) \quad (24)$$

where Γ is the specific adsorption, i.e., the weight of adsorbed polymer per unit weight of adsorbent, K_L is an equilibrium constant, Γ_m is the maximum or limiting specific adsorption, and C is the equilibrium concentration.

To test the conformance of an adsorption system to the Langmuir isotherm, it is necessary (5, 80) to include data in the dilute solution region over a wide range of surface coverage. Equilibrium adsorption data were obtained in that region from Adsorption Run no. 3S-ECB, employing Polystyrene B6. These data pertain to concentrations from 0.009 to 0.80 mg./cc. Because of the limited amount of polymer in solution in this region, concentrations had to be determined spectrophotometrically. However, unpurified Polystyrene B6 had a significantly different ultraviolet spectrum than the highly purified polystyrenes, making it impossible to use the concentration-calibration curves in the usual manner.

It was found, however, that the decrease in spectrophotometric absorbance between the initial and final solutions could be used quite satisfactorily. Apparently, the impurities present were not adsorbed to any significant degree. This was established in two ways. First, the highest concentration employed was determined both gravimetrically and spectrophotometrically, and excellent

agreement was obtained. Second, the use of different wavelengths (those previously calibrated) gave essentially the same results. It is very unlikely that impurities were adsorbed in the same spectrophotometric ratios as polymer.

The results obtained from the ultraviolet analysis are summarized in Table XIII. Using the average concentration decrease obtained from three wavelengths ($\lambda = 260, 262, \text{ and } 269 \text{ m}\mu$), the results shown in Table XIV were calculated.

TABLE XIII

RESULTS FROM ULTRAVIOLET ANALYSIS OF DILUTE
SOLUTIONS FROM ADSORPTION RUN NO. 3S-ECB

Initial Concentration, weight %	Concentration Decrease ^a , weight %			
	A	B	C	D
0.1430	0.0798	0.0785	0.0776	0.0793
0.1027	0.0735	0.0731	0.0721	
0.07196	0.0600	0.0598	0.0595	
0.05804	0.0499	0.0506	0.0505	
0.04041	0.0390	0.0389	0.0387	
0.02325	0.0211	0.0213	0.0212	
0.01193	0.0112	0.0112	0.0111	

^aCode

- A - Results using only a single wavelength, $\lambda = 269 \text{ m}\mu$.
- B - Results using $\lambda = 260, 262, \text{ and } 269 \text{ m}\mu$.
- C - Results using $\lambda = 255, 260, 262, \text{ and } 269 \text{ m}\mu$.
- D - Gravimetric determination.

The Langmuir isotherm can be written in its linear form as follows:

$$C/\Gamma = C/\Gamma_m + 1/(K_1\Gamma_m) \quad (25).$$

The adsorption data obtained from the dilute solution region (Table XIV) were plotted in accordance with the above equation, as shown in Fig. 12.

TABLE XIV
RESULTS FROM DILUTE SOLUTION REGION
OF ADSORPTION RUN NO. 3S-ECB

Initial Concentration, weight %	Equilibrium Concentration, mg./cc.	Specific Adsorption, mg./g.
0.1430	0.803	14.7
0.1027	0.370	13.7
0.07196	0.152	11.2
0.05804	0.0923	9.46
0.04041	0.0189	7.27
0.02325	0.0241	3.99
0.01193	0.00926	2.09

A statistical analysis of the data (method of least squares) yielded a correlation coefficient of 0.9986, $\Gamma_m = 15.63$ mg./g., and $K_1 = 18.45$ cc./mg.

It has been pointed out (5, 80) that a plot of adsorption data is not a very sensitive test of Langmuir behavior in regions of nearly constant surface coverage, i.e., regions of nearly constant Γ . The fraction of surface covered, θ , can be calculated according to:

$$\theta = \Gamma/\Gamma_m \quad (26).$$

The above relationship assumes with no justification that the fraction of surface covered is directly proportional to the weight of adsorbed polymer. Consequently, the surface coverage quantities should not be interpreted literally.

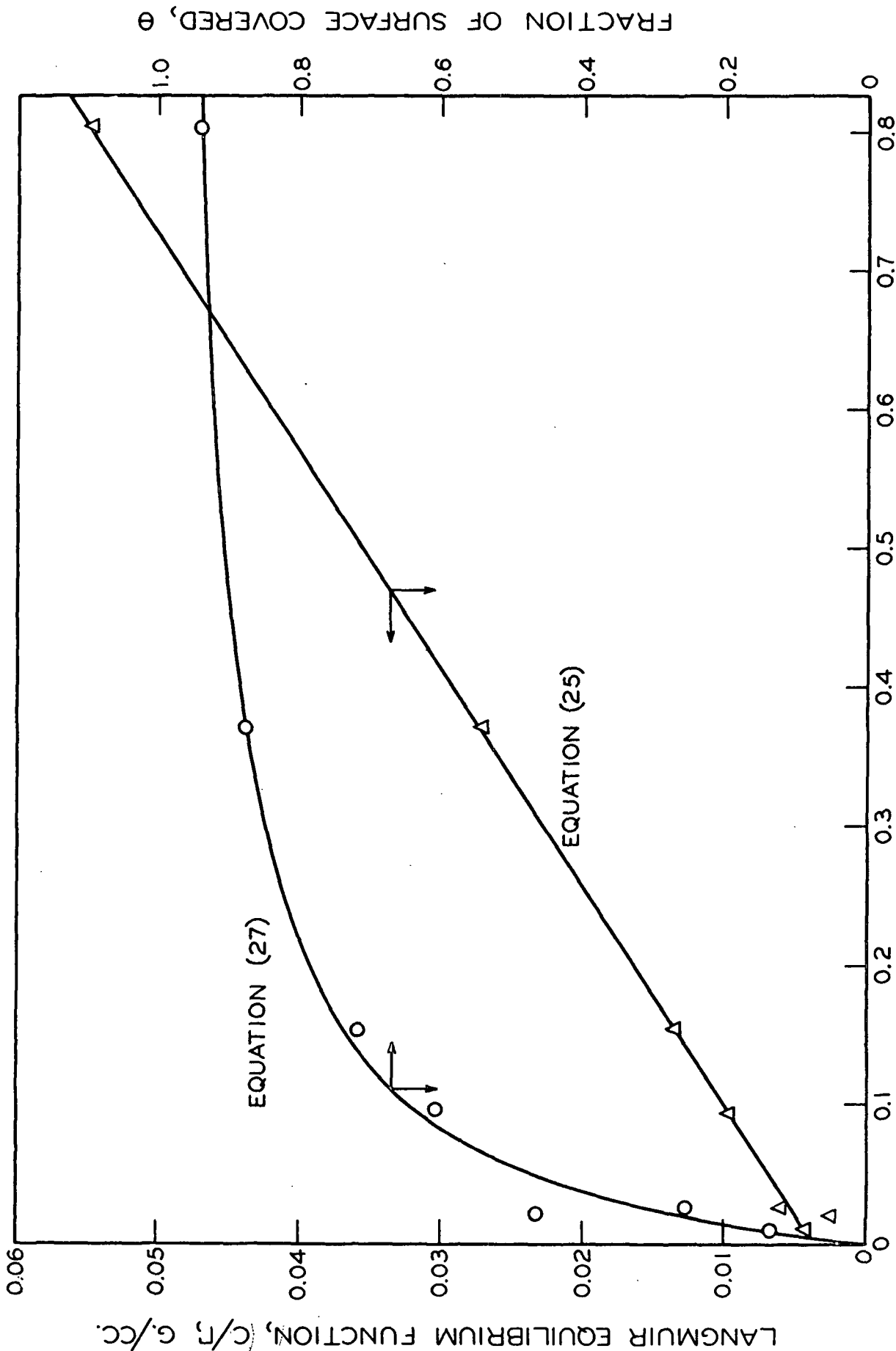


Figure 12. Langmuir Plot for the Dilute Solution Region Compared to the Fraction of Surface Covered (Adsorption Run No. 3S-ECB)

Surface coverage values were calculated with Equation (26) and compared with Langmuir quantities, as shown in Fig. 12. Note that Langmuir behavior was observed over a wide range of surface coverage, i.e., over a wide range of specific adsorption.

Data from the high concentration region of Adsorption Run no. 3S-ECB indicate that the system exhibited Langmuir behavior at substantially higher equilibrium concentrations. These adsorption data were plotted in accordance with Equation (25), as shown in Fig. 13. A statistical analysis of the data yielded a correlation coefficient of 0.9988 and $\Gamma_m = 15.66$ mg./g. The limits of the dilute solution region are indicated in Fig. 13 to emphasize the wide range of concentration over which Langmuir behavior was observed.

The combined data obtained from Adsorption Run no. 3S-ECB also was analyzed statistically, yielding a correlation coefficient of 0.9993 and $\Gamma_m = 15.93$ mg./g. The latter value was used in Equation (26) to calculate the surface coverage shown in Fig. 12. The solid curve passing through the surface coverage points in that figure was obtained by combining Equations (24) and (26) as follows:

$$\theta = K_1 C / (1 + K_1 C) \quad (27).$$

The equilibrium constant, K_1 , was taken as 18.45 cc./mg., obtained from the dilute solution data.

The Langmuir isotherm obtained from the combined adsorption data is compared in Fig. 14 with that obtained from the dilute solution data. Note that the constants, K_1 and Γ_m , obtained from the dilute solution data can predict the adsorption isotherm over the entire concentration range with a high degree of accuracy.

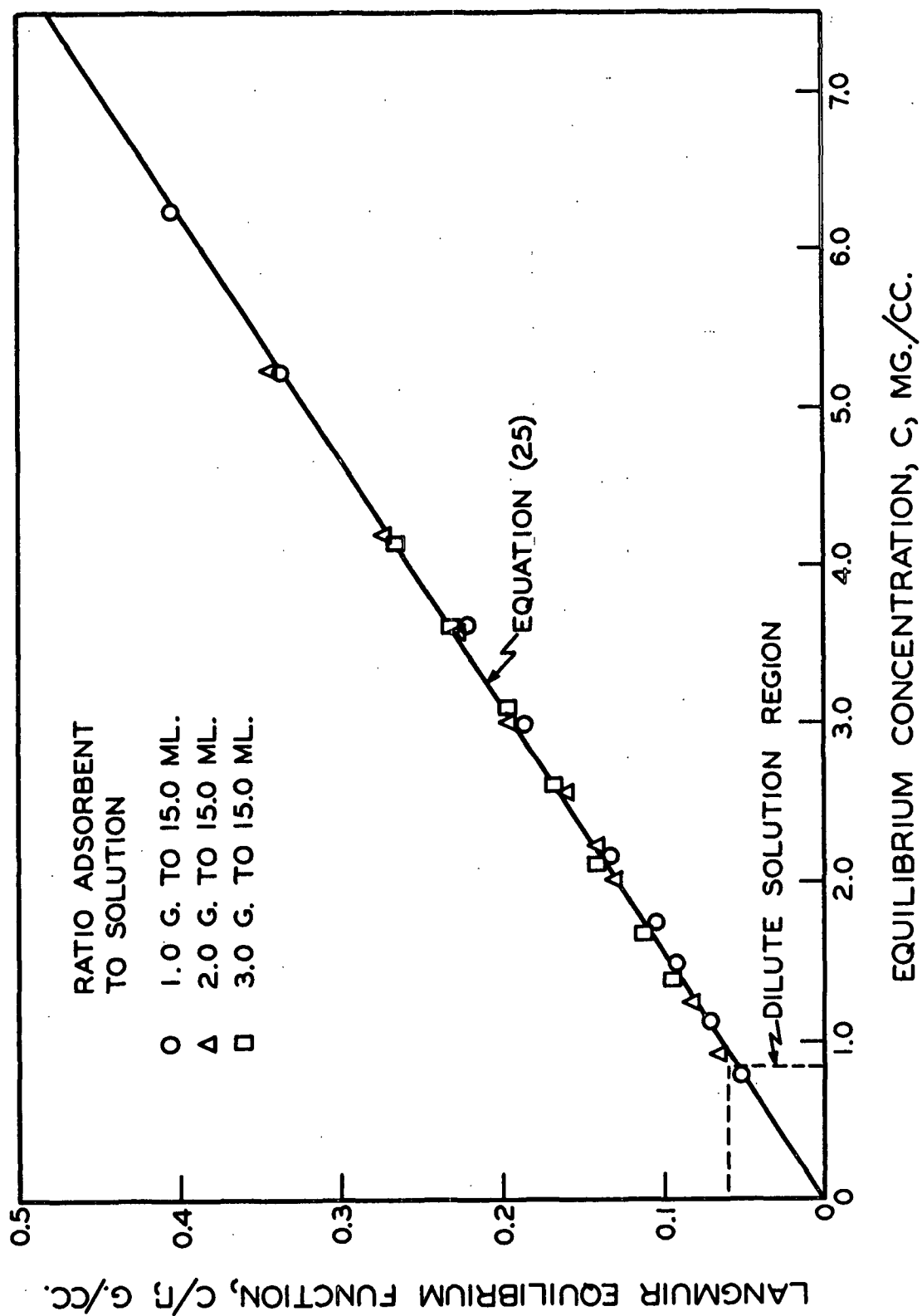


Figure 13. Langmuir Plot for Higher Concentration Region of Run No. 3S-ECB (Polystyrene B6)

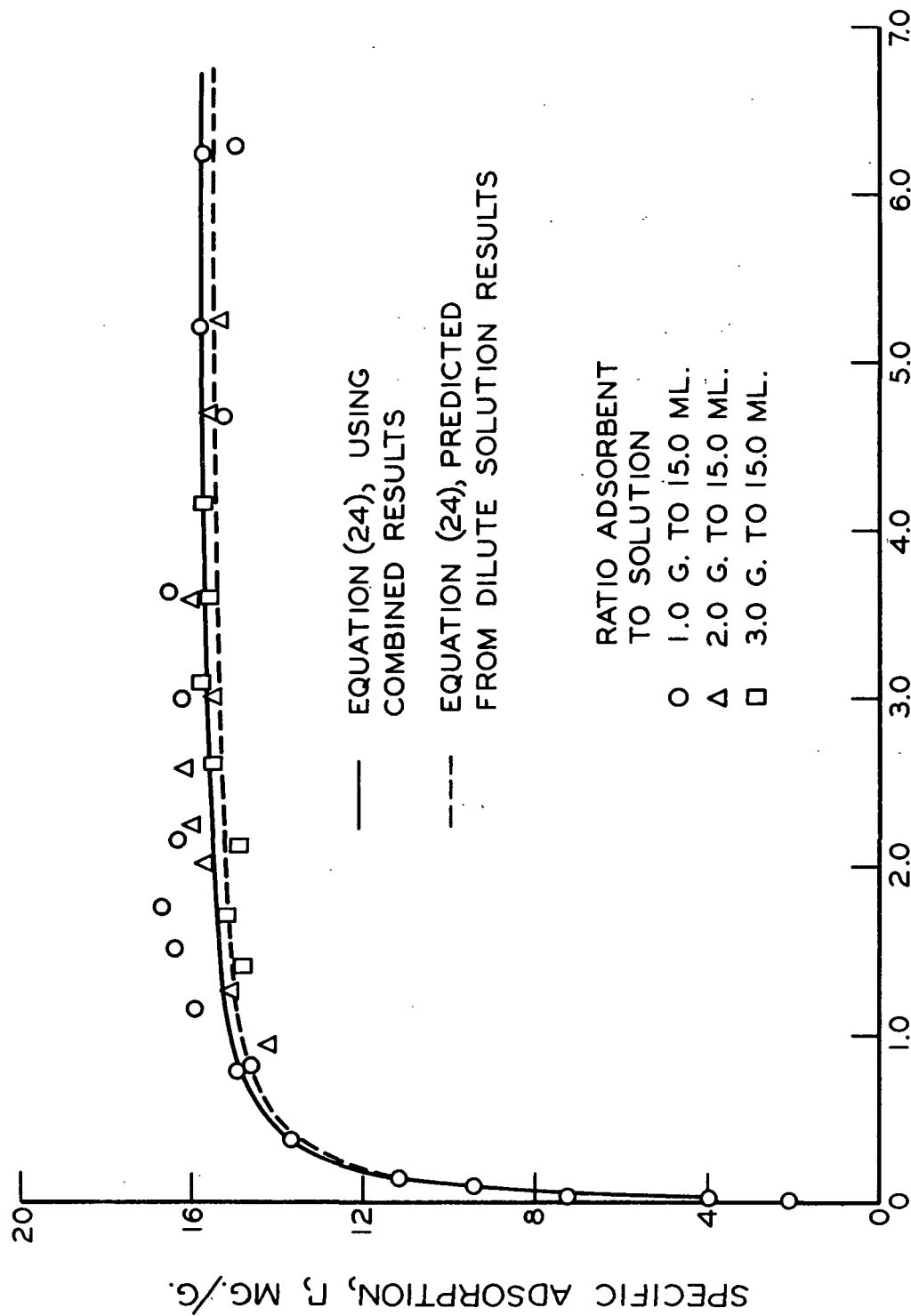


Figure 14. Langmuir Adsorption Isotherm for Run No. 3S-ECB (Polystyrene B6)

Additional evidence of Langmuir behavior was obtained from Adsorption Run no. 4S4-ECB, employing Polystyrene PB6. The adsorption data were plotted in accordance with Equation (25), as shown in Fig. 15. It is not known whether the deviations from linearity at the higher concentrations are significant or not. The relative decreases in concentration which resulted from adsorption were much lower for these determinations than for those at lower equilibrium concentrations, making the determination of Γ much less certain. On the other hand, the deviations may represent a change in the adsorption process, although the data are too limited to support such a conclusion. A linear regression of the adsorption data in the concentration range, $0 < C < 6.0$ mg./cc., yielded a correlation coefficient of 0.9977 and $\Gamma_m = 15.36$ mg./g.

Fractionation Behavior in the Bulk Phase

The intrinsic viscosity data obtained from Adsorption Run no. 3S-ECB (Polystyrene B6) are shown in Fig. 16. It appears that the fractionation (as measured by intrinsic viscosity) of Polystyrene B6 was strongly dependent on the ratio of adsorbent to solution and the equilibrium concentration. However, the viscosity data can be described by a single parameter, irrespective of the ratio of adsorbent to solution or equilibrium concentration. This is demonstrated in Fig. 17 in which intrinsic viscosity was plotted against the weight fraction of polymer adsorbed, $\underline{X_A}$.

On first consideration, the variables which seemed important in Fig. 16, i.e., the ratio of adsorbent to solution and equilibrium concentration, appear to be unnecessary to describe the fractionations obtained. However, it must be emphasized that the quantity, $\underline{X_A}$, actually is related to these variables according to:

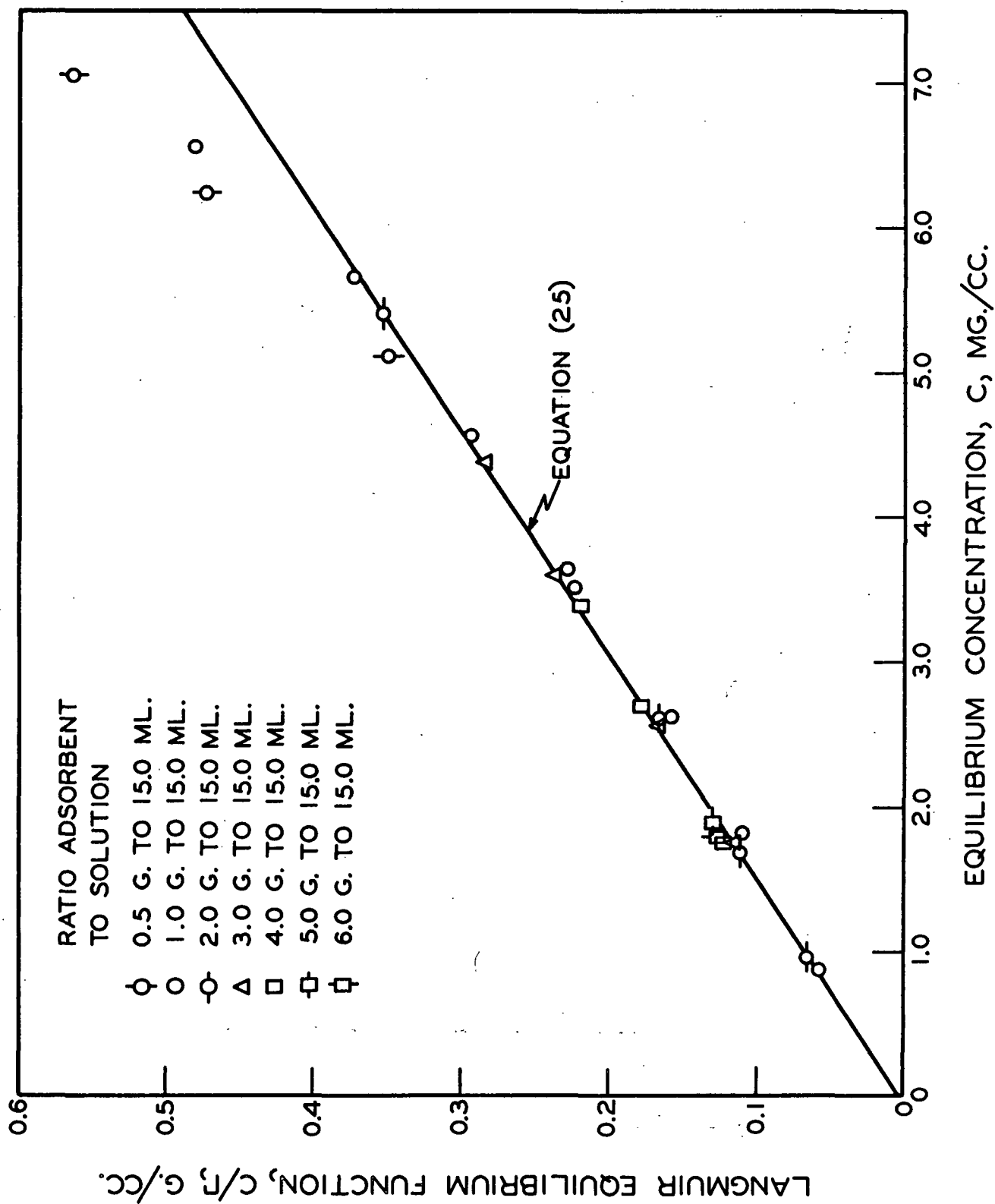


Figure 15. Langmuir Plot for Run No. 4S4-ECB (Polystyrene PB6)

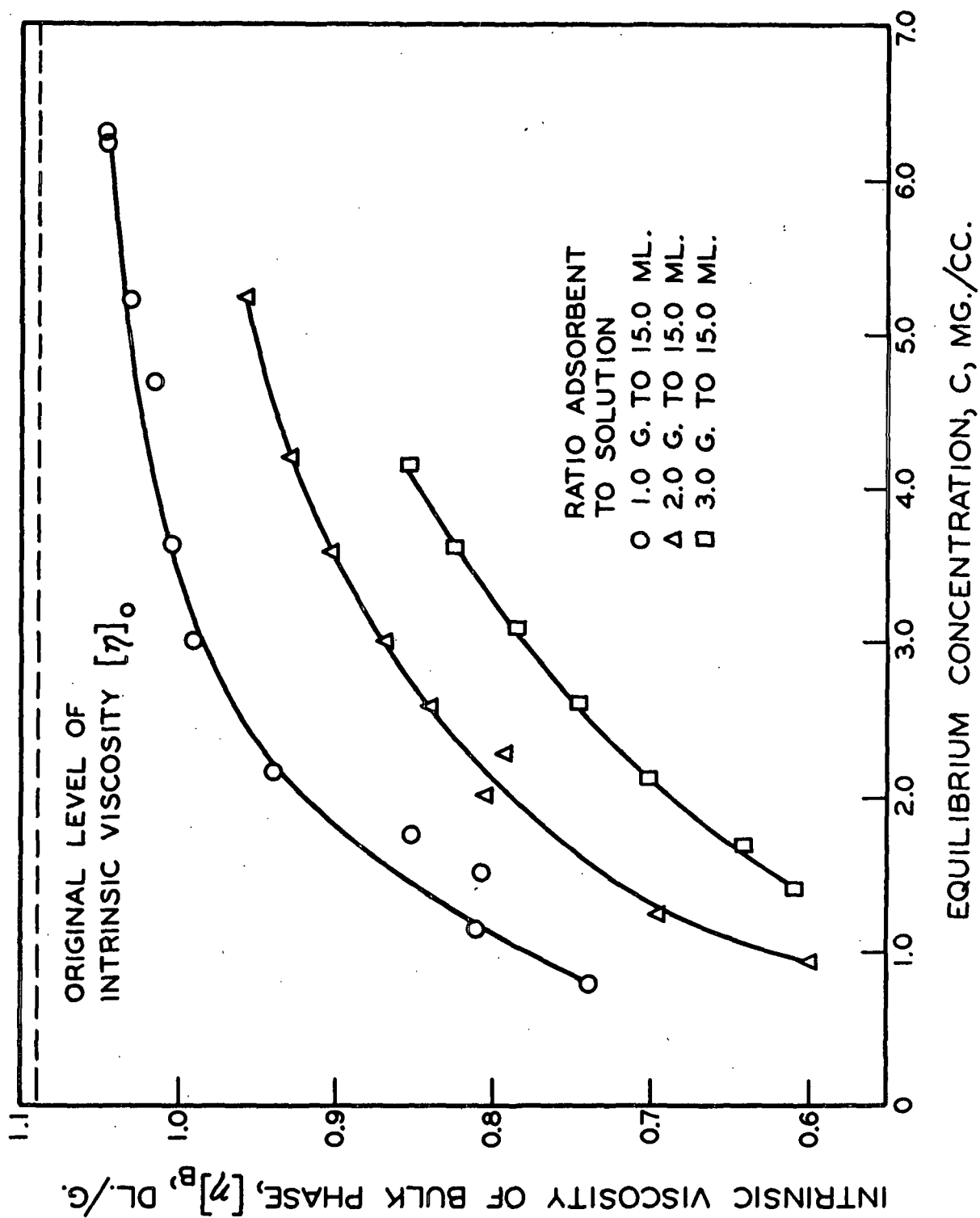


Figure 16. Effect of System Variables on the Intrinsic Viscosity of Bulk Phase at Equilibrium (Adsorption Run No. 3S-ECB)

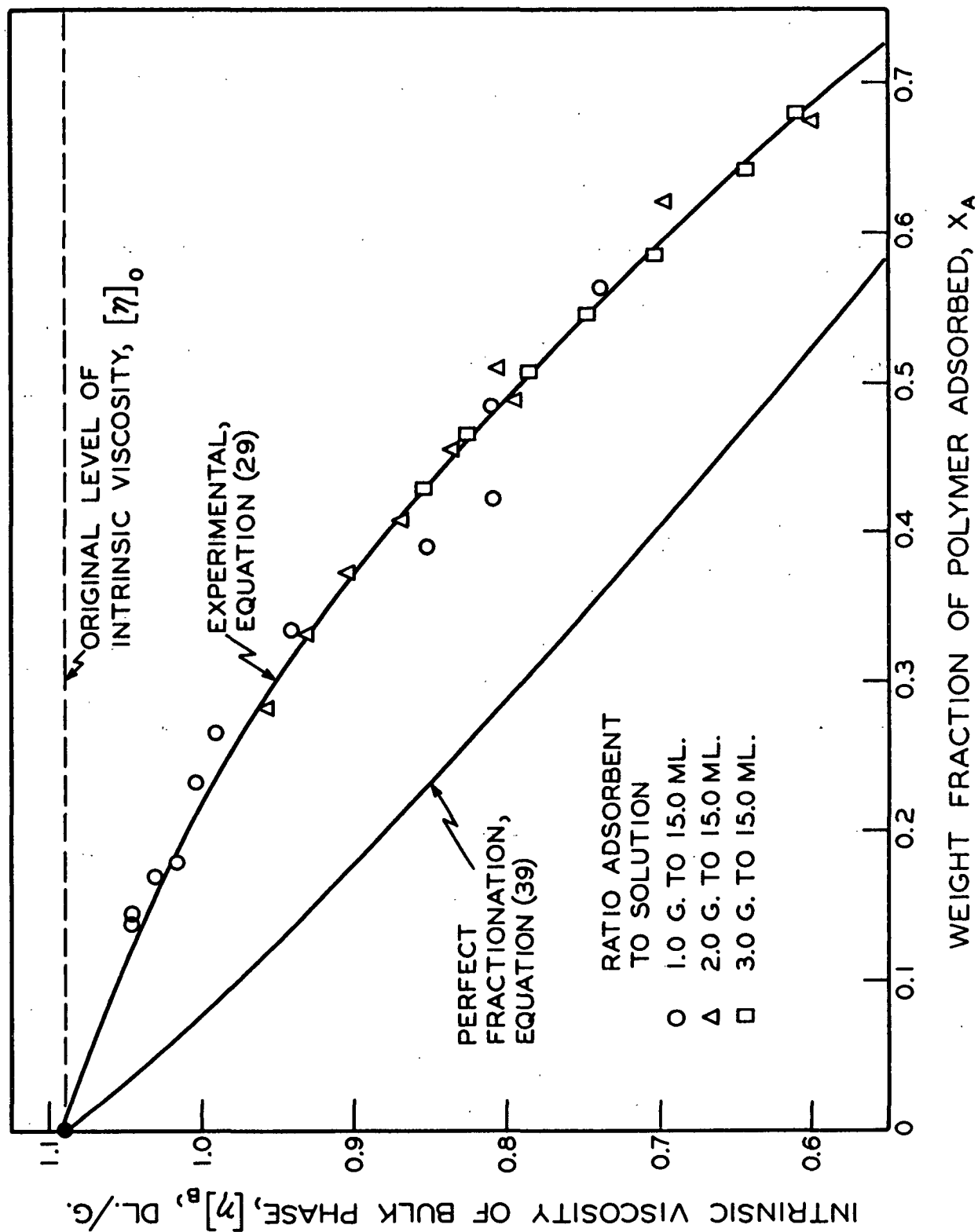


Figure 17. Equilibrium Fractionation Behavior of Polystyrene B6 in Bulk Phase (Adsorption Run No. 3S-ECB)

$$X_A = \Gamma W_a / C_o V = 1 - C/C_o \quad (28)$$

where Γ is the specific adsorption, \underline{W}_a is the weight of adsorbent, \underline{C}_o is the initial solution concentration, \underline{V} is the volume of solution, and \underline{C} is the equilibrium concentration.

The intrinsic viscosity determinations were limited to the plateau region (see Fig. 14) where solution concentrations were high enough for accurate efflux time determinations. Because of the near constancy of Γ in that region, variations in \underline{W}_a and \underline{C}_o for fixed values of $\underline{W}_a/\underline{C}_o$ and \underline{V} would not change the value of \underline{X}_A . However, it is evident from Equation (28) that such variations would change the level of \underline{C} in each case.

Experimentally, both \underline{W}_a and \underline{C}_o were varied for fixed values of \underline{V} . In effect, this produced different levels of \underline{C} at each value of \underline{X}_A . In other words, different ratios of adsorbent to solution at a fixed value of \underline{X}_A actually represent different levels of \underline{C} . Consequently, that ratio was included on all the appropriate plots to indicate the effect of \underline{C} on the quantity under investigation.

Note that the viscosity results shown in Fig. 17 depended only on the weight fraction of polymer adsorbed, irrespective of the ratio of adsorbent to solution or final equilibrium concentration. It must be emphasized that the viscosity data were limited to the region of nearly complete surface coverage, thereby limiting the validity of the observed relationship to that region.

The viscosity results shown in Fig. 17 were evaluated statistically, using a curvilinear regression with a prescribed constant term. It is obvious that the intrinsic viscosity of the bulk phase, $[\eta]_{\underline{B}}$, is equal to that of the

original solution, $[\eta]_{\underline{O}}$, when $\underline{X}_A = 0$. In that case, since $[\eta]_{\underline{O}}$ is known with more certainty than the $[\eta]_{\underline{B}}$ observations, the use of a regression with a prescribed constant term appears to be justified. The prescribed constant term forces the regression through the point $[\eta]_{\underline{O}}$ at $\underline{X}_A = 0$. From analysis of variance, it was found that the results in Fig. 17 (for the regression of $[\eta]_{\underline{B}}$ on \underline{X}_A) are best fitted by a parabolic relationship:

$$[\eta]_{\underline{B}} = 1.090 - 0.2794(\underline{X}_A) - 0.6380(\underline{X}_A)^2 \quad (29)$$

From the sum of the squares removed by regressions with and without a prescribed constant term, it was found that the restriction imposed on the curve by the prescribed constant did not alter significantly the goodness of the fit. By including the prescribed constant term the regression is more reliable in the low \underline{X}_A -range.

The order of the regression was adjudged from an analysis of the variance; the significance of each successive term was tested by the F-ratio (81). This procedure was employed throughout this work, using the 0.05 probability level as the criterion for significance.

The curves representing no fractionation and "perfect" fractionation are also included in Fig. 17. If no fractionation occurred during the adsorption process, the molecular weight distribution would remain unchanged and independent of \underline{X}_A . In this case, $[\eta]_{\underline{B}}$ would have to be constant and equal to $[\eta]_{\underline{O}}$. Hence, the straight line located at $[\eta]_{\underline{O}}$ represents the no-fractionation curve. (The perfect fractionation curve will be discussed in the next section.)

Equilibrium adsorption experiments were conducted with Polystyrene PB6 (Run no. 4S4-ECB) to substantiate the behavior shown in Fig. 17. A minimum

of four days was allowed for equilibration. The viscosity data were plotted against the weight fraction of polymer adsorbed, as shown in Fig. 18. These results clearly support the behavior originally observed for Polystyrene B6, namely that $[\eta]_{\underline{B}}$ depended only on \underline{X}_A . A curvilinear regression of $[\eta]_{\underline{B}}$ on \underline{X}_A yielded the following relationship:

$$[\eta]_{\underline{B}} = 1.070 - 0.3055(\underline{X}_A) - 0.6069(\underline{X}_A)^2 \quad (30).$$

The regression was not restricted by the inclusion of a prescribed constant term because of the data available in the low \underline{X}_A -range.

The intrinsic viscosity of the bulk phase was used to detect any polymer fractionation resulting from adsorption. Intrinsic viscosity, $[\eta]$, can be related empirically to the viscosity - average molecular weight, \overline{M}_V , by the Mark-Houwink relationship as follows:

$$[\eta] = K(\overline{M}_V)^a \quad (31)$$

where \underline{K} and \underline{a} are constants for a given polymer-solvent pair and temperature.

The viscosity - average molecular weight, unlike the fundamental number- and weight-average molecular weights, generally is not constant for a given polymer sample but varies from one solvent system to another (depending on the degree of polymolecularity and the change in magnitude of the solvent-polymer interactions) and also exhibits a slight variation with temperature (depending on how far removed from the theta temperature). In spite of these characteristics, intrinsic viscosity was superior to the use of other average molecular weight methods because of the comparative ease and precision of the determinations.

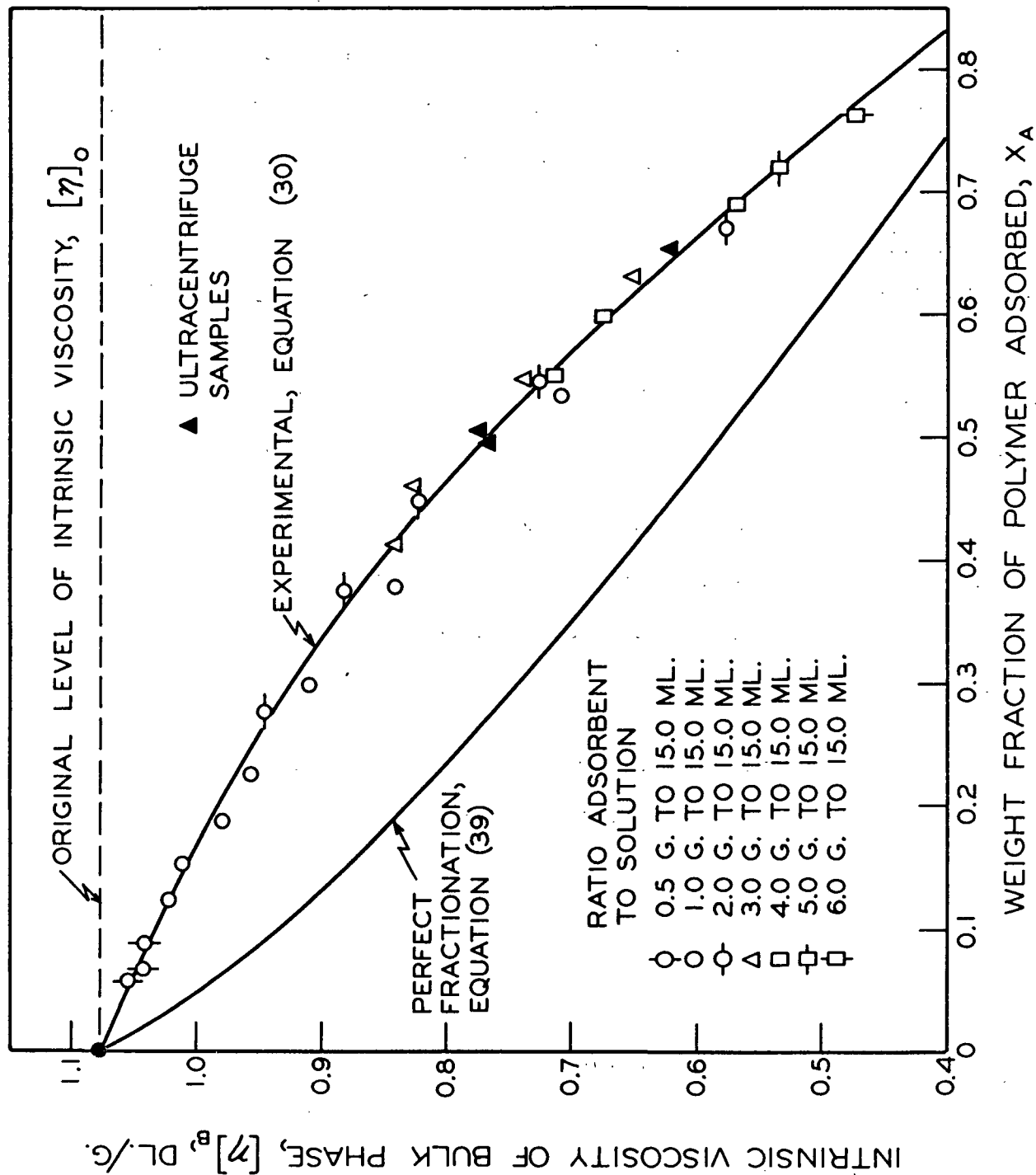


Figure 18. Equilibrium Fractionation Behavior of Polystyrene PB6 in Bulk Phase (Adsorption Run No. 4S4-ECB)

The main objection to intrinsic viscosity as a measure of fractionation is one commonly encountered wherever an average quantity is used to describe a distribution. Unless the mathematical form of the distribution is known, a single parameter (or even several parameters) is not sufficient to characterize the distribution. However, in cases where one of the tails is reduced substantially while the other remains essentially unchanged, average quantities yield valuable information about the change that has occurred.

Perfect Fractionation

The results shown in Fig. 17 and 18 indicate that the higher molecular weight species were adsorbed preferentially at equilibrium, irrespective of the weight fraction of polymer adsorbed. To judge the extent of the fractionations obtained, the "perfect fractionation" concept was employed.

For perfect fractionation, the highest molecular weight molecules in the bulk phase must be removed successively via adsorption as $\frac{X}{A}$ is increased. To obtain the perfect fractionation curve, knowledge of the complete molecular weight distribution or its equivalent is required.

Assuming that the polymer molecules are continuously distributed with respect to molecular weight, the viscosity - average molecular weight (82) can be written as:

$$M_v = \left[\frac{\int_0^{\infty} M^a f(M) dM}{\int_0^{\infty} f(M) dM} \right]^{1/a} \quad (32)$$

where $f(M)$ is the differential weight distribution function of M , the molecular weight, and a is the exponential constant in Equation (31). The differential weight distribution function is given by:

$$f(M) = dW(M)/dM \quad (33)$$

where $\underline{W}(\underline{M})$ is the integral weight distribution function. At a given molecular weight, \underline{M}_i , the integral distribution function, $\underline{W}(\underline{M}_i)$, yields the weight fraction of the sample containing all the species with molecular weights equal to or less than \underline{M}_i . The function, $\underline{f}(\underline{M})$, is normalized in the range $0 < \underline{M} < \infty$. This fact is expressed readily by the following:

$$\int_0^{\infty} f(M)dM = 1 \quad (34).$$

By combining Equations (31) and (32), one finds that

$$[\eta] = K \int_0^{\infty} M^a f(M)dM / \int_0^{\infty} f(M)dM \quad (35).$$

The above relationship can be written in terms of the distribution of sedimentation coefficient, $\underline{S}-\underline{g}(\underline{S})$, which is related to the molecular weight distribution according to (64):

$$g(S)dS = f(M)dM \quad (36)$$

where \underline{S} is the sedimentation coefficient and $\underline{g}(\underline{S})$ is the differential weight distribution function of \underline{S} . The function, $\underline{g}(\underline{S})$, is a normalized function in the range $0 < \underline{S} < \infty$. Generally, the sedimentation coefficient can be related empirically to molecular weight according to (63):

$$S = kM^b \quad (37)$$

where \underline{k} and \underline{b} are constants which depend on the solvent-polymer pair and temperature. By combining Equations (35), (36), and (37), the following is obtained:

$$[\eta] = K(k)^{-a/b} \int_0^{\infty} S^{a/b} g(S) dS / \int_0^{\infty} g(S) dS \quad (38).$$

Equation (38) permits a direct calculation of $[\eta]$ from the distribution of sedimentation coefficient when the empirical constants are known. Note that \underline{K} and \underline{a} pertain to the solvent system for which the intrinsic viscosity calculation is desired. On the other hand, \underline{k} and \underline{b} refer to the solvent system in which the distribution, $\underline{S}-\underline{g}(\underline{S})$, was determined. In other words, the distribution can be determined in one solvent and the intrinsic viscosity calculated for another.

To determine the perfect fractionation curve for the bulk phase, Equation (38) need only be integrated to the level of \underline{S} for which $[\eta]_{\underline{B}}$ is desired:

$$[\eta]_{\underline{B}i} = K(k)^{-a/b} \int_0^{\underline{S}_i} S^{a/b} g(S) dS / \int_0^{\underline{S}_i} g(S) dS \quad (39).$$

This relationship yields the value of $[\eta]_{\underline{B}}$ which the solution would exhibit if all the species with $\underline{S} \geq \underline{S}_i$ were removed from the sample (via adsorption in this case). The corresponding weight fraction of polymer adsorbed is given by:

$$X_{\underline{A}i} = \int_{\underline{S}_i}^{\infty} g(S) dS \quad (40).$$

In this way, mutually related pairs, $[\eta]_{\underline{B}i}$ and $X_{\underline{A}i}$, can be evaluated for various levels of \underline{S} , yielding the perfect fractionation curve.

The perfect fractionation curve shown in Fig. 17 was calculated with Equations (39) and (40), using the distribution of sedimentation coefficient determined by Taylor (29) for Polystyrene B6. The constants, \underline{k} and \underline{b} , were taken from the following relationship reported by McCormick (27) for the

polystyrene - cyclohexane system at 35°C.:

$$S = (1.69 \times 10^{-2})M^{0.48} \quad (41)$$

where \underline{S} is given in svedberg units (10^{-13} sec.). The constants in the Mark-Houwink equation, i.e., \underline{K} and \underline{a} , were obtained from the following relationship reported by Outer, et al. (83) for the polystyrene - dichloroethane system at 25°C.:

$$[\eta] = (2.1 \times 10^{-4})M^{0.66} \quad (42)$$

where $[\eta]$ is given in dl./g. Equation (42) was used throughout this work for calculations needed at 30°C. (It is demonstrated in Appendix I that the change in $[\eta]$ from 25 to 30°C. for the polystyrene - dichloroethane system is negligible.)

The perfect fractionation curve shown in Fig. 18 was calculated from the distribution of sedimentation coefficient for Polystyrene PB6, which is shown in Fig. 11 as the concentration-corrected distribution. The accuracy of empirical constants employed in the calculation of perfect fractionation curves is discussed in Appendix III.

Behavior in the Surface Phase

From the weight additivity of intrinsic viscosity quantities (67, 82), the intrinsic viscosity of polymer in the surface phase, $[\eta]_{\underline{A}}$, can be calculated according to:

$$[\eta]_{\underline{A}} = ([\eta]_{\underline{O}} - X_{\underline{B}}[\eta]_{\underline{B}})/X_{\underline{A}} \quad (43)$$

where

$[\eta]_{\underline{O}}$ = intrinsic viscosity of original solution

$[\eta]_{\underline{B}}$ = intrinsic viscosity of solution, i.e., the bulk phase, following adsorption

\underline{X} = weight fraction of polymer remaining in solution following adsorption

\underline{X}_A = weight fraction of polymer in the surface phase.

The above relationship is valid irrespective of the polymolecularity involved. The quantity, $[\eta]_A$, is the intrinsic viscosity that the polymer in the surface phase would exhibit if completely desorbed (with no changes in its molecular weight distribution) and redissolved in pure solvent.

Using Equation (43), the $[\eta]_A$ quantities were calculated for equilibrium Adsorption Runs no. 3S-ECB and 4S4-ECB, as shown in Fig. 19 and 20, respectively. The solid curve passing the experimental points in Fig. 19 was obtained by combining Equations (29) and (43) as follows:

$$[\eta]_A = [\eta]_0 + 0.2794(X_B) + 0.6380(X_A X_B) \quad (44).$$

This procedure was favored over a direct regression on the $[\eta]_A$ quantities because Equation (29) was guided in the low \underline{X}_A -range by the prescribed constant term, $[\eta]_0$. The solid curve passing through the experimental points in Fig. 20 was obtained from a curvilinear regression of the $[\eta]_A$ quantities on \underline{X}_A , yielding:

$$[\eta]_A = 1.495 - 0.06033(X_A) - 0.3109(X_A)^2 \quad (45).$$

The perfect fractionation curves shown in Fig. 19 and 20 for the surface phase were calculated with Equations (39) and (40), replacing the integration limits, $0 \leq \underline{S} \leq \underline{S}_1$, in the former with limits, $\underline{S}_1 \leq \underline{S} < \infty$, as follows:

$$[\eta]_{Ai} = K(k)^{-a/b} \int_{\underline{S}_1}^{\infty} \underline{S}^{a/b} g(\underline{S}) d\underline{S} / \int_{\underline{S}_1}^{\infty} g(\underline{S}) d\underline{S} \quad (46).$$

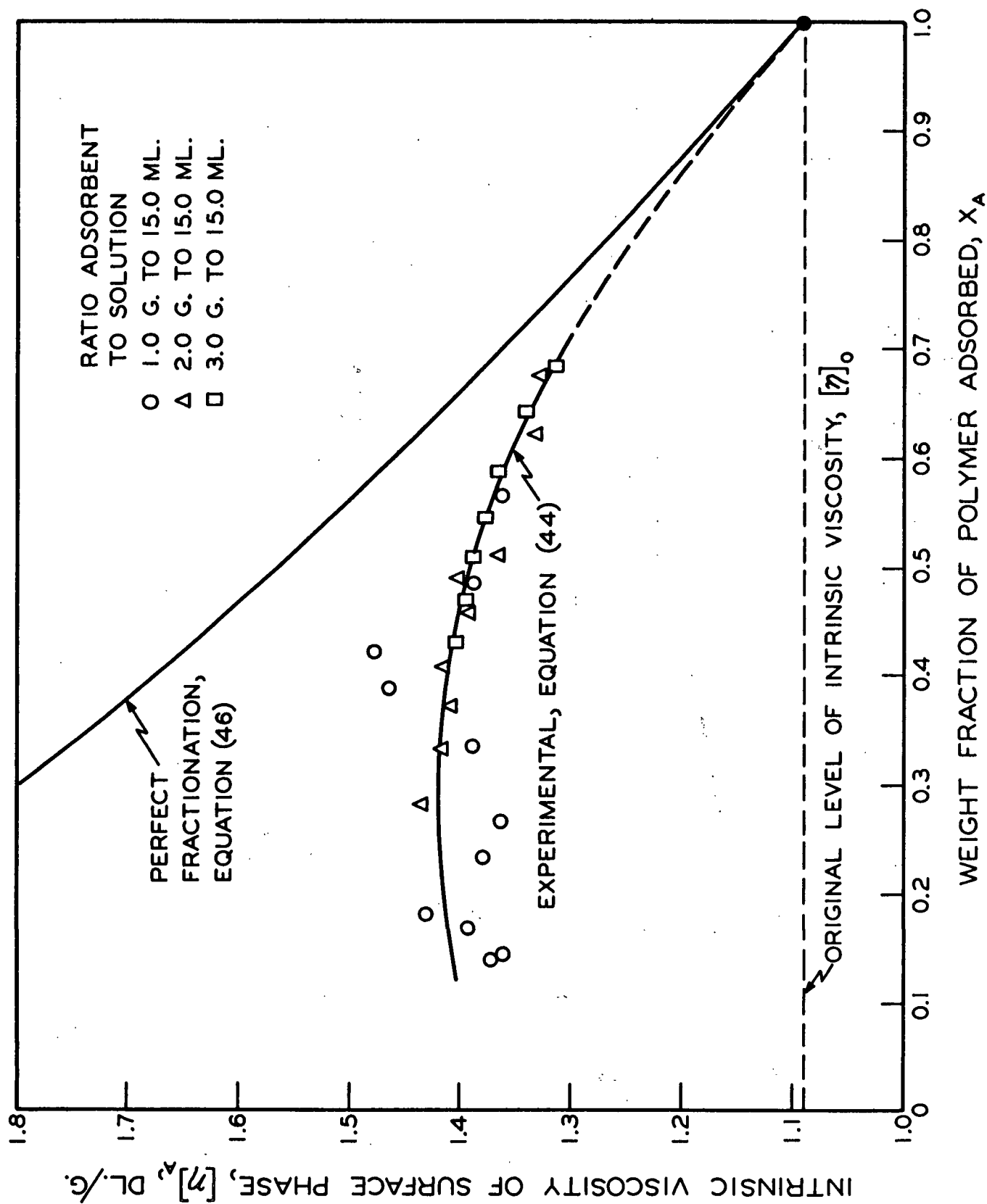


Figure 19. Equilibrium Fractionation Behavior of Polystyrene B6 in Surface Phase (Adsorption Run No. 3S-ECB)

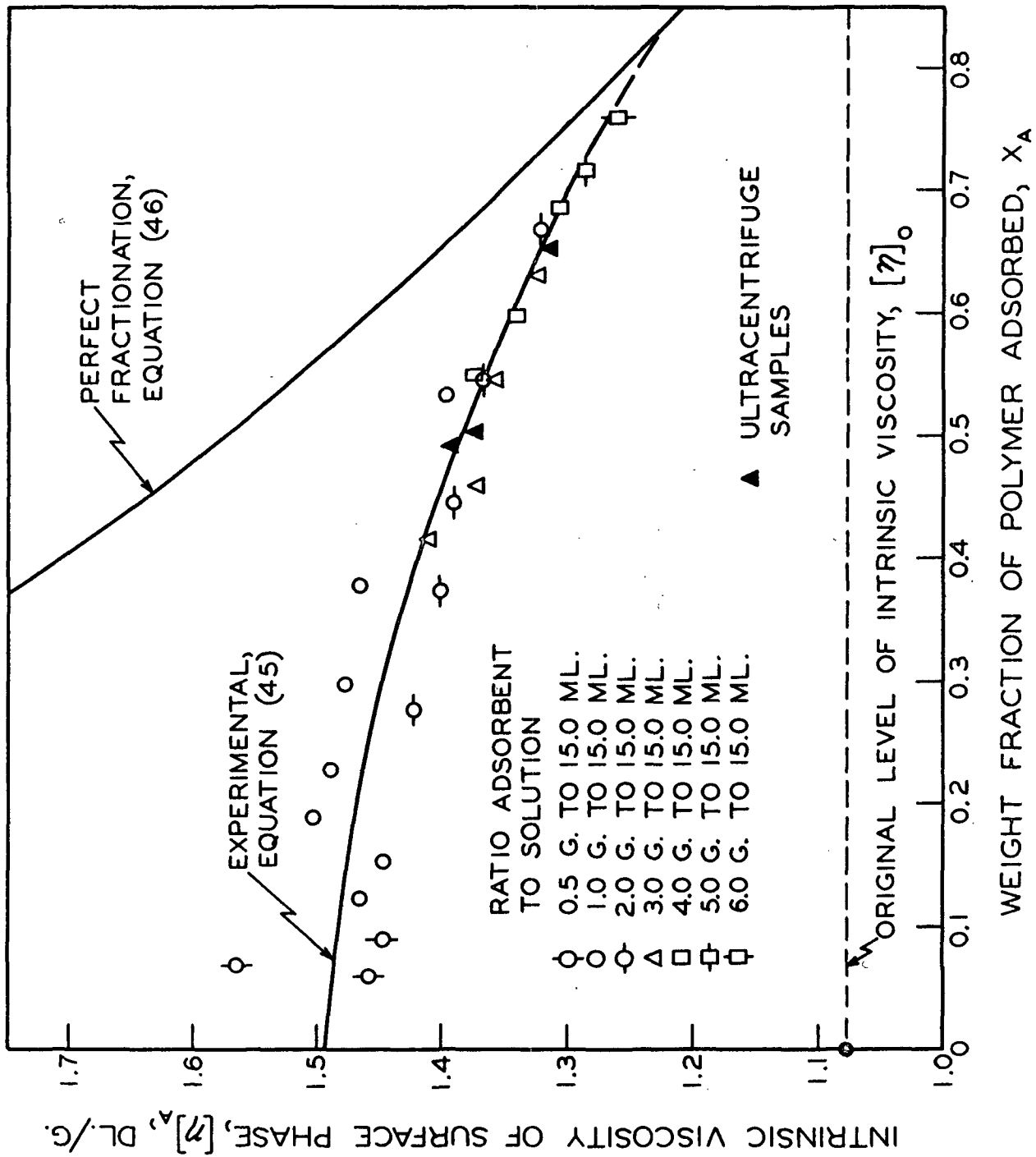


Figure 20. Equilibrium Fractionation Behavior of Polystyrene PB6 in Surface Phase (Adsorption Run No. 4S4-ECB)

Degree of Fractionation

Before discussing the fractionations obtained at equilibrium, it is necessary to define fractionation and to examine intrinsic viscosity as a measure of fractionation. The subsequent development presumes that the higher molecular weight species are adsorbed preferentially under all equilibrium conditions, in accordance with the results shown in Fig. 19 and 20.

The differential weight distribution function of molecular weight for the polymer in the original solution is given by $f_o(\underline{M})$. Following adsorption, the distribution function for the bulk phase (based on the weight of polymer originally present) can be represented by $f'_B(\underline{M})$. Since the function, $f_o(\underline{M})$, is normalized in the range $0 < \underline{M} < \infty$, the following relationships are evident:

$$\int_0^{\infty} f_o(\underline{M}) d\underline{M} = 1, \text{ and} \quad (47)$$

$$\int_0^{\infty} f'_B(\underline{M}) d\underline{M} = X_B \quad (48).$$

In order to renormalize the distribution following adsorption, X_B is employed as a common divisor over the range of species:

$$\int_0^{\infty} (f'_B(\underline{M})/X_B) d\underline{M} = \int_0^{\infty} f_B(\underline{M}) d\underline{M} = 1 \quad (49)$$

where $f_B(\underline{M})$ is the distribution function for the bulk phase following adsorption, a normalized function in the range $0 < \underline{M} < \infty$.

A quantity represented by \underline{M}_0 can be defined as the molecular weight at which the weight fraction containing all of the original species with $\underline{M} \leq \underline{M}_0$ is equal to X_B . This is readily expressed by the following:

$$\int_0^{M_0} f_0(M) dM = X_B \quad (50).$$

By comparing Equations (47) and (50), it is evident that

$$\int_{M_0}^{\infty} f_0(M) dM = X_A \quad (51).$$

For perfect fractionation, all species with $\underline{M} > \underline{M}_0$ must be adsorbed from the solution. In this case, the differential distribution functions before and after adsorption, $f_0(\underline{M})$ and $f'_{Bp}(\underline{M})$, respectively, are identical in the range $0 < \underline{M} \leq \underline{M}_0$. In the molecular weight range above \underline{M}_0 , the distribution function representing perfect fractionation for the bulk phase, $f'_{Bp}(\underline{M})$, must be zero because all of these species supposedly have been removed from the solution by adsorption.

The function, $f'_{Bp}(\underline{M})$, can be renormalized as follows:

$$\int_0^{\infty} (f'_{Bp}(M)/X_B) dM = \int_0^{\infty} f_{Bp}(M) dM = 1, \text{ and} \quad (52)$$

$$\int_0^{M_0} f_{Bp}(M) dM = 1 \quad (53)$$

where $f_{Bp}(\underline{M})$ is the normalized distribution function for the bulk phase following adsorption with perfect fractionation. Finally, the resulting molecular weight distribution functions can be represented by the curves shown in Fig. 21.

With the assumption that adsorption of higher molecular weight species is always preferred, the degree of fractionation, \underline{DF} , can be defined by the following:

$$DF = (A - A_{\min}) / (A_{\max} - A_{\min}) \quad (54)$$

where \underline{A} is the area of displacement between the distribution curves, and \underline{A}_{\max} and \underline{A}_{\min} represent the respective maximum and minimum displacement areas possible.

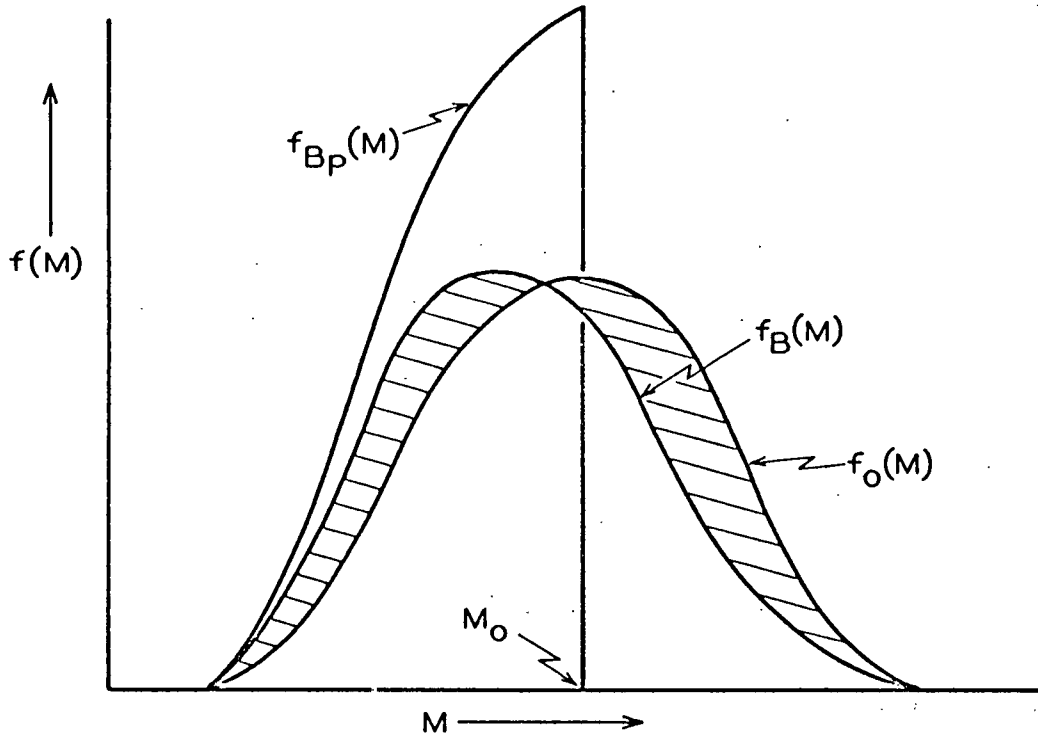


Figure 21. Normalized Molecular Weight Distributions Before and After Adsorption with Perfect and Real Fractionation

The displacement area, \underline{A} , represented by the lined section in Fig. 21, is given by:

$$A = \int_0^{\infty} |f_O(M) - f_B(M)| dM \quad (55)$$

The minimum displacement area possible, \underline{A}_{\min} , is obtained only when there is no change in the molecular weight distribution via adsorption, i.e., when $\underline{f}_B(M) = \underline{f}_O(M)$. In this case, $\underline{A} = \underline{A}_{\min} = 0$.

The maximum displacement area, A_{\max} , is obtained only when perfect fractionation occurs and is given by:

$$A_{\max} = \int_0^{\infty} \left| f_o(M) - f_{Bp}(M) \right| dM \quad (56).$$

The integral in Equation (56) can be broken up as follows:

$$A_{\max} = \int_0^{M_o} \left| f_o(M) - f_{Bp}(M) \right| dM + \int_{M_o}^{\infty} \left| f_o(M) - f_{Bp}(M) \right| dM. \quad (57).$$

From knowledge of the relationship between $f_{Bp}(M)$ and $f_o(M)$, i.e.,

$f_{Bp}(M) = f_o(M)/X_B$ for $0 < M \leq M_o$ and $f_{Bp}(M) = 0$ for $M_o \leq M < \infty$, Equation (57) can be rewritten as follows:

$$A_{\max} = (1 - X_B) \int_0^{M_o} f_{Bp}(M) dM + \int_{M_o}^{\infty} f_o(M) dM \quad (58).$$

By combining Equations (51), (53), and (58), it is seen that $A_{\max} = 2(X_A)$.

The degree of fractionation defined by Equation (54) can now be written as follows:

$$DF_B = \int_0^{\infty} \left| f_o(M) - f_B(M) \right| dM / 2(X_A) \quad (59).$$

The degree of fractionation is defined so that it ranges from zero to unity, being zero for no fractionation and unity for perfect fractionation. A DF_B of zero implies that the molecular weight distribution is unchanged by adsorption.

Equation (59) requires the molecular weight distribution for the bulk phase following adsorption, i.e., $f_B(M)$. Using a similar approach, the degree of

fractionation can be defined in terms of the molecular weight distribution in the surface phase as follows:

$$DF_A = \int_0^{\infty} \left| f_O(M) - f_A(M) \right| dM / 2(X_B) \quad (60)$$

where $f_A(M)$ is the normalized distribution function of molecular weight for the adsorbed polymer. It is easily demonstrated that Equations (59) and (60) are equivalent and yield the same DF values for a given condition.

Intrinsic Viscosity as a Measure of Fractionation

Ideally, the molecular weight distribution function following adsorption would be known for the polymer in either the bulk or surface phase. This would permit calculation of DF_A or DF_B , and the molecular weight distribution for either phase would be uniquely defined. However, the determination of molecular weight distributions is quite involved, and time considerations seriously limit the number of observations which can be made.

Since intrinsic viscosity was used as a convenient measure of fractionation, it is important to understand the nature of that information, particularly in reference to the degree of fractionation.

Any method which determines an average molecular weight (or a property which depends on some average molecular weight) involves the entire molecular weight distribution. The measured property or average is actually the result of an integration of a particular function over the entire molecular weight range (more exactly, the summation of a particular weighting function over all the species present).

The degree of fractionation defined by Equations (59) and (60) cannot be determined from average measurements; however, an alternative procedure is available, requiring only the molecular weight distribution of the original polymer and a few empirical constants.

For intrinsic viscosity methods, the degree of fractionation, \underline{DF}_v , can be defined by:

$$\underline{DF}_v = ([\eta]_o - [\eta]_B) / ([\eta]_o - [\eta]_{Bp}) \quad (61)$$

where

$[\eta]_o$ = intrinsic viscosity of the original solution

$[\eta]_B$ = intrinsic viscosity of the solution following adsorption

$[\eta]_{Bp}$ = intrinsic viscosity that the solution would exhibit if perfect fractionation had occurred for the same quantity of polymer adsorbed.

By substituting Equations (31) and (32) into Equation (61), the latter relationship can be written in a more revealing manner as follows:

$$\underline{DF}_v = \int_0^{\infty} M^2 [f_o(M) - f_B(M)] dM / \int_0^{\infty} M^2 [f_o(M) - f_{Bp}(M)] dM \quad (62).$$

Since the distribution functions are normalized in the range $0 < M < \infty$, it is apparent that the following equations are valid:

$$\begin{aligned} \int_0^{\infty} [f_o(M) - f_B(M)] dM &= 0, \text{ and} \\ \int_0^{\infty} [f_o(M) - f_{Bp}(M)] dM &= 0. \end{aligned} \quad (63)$$

By comparing Equations (62) and (63) it is evident that the degree of fractionation obtained from an averaging method (viscometry, osmometry, light scattering, etc.) relies on a weighting function to reveal any changes in the molecular weight distribution. For viscometry and light scattering, the respective weighting functions are \underline{M}^a and \underline{M} . The situation is more complex for osmometry, but the effective weighting function is \underline{M}^{-1} . The degree of fractionation determined by an averaging method is strongly biased by the weighting function.

The degree of fractionation defined by Equations (59) and (60) uses a weighting function of unity; each increment of molecular weight is weighted only according to its weight fraction, making a much more preferable definition. The viscosity degree of fractionation, \underline{DF}_v , is quite sensitive to fractionation of higher molecular weight species but to a lesser extent than that obtained from light scattering, depending on the magnitude of \underline{a} . The degree of fractionation which can be determined from osmotic measurements probably would be unacceptable for these studies; this quantity would be extremely sensitive to fractionation of lower molecular weight species. In addition to the convenience and precision offered by viscometry, its weighting function is preferable to those of osmometry and light scattering.

The degree of fractionation determined by viscosity also can be defined in terms of the surface phase as follows:

$$\underline{DF}_v = ([\eta]_A - [\eta]_o) / ([\eta]_{Ap} - [\eta]_o) \quad (64)$$

where $[\eta]_A$ is the intrinsic viscosity of polymer in the surface phase, and $[\eta]_{Ap}$ is the intrinsic viscosity that the polymer in the surface phase would possess if perfect fractionation had occurred for the same quantity of polymer adsorbed. It is demonstrated easily that Equations (61) and (64) are equivalent

and that the resulting $\underline{DF}_{\underline{v}}$ values are identical irrespective of the phase employed.

The $\underline{DF}_{\underline{v}}$ values were determined for Adsorption Runs no. 3S-ECB and 4S4-ECB using Equations (61) and (64) and are shown in Fig. 22. (Some additional results included in this figure will be discussed later.) Values of $[\eta]_{\underline{Bp}}$ and $[\eta]_{\underline{Ap}}$ needed in these calculations were determined previously with Equations (39) and (46) in connection with the perfect fractionation curves.

Summary

The polystyrene - dichloroethane - carbon black adsorption system employed in this work exhibited Langmuir behavior over nearly four decades of concentration and for a wide range of surface coverage. The polymer was strongly adsorbed in the system, nearly saturating the adsorbent surfaces at solution concentrations as low as 0.05% by weight.

The polystyrene samples employed in this portion of the work were of broad molecular weight distribution and were fractionated significantly by the adsorption process, the higher molecular weight species being preferentially adsorbed for all the equilibrium conditions investigated. Both the fractionation and preferential adsorption were adjudged by intrinsic viscosity methods.

The intrinsic viscosity and degree of fractionation at equilibrium depended only on the weight fraction of polymer adsorbed. The viscometric results were limited, however, to the region of nearly complete surface coverage because of the strong affinity of polymer for the adsorbent surfaces. The surface coverage was in excess of 85% for equilibrium solution concentrations of only 0.02% polystyrene by weight.

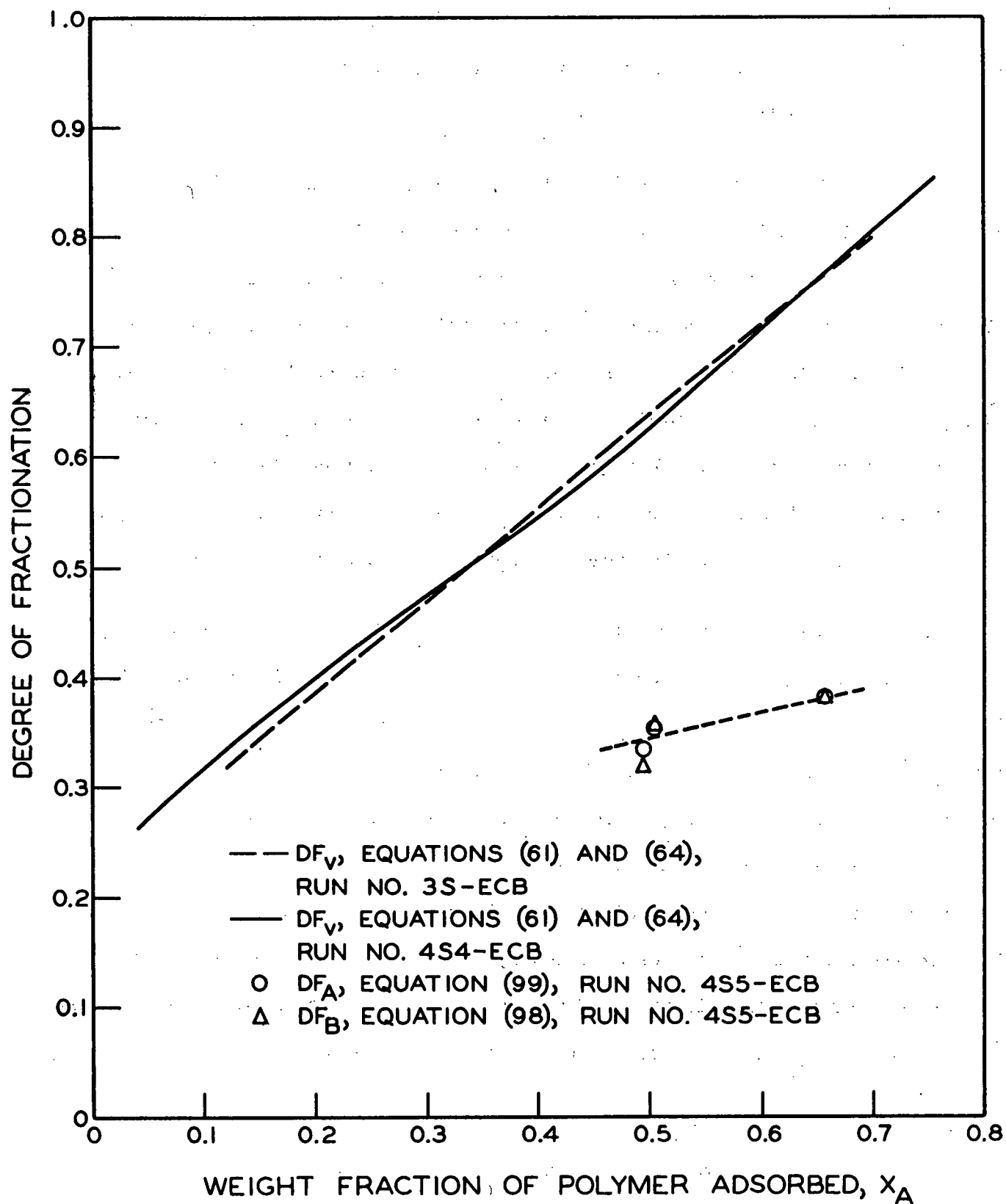


Figure 22. Effect of the Weight Fraction of Polymer Adsorbed on the Degree of Fractionation

The fact that the adsorption and fractionation results are independent of the ratio of adsorbent to solution indicates that the adsorbent was dispersed readily in the solutions and that a consistent fraction of the surface area was available for adsorption.

The degree of fractionation determined by intrinsic viscosity methods, i.e., $\underline{\underline{DF}}_{\underline{\underline{v}}}$, exhibited a nearly linear relationship with the weight fraction of polymer adsorbed. The $\underline{\underline{DF}}_{\underline{\underline{v}}}$ results should not be associated with the fractionation efficiency of the adsorption process, because this quantity is strongly biased by the weighting function and is thereby strongly influenced by any fractionation of higher molecular weight species. The $\underline{\underline{DF}}_{\underline{\underline{v}}}$ results shown in Fig. 22 indicate that the higher molecular weight species were essentially completely adsorbed at high levels of $\underline{\underline{X}}_{\underline{\underline{A}}}$. At lower levels of $\underline{\underline{X}}_{\underline{\underline{A}}}$, the higher molecular weight species were preferentially adsorbed but were not depleted to a significant extent.

The intrinsic viscosity results, i.e., $[\eta]$ and $\underline{\underline{DF}}_{\underline{\underline{v}}}$, depended only on the weight fraction of polymer adsorbed, irrespective of the solution concentrations involved. In the region of low $\underline{\underline{X}}_{\underline{\underline{A}}}$, the ratio of polymer in the bulk phase to that in the surface phase was quite high, yielding large excesses of adsorbable species. In this region, $[\eta]_{\underline{\underline{A}}}$ increased only slowly with increased excesses of adsorbable species even though the limiting values, i.e., the values given by the perfect fractionation curve, increased sharply. This behavior suggests that the bulk phase contained an excess of nearly all the species originally present and that the distribution in the surface phase had become fairly well established at low values of $\underline{\underline{X}}_{\underline{\underline{A}}}$, changing very little with further excesses.

This point is made clearer by observing the intrinsic viscosity as a function of the weight ratio of polymer to adsorbent, as shown in Fig. 23 and 24

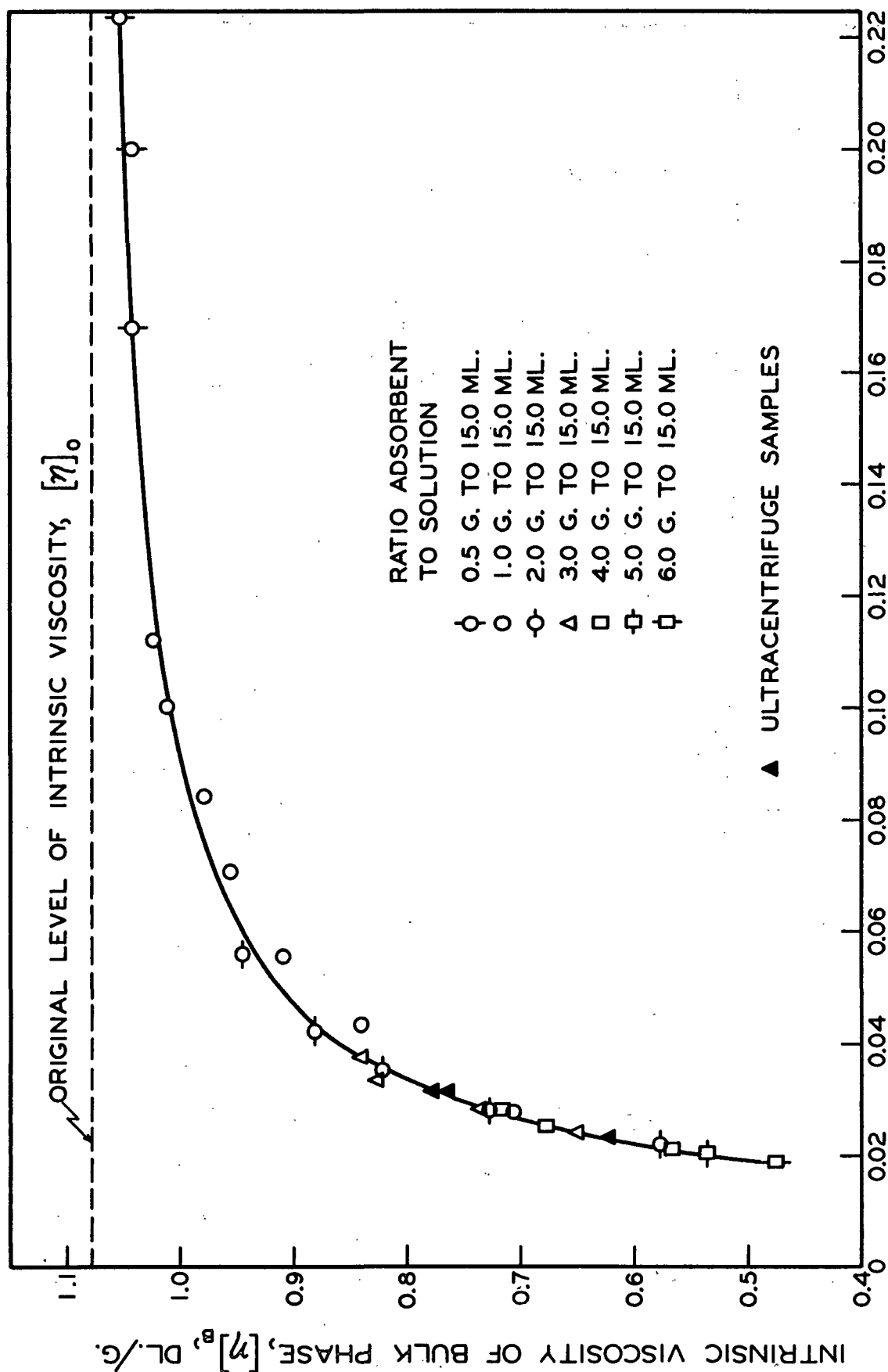


Figure 23. Equilibrium Fractionation Behavior of Polystyrene PB6 in Bulk Phase (Adsorption Run No. 4S4-ECB)

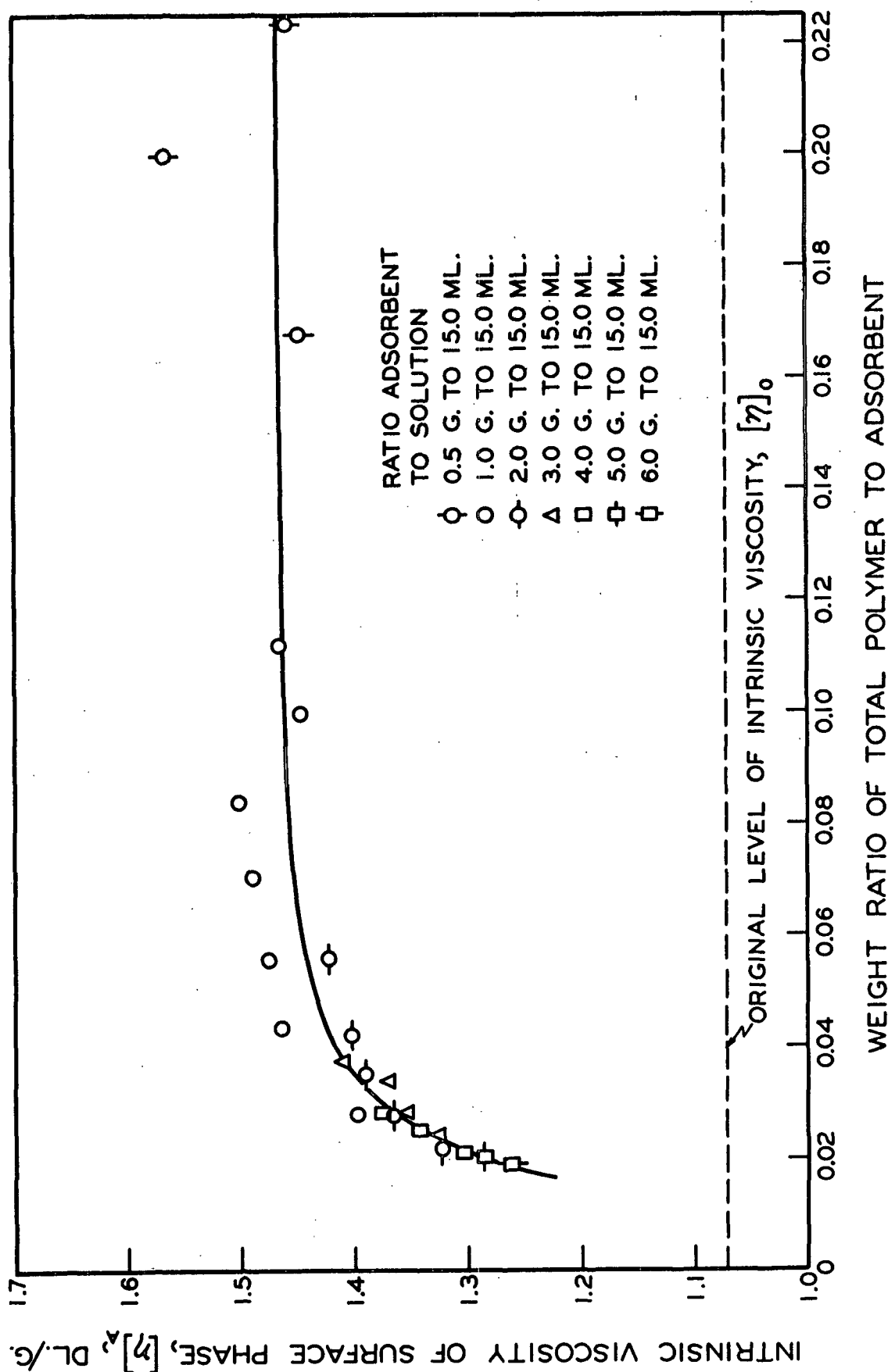


Figure 24. Equilibrium Fractionation Behavior of Polystyrene PB6 in Surface Phase (Adsorption Run No. 4S4-ECB)

for the bulk and surface phases, respectively. Note that $[\eta]_A$ was fairly constant above a certain ratio of polymer to adsorbent and changed very little beyond that point regardless of the excess of species available for adsorption. It appears that the distribution in the surface phase had become fairly well established at that point and, thereafter, remained nearly independent of further excesses.

This interpretation of the adsorption process, based entirely on the response of viscometric quantities, must be regarded as tentative. In order to explore the fractionation behavior more fully, complete distributions were determined before and after adsorption.

SEDIMENTATION VELOCITY STUDIES

Experimental

In preparing samples for sedimentation velocity studies, the adsorption work (Run no. 4S5-ECB) was conducted in 1,2-dichloroethane with Polystyrene PB6, allowing four days for equilibration. Each adsorption tube contained 25.0 ml. of solution, and the shaker speed and angle were fixed at 24.0 r.p.m. and 15°, respectively. Following equilibration, the tubes were centrifuged and the supernatant solutions were filtered to remove the adsorbent. A portion of the adsorption solution was used for a one-point intrinsic viscosity determination at 30°C.

The adsorption work was carried out in 1,2-dichloroethane at 25°C. whereas the sedimentation velocity experiments were performed in cyclohexane at 35°C. Caution was taken to prevent changes in the molecular weight distributions following adsorption.

Sedimentation Coefficient Distributions

Distributions of sedimentation coefficient were determined for Polystyrene PB6 before and after adsorption had occurred and were corrected for the effects of diffusion and concentration. The distribution shown in Fig. 11 for Polystyrene PB6 is the original distribution, and its differential weight distribution function is represented by $\underline{g}_0(\underline{S})$.

Distributions for the bulk phase were determined from three samples for which equilibrium adsorption had occurred. The adsorption data for these samples are given in Table XV. The intrinsic viscosity of each sample was plotted in Fig. 18, 20, and 23 to illustrate the relationship between the samples and Adsorption Run no. 4S4-ECB (Polystyrene PB6 in both cases).

TABLE XV

RESULTS OF ADSORPTION RUN NO. 4S5-ECB FOR SAMPLES
EMPLOYED IN SEDIMENTATION VELOCITY STUDIES

Sample	Adsorbent ^a Weight, g.	Initial Concentration ^b , %	Equilibrium ^b Concentration ^b , %	\underline{X}_A
3	8.200	0.5990	0.2070	0.654
4	3.760	0.3761	0.1909	0.493
5	6.000	0.5990	0.2975	0.503

Sample	$[\eta]$, dl./g. ^c	Weight Polymer Adsorbed, mg.	Γ , mg./g.
3	0.624	122.1	14.9
4	0.769	57.7	15.3
5	0.776	93.9	15.7

^aFurnace-treated FT-D4 graphitized carbon black.

^bWeight per cent of Polystyrene PB6 in 1,2-dichloroethane.

^cIntrinsic viscosity in 1,2-dichloroethane at 30°C. compared with original level of 1.078 dl./g.

The distribution of polymer in the surface phase can be determined from knowledge of the bulk phase distributions before and after adsorption has taken place. It can be demonstrated from a material balance that the differential weight distribution function of sedimentation coefficient for the surface phase, i.e., $\underline{g}_A(\underline{S})$, is given by the following:

$$g_A(S_i) = [g_O(S_i) - X_B g_B(S_i)] / \int_0^{\infty} [g_O(S) - X_B g_B(S)] dS \quad (65)$$

where $\underline{g}_B(\underline{S})$ is the distribution function for the bulk phase.

The distribution functions for the surface phase were calculated with Equation (65) and are compared with the bulk phase distributions in Fig. 25, 26, and 27 for Samples 3, 4, and 5, respectively. Some smoothing of the resulting surface-phase distributions was necessary, particularly in regions where the first derivatives of either the original or bulk phase distribution were rather high, and is indicated by broken lines in the figures.

Two determinations of the sedimentation coefficient distribution were made for the original polystyrene, using Samples 100 and 101. Since the diffusion extrapolations were considerably better for Sample 101, the distribution function obtained from that sample was used in Equation (65) to calculate the surface-phase distributions.

Distributions of sedimentation coefficient can be transformed to molecular weight distributions if the relationship between the sedimentation coefficient and molecular weight is known. Equations (36) and (37) can be combined to obtain the differential weight distribution function of molecular weight:

$$f(M) = b(k)^{1/b} \left[S^{(b-1)/b} \right] g(S) \quad (66).$$

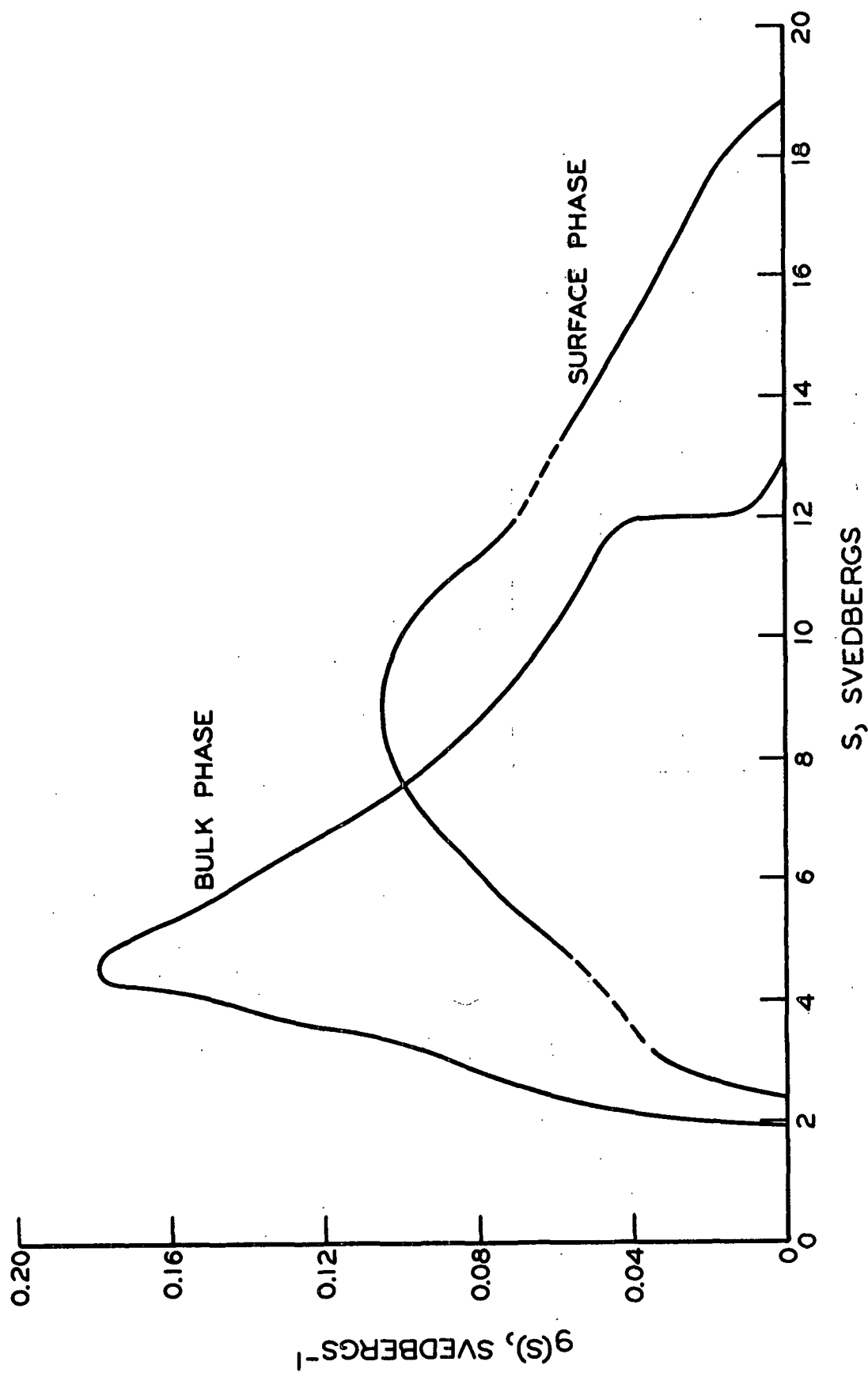


Figure 25. Normalized Distributions of Sedimentation Coefficient for Polystyrene PB6 Following Equilibrium Adsorption (Sample 3)

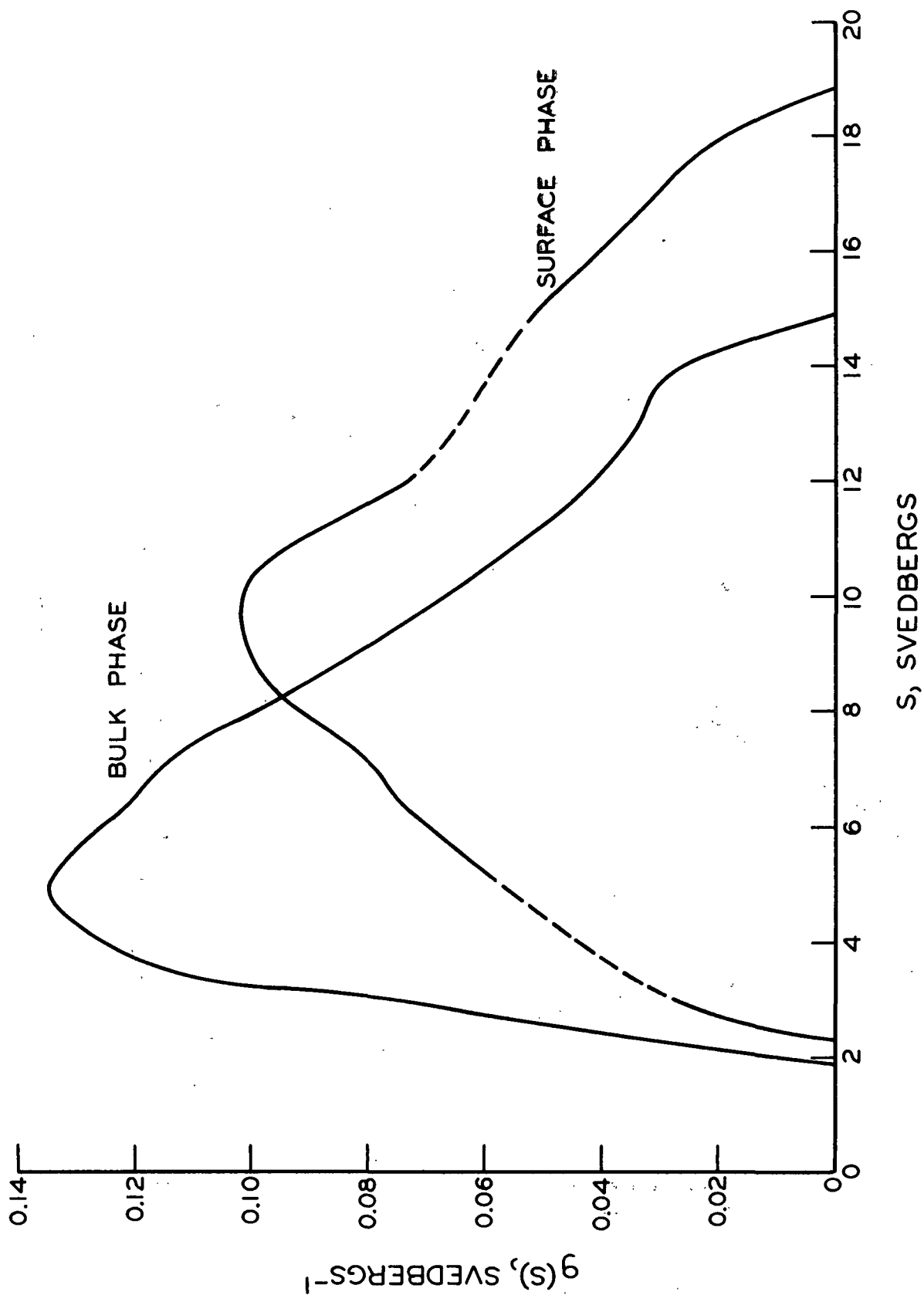


Figure 26. Normalized Distributions of Sedimentation Coefficient for Polystyrene PB6 Following Equilibrium Adsorption (Sample 4)

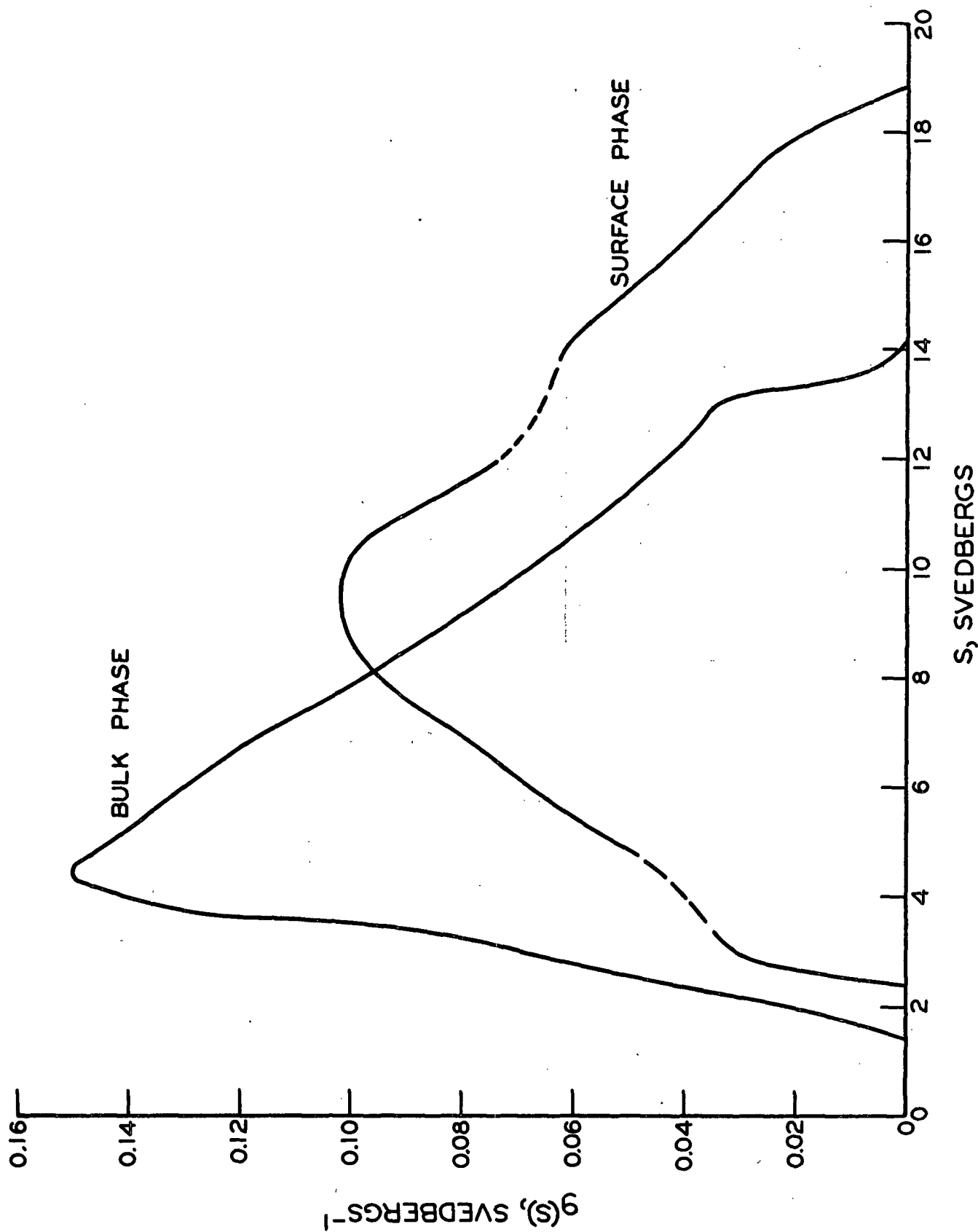


Figure 27. Normalized Distributions of Sedimentation Coefficient for Polystyrene PB6 Following Equilibrium Adsorption (Sample 5)

The molecular weight is obtained readily from Equation (37):

$$M = (S/k)^{1/b} \quad (67).$$

Using Equations (66) and (67), the molecular weight distributions were calculated for the original polymer (Polystyrene PB6) and for the polymer in the corresponding bulk and surface phases for $\underline{X_A} = 0.493$ (Sample 4), as shown in Fig. 28.

The defining equations for the number-, weight-, and z-average molecular weights are given, respectively, as follows:

$$\overline{M_n} = \int_0^{\infty} f(M) dM / \int_0^{\infty} [f(M)/M] dM \quad (68),$$

$$\overline{M_w} = \int_0^{\infty} M f(M) dM / \int_0^{\infty} f(M) dM, \text{ and} \quad (69)$$

$$\overline{M_z} = \int_0^{\infty} M^2 f(M) dM / \int_0^{\infty} M f(M) dM \quad (70).$$

By combining Equations (36) and (67) with Equations (68), (69), and (70), the defining relationships for the molecular weight averages can be written in terms of the sedimentation coefficient distribution as follows:

$$\overline{M_n} = k^{-1/b} \int_0^{\infty} g(S) dS / \int_0^{\infty} S^{-1/b} g(S) dS \quad (71),$$

$$\overline{M_w} = k^{-1/b} \int_0^{\infty} S^{1/b} g(S) dS / \int_0^{\infty} g(S) dS, \text{ and} \quad (72)$$

$$\overline{M_z} = k^{-1/b} \int_0^{\infty} S^{2/b} g(S) dS / \int_0^{\infty} S^{1/b} g(S) dS \quad (73).$$

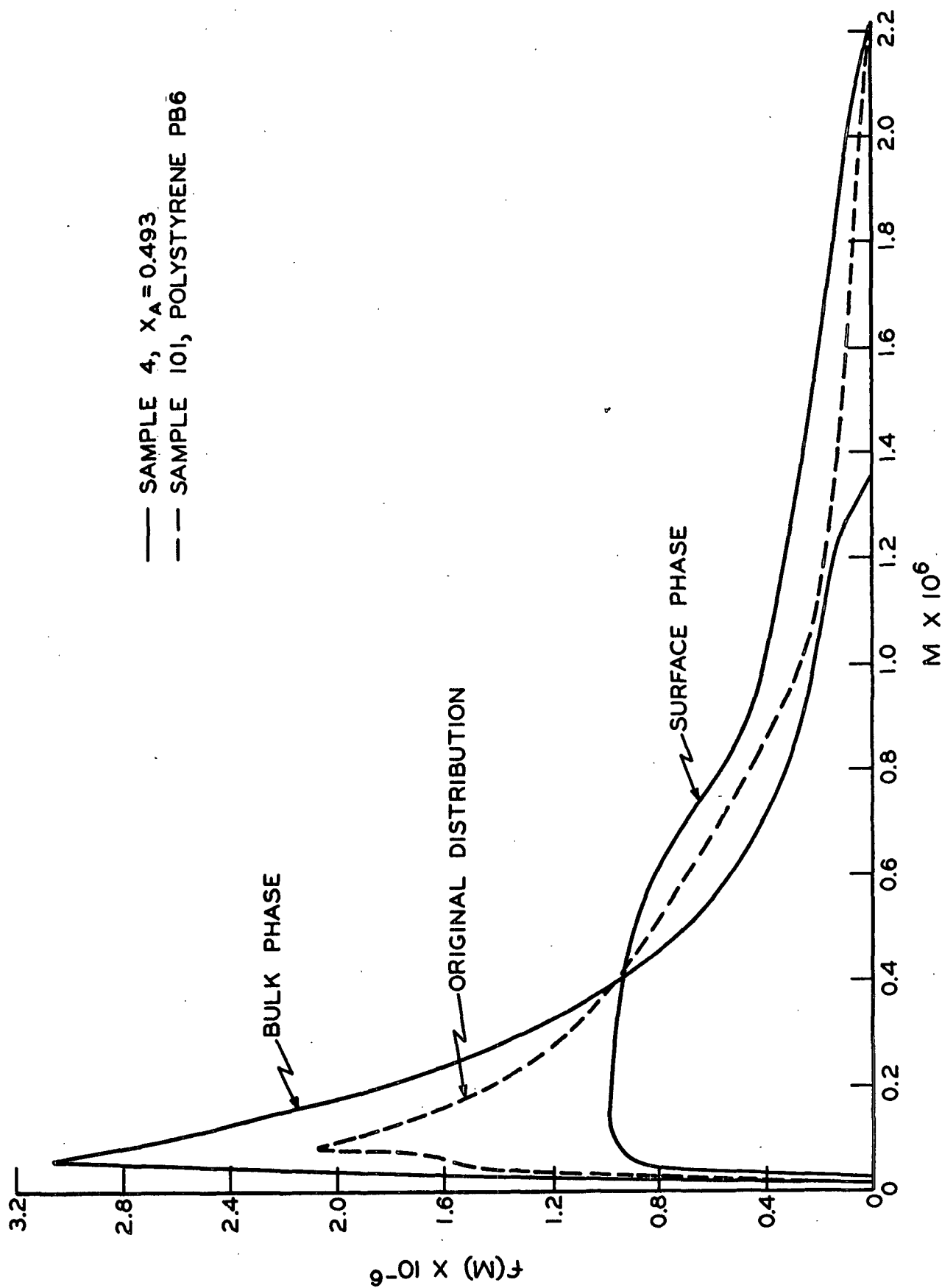


Figure 28. Normalized Distributions of Molecular Weight for Polystyrene PB6 Before and After Adsorption

Using the above relationships, the average molecular weights were calculated for each of the distributions and are shown in Table XVI along with the first and second moments. The first and second moments, \overline{S}_1 and \overline{S}_2 , respectively, are defined as follows:

$$\overline{S}_1 = \int_0^{\infty} Sg(S)dS / \int_0^{\infty} g(S)dS, \text{ and} \quad (74)$$

$$\overline{S}_2 = \left[\int_0^{\infty} S^2 g(S)dS / \int_0^{\infty} g(S)dS \right]^{1/2} \quad (75).$$

Note that each of the molecular weight averages for corresponding bulk and surface phases (Table XVI) differ by approximately a factor of two. That difference was anticipated, of course, from the intrinsic viscosity results.

Molecular weight distributions determined by sedimentation velocity analysis compare favorably with determinations by other methods. Using the system employed in the present study, i.e., polystyrene in cyclohexane at 35°C., Cantow (68) found that distributions obtained from sedimentation velocity and fractional precipitation methods were in excellent agreement. McCormick (27) demonstrated that mixtures of narrow polystyrene fractions in cyclohexane at 35°C. can be separated almost completely by sedimentation. A more severe test of the sedimentation velocity method was provided recently. Using a synthetic mixture of high and low molecular weight fractions of polyethylene in α -bromonaphthalene at 110°C., McCormick (84) found that distributions obtained from sedimentation velocity and fractional precipitation methods were in good agreement.

TABLE XVI

SEDIMENTATION COEFFICIENT MOMENTS AND MOLECULAR WEIGHT
AVERAGES CALCULATED FROM SEDIMENTATION COEFFICIENT DISTRIBUTIONS

Sample	Description of Distribution	\overline{S}_1 , svedbergs	\overline{S}_2 , svedbergs	$\overline{M} \times 10^{-5}$ \overline{M}_n	$\overline{M} \times 10^{-5}$ \overline{M}_w	$\overline{M} \times 10^{-5}$ \overline{M}_z
101	Original	8.49	9.24	2.11	5.12	8.83
100	Original	8.45	9.10	2.32	4.96	7.99
3	Bulk phase	6.36	6.83	1.33	2.72	4.40
3	Surface phase	9.61	10.28	3.00	6.37	9.85
4	Bulk phase	7.12	7.72	1.58	3.52	5.98
4	Surface phase	9.98	10.66	3.16	6.88	10.43
5	Bulk phase	6.89	7.43	1.47	3.25	5.34
5	Surface phase	10.03	10.70	3.22	6.94	10.44

Concentration Dependence of the Fractionation Process

Samples 4 and 5 (Table XV) had nearly the same weight fractions of polymer adsorbed (and like ratios of polymer to adsorbent) but differed in their final equilibrium concentrations. Intrinsic viscosity studies had indicated that solution concentration probably was not important in the fractionation process; however, those studies were limited to average measurements, and the actual behavior of the distributions was not established. It was believed that the resulting distributions were not affected by concentration but depended only on the weight fraction of polymer adsorbed. Although the concentration range represented by Samples 4 and 5 is limited, the surface-phase distributions compared in Fig. 29 indicate that solution concentration did not affect the fractionation process significantly. The surface-phase distributions were chosen for the comparison rather than the bulk-phase distributions because the former appeared to be less sensitive to small differences in \underline{X}_A , as indicated by intrinsic viscosity studies. (This was particularly true in the region $\underline{X}_A = 0.5$, as seen in Fig. 18 and 20.)

The distributions shown in Fig. 29 also demonstrate the excellent reproducibility of the sedimentation velocity method. In spite of high reproducibility, irregularities present in the distribution curves probably are not accurate, i.e., do not represent actual fluctuations in the polymer distributions, because these curves reflect any irregularities or errors present in the original distribution as well as their respective bulk-phase distributions.

Partitioning of Polymer Homologs Between the Bulk and Surface Phases

Because of the similarities in phase separation in polymer solutions and polymer adsorption, the fractionation results were compared with the well-known behavior encountered in phase separation.

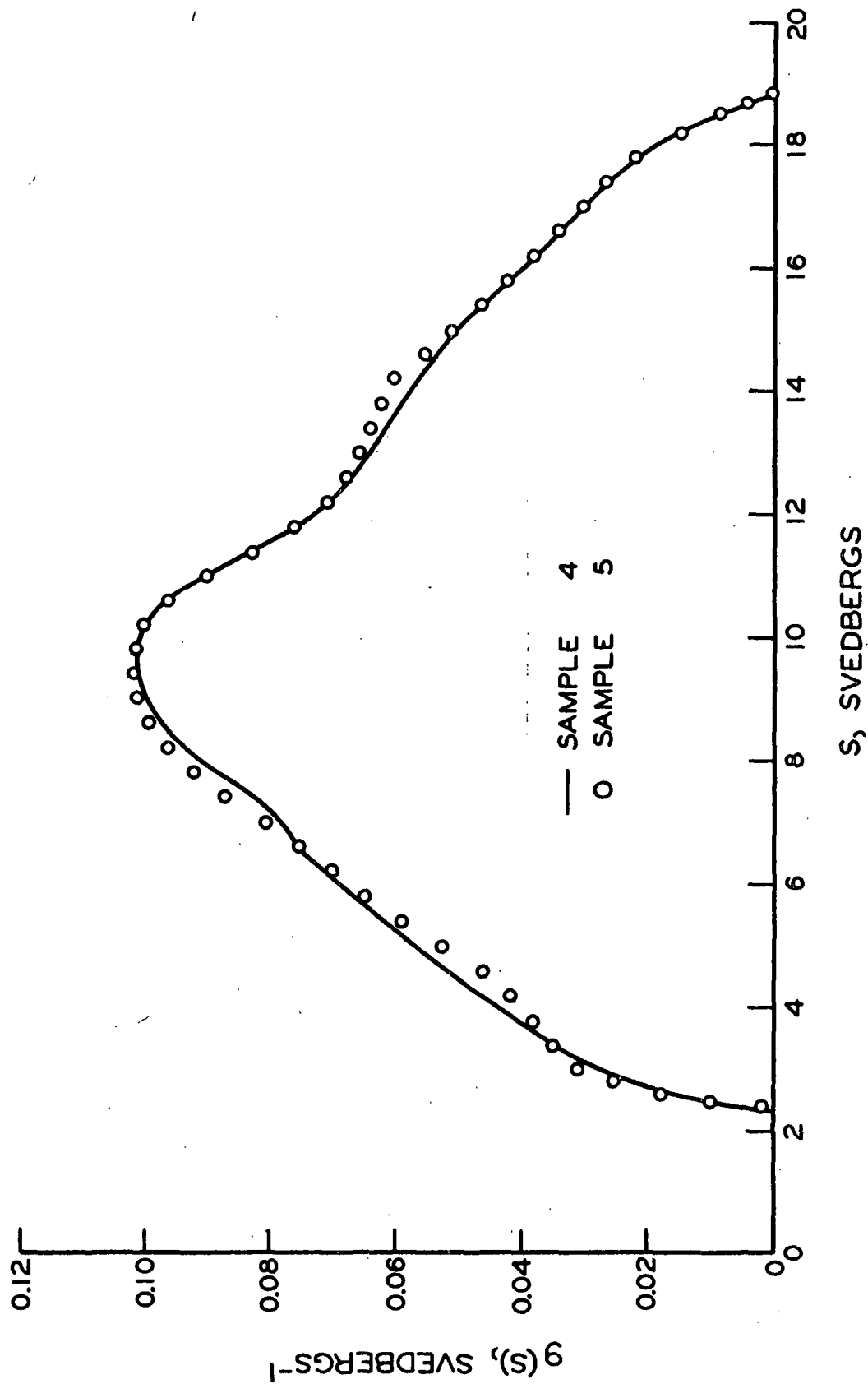


Figure 29. Comparison of Surface Phase Distributions for Two Samples of Different Equilibrium Concentration and Nearly Identical Weight Fractions of Polymer Adsorbed

The fractionation obtained in phase separation (67) is described by:

$$\ln(v'_x/v_x) = \sigma x \quad (76)$$

where

- \underline{x} = degree of polymerization (D.P.)
- $\frac{v'_x}{\underline{x}}$ = volume fraction of the "precipitated" or concentrated phase occupied by polymer of D.P. = \underline{x}
- $\frac{v_x}{\underline{x}}$ = volume fraction of the dilute phase occupied by polymer of D.P. = \underline{x}
- σ = a constant dependent on the volume fraction of polymer and the number-average molecular weight in each of the two phases and on the interaction between the solvent and polymer homologs.

Assuming that the partial specific volume of the polymer is independent of concentration and molecular weight, Equation (76) can be written as:

$$\ln(W'_x/W_x) = \sigma x + \ln(R) \quad (77)$$

where

- $\frac{W'_x}{\underline{x}}$ = weight of species of D.P. = \underline{x} in the concentrated phase
- $\frac{W_x}{\underline{x}}$ = weight of species of D.P. = \underline{x} in the dilute phase
- \underline{R} = ratio of total volume of concentrated phase to total volume of dilute phase.

Assuming that the polymer molecules are continuously distributed with respect to molecular weight, the weight ratio, $\frac{W'_x}{W_x}$, for the adsorption system is given by the following:

$$\frac{W'_x}{W_x} = \frac{X_A f_A(M)}{X_B f_B(M)} \quad (78).$$

Since distribution functions of molecular weight and sedimentation coefficient are related by Equation (36), it is evident that ratios of the distribution functions are related by the following:

$$f_A(M)/f_B(M) = g_A(S)/g_B(S) \quad (79).$$

The corresponding value of \underline{x} can be obtained from Equation (67) as follows:

$$x = [(S/k)^{1/b}]/m_o \quad (80)$$

where \underline{m}_o is the molecular weight of a mer ($\underline{m}_o = 104.14$ for polystyrene). Investigation of these variables revealed the relationships shown in Fig. 30. The partitioning of species between the bulk and surface phases was described by the following equation:

$$\ln[X_A f_A(M)/X_B f_B(M)] = B[\ln(x)] + \ln(I) \quad (81)$$

where \underline{B} and \underline{I} are constants for a given equilibrium condition.

Earlier studies indicated that the fractionation behavior depended only on the weight fraction of polymer adsorbed, being independent of solution concentration. Consequently, it is anticipated that the constants, \underline{B} and \underline{I} , for a given system depend only on \underline{X}_A .

Other functional relationships were investigated for the partitioning behavior, and equally good regressions were obtained for the following:

$$\ln[g_A(S)/g_B(S)] = B[\ln(x)] + \ln(I), \text{ and} \quad (82)$$

$$\ln[g_A(S)/g_B(S)] = B[\ln(S)] + \ln(I) \quad (83).$$

The results of the partitioning regressions are summarized in Table XVII.

Note that the slopes can be reduced to a constant for each regression by the factor, $(1/\underline{X}_A)$. On this basis, the general equation describing the partitioning behavior can be written as follows:

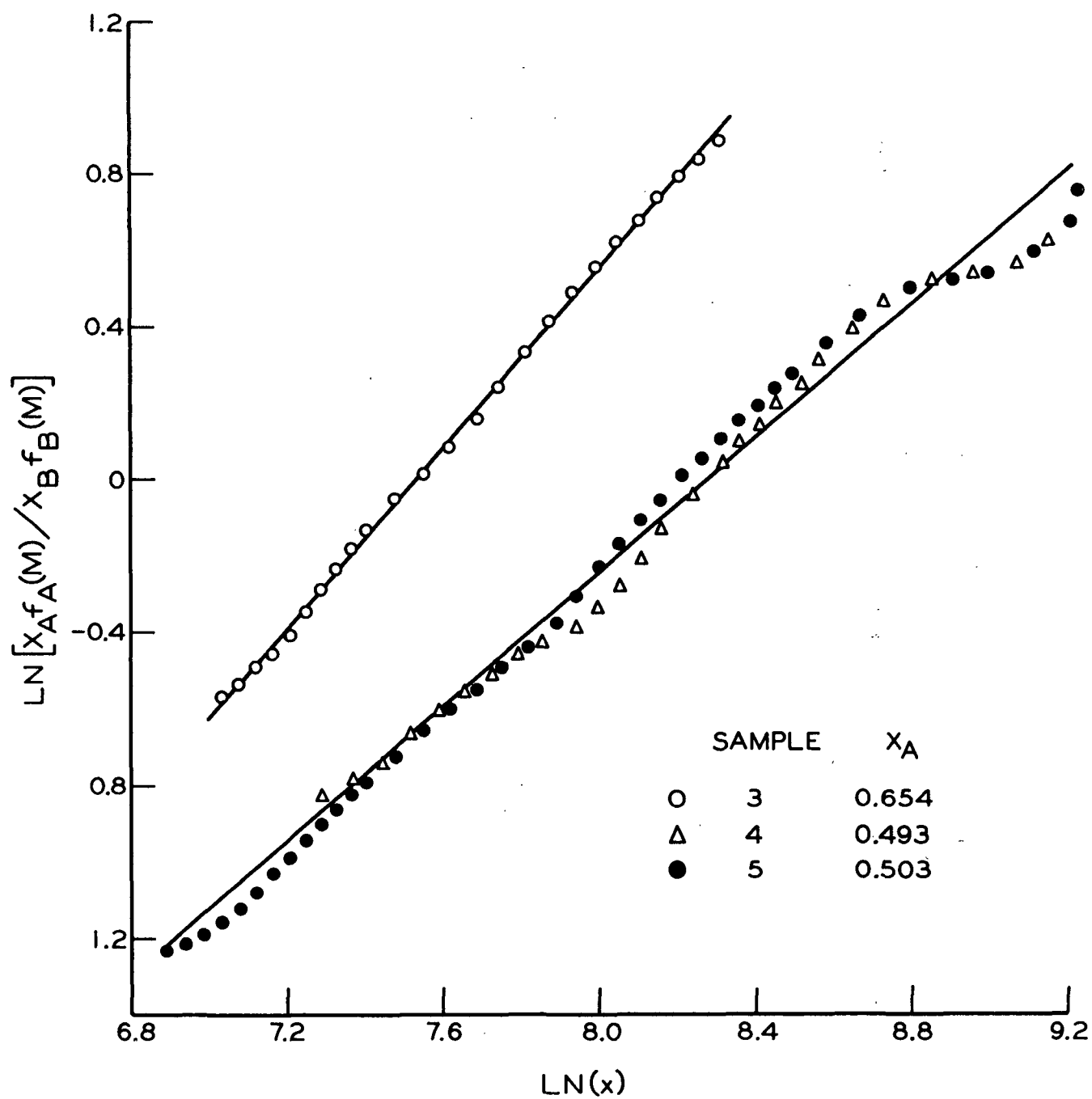


Figure 30. Partitioning of Polystyrene PB6 Homologs Between the Bulk and Surface Phases

TABLE XVII

REGRESSION RESULTS FOR THE PARTITIONING RELATIONSHIPS

Dependent Variable	Independent Variable	Sample	Slope, \underline{B}	Intercept, $\ln[\underline{I}(\underline{x})]$	$(\underline{B}/\underline{x})$	Correlation Coefficient
$\ln[\underline{x}_A^f(\underline{M})/\underline{x}_B^f(\underline{M})]$	$\ln(\underline{x})$	3	1.167	-8.792	1.783	0.9994
		4	0.8502	-7.064	1.726	0.9903
		5	0.8701	-7.212	1.729	0.9918
$\ln[\underline{g}_A(\underline{s})/\underline{g}_B(\underline{s})]$	$\ln(\underline{x})$	3	1.167	-9.430	1.783	0.9993
		4	0.8503	-7.034	1.727	0.9903
		5	0.8701	-7.225	1.729	0.9918
$\ln[\underline{g}_A(\underline{s})/\underline{g}_B(\underline{s})]$	$\ln(\underline{s})$	3	2.431	-4.934	3.673	0.9995
		4	1.772	-3.756	3.597	0.9903
		5	1.813	-3.871	3.602	0.9918

$$\ln[g_A(S)/g_B(S)] = B_O X_A [\ln(S)] + \ln[I(X_A)] \quad (84)$$

where B_O is a constant for the system and $I(X_A)$ is a function of X_A . The data are too limited to determine the functional relationship for the intercept, i.e., $I(X_A)$.

From a material balance of the polymer in the adsorption system, it can be demonstrated that

$$g_O(S) = X_A g_A(S) + X_B g_B(S) \quad (85).$$

By combining Equations (84) and (85), the equilibrium distributions for the bulk and surface phases can be predicted from the original distribution. In this case, the distribution for the bulk phase is given by:

$$g_B(S) = g_O(S) / [X_B(1 + Q)] \quad (86)$$

$$\text{where } Q = [X_A/X_B] [S^{B_O X_A}] I(X_A) \quad (87).$$

Similarly, the distribution for the surface phase is given by:

$$g_A(S) = [Q g_O(S)] / [X_A(1 + Q)] \quad (88).$$

Equations (86) and (87) were used to calculate the distribution for the bulk phase at $X_A = 0.5$. The value of B_O , taken as 3.624, was obtained by averaging the results from the partitioning regressions. The value of $\ln[I(X_A)]$, taken as -3.836, was obtained by linear interpolation of the results from Samples 4 and 5. The distributions obtained from Samples 101 and 100 were each employed as the original distribution, $g_O(S)$. The calculated distributions ($X_A = 0.5$) are compared in Fig. 31 with the experimental distributions obtained from Samples 4 ($X_A = 0.493$) and 5 ($X_A = 0.503$).

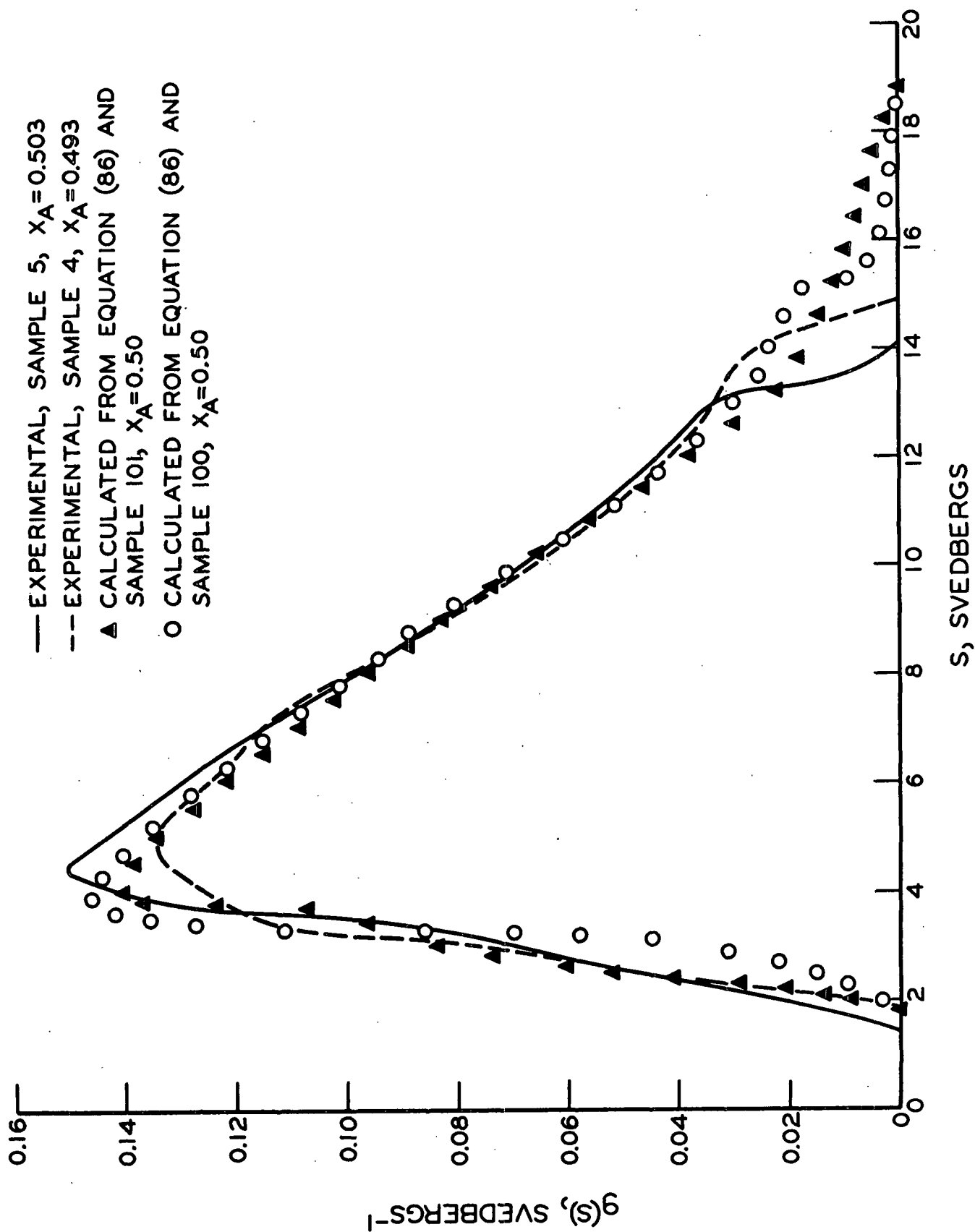


Figure 31. Comparison of Experimental Bulk-Phase Distributions with Those Predicted from Partitioning Relationship

Note that the partitioning relationship given by Equation (84) accurately describes the bulk-phase distribution over the entire range of \underline{S} with the exception of the high molecular weight region. In that region, a finite and measurable distribution of species is predicted for both the bulk and surface phases. Although the results obtained from Sample 100 for the original distribution were not particularly satisfactory (because of scatter in the diffusion extrapolations), they do provide a possible explanation for the discrepancy.

The original distributions obtained from Samples 100 and 101 exhibit a substantial difference in the high molecular weight region, as shown in Fig. 32. The distribution determined at the higher solution concentration, i.e., Sample 101 (Table XVIII), possesses a very regular shape in that region, whereas the distribution determined at the lower concentration, i.e., Sample 100, exhibits a rather abrupt change. In fact, all of the distributions determined at low concentrations (Table XVIII) exhibited an abrupt change in the same region, i.e., $0.2 \leq \underline{g}(\underline{S})/\underline{g}(\underline{S})_{\max} \leq 0.4$ on the leading side of the boundary.

TABLE XVIII
ORIGINAL SOLUTION CONCENTRATIONS EMPLOYED
IN SEDIMENTATION VELOCITY RUNS

Ultracentrifuge Sample	$\frac{C}{\rho}$, dl./g.
101	0.2220
100	0.1159
3	0.1197
4	0.1289
5	0.1341

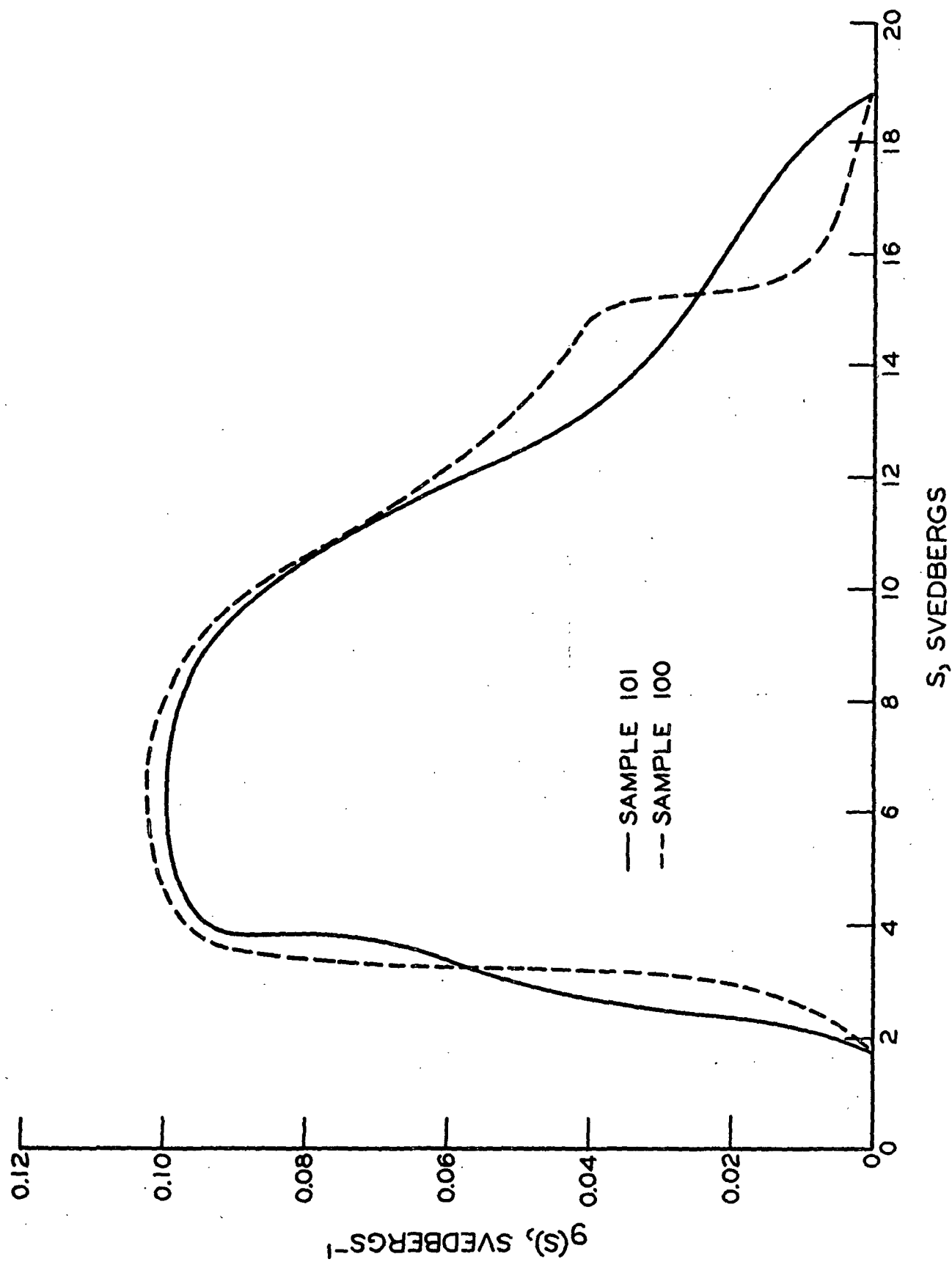


Figure 32. Comparison of Original Distribution Determinations for Polystyrene PB6

This behavior is likely the result of localized convective disturbances which frequently occur in regions of low concentration gradient (65). Significantly, abrupt changes occurred in the same region of the boundary, i.e., $0.2 \leq g(\underline{S})/g(\underline{S})_{\max} \leq 0.4$, and not at similar levels of \underline{S} . When boundaries were allowed to sediment for sufficiently long periods, distinct peaks appeared in that region and eventually resulted in a complete breakup of the boundary.

Additional support in favor of a gradually dissipating tail as predicted by the partitioning relationship is provided by thermodynamics. The chemical potential of a given solute is identical for the bulk and surface phases when species of that type are found in both phases at equilibrium. There is no reason to suspect that the chemical potential of a given polymer homolog in either phase can change abruptly enough with increasing chain length to explain the behavior observed in the tail region for the bulk phase. There is probably more depletion of high molecular weight species from the bulk phase than predicted by the partitioning relationship (complete depletion of a solute type will occur when the chemical potential of the solute is higher under all conditions in the bulk phase than in the surface phase), but the transition from some finite level of partitioning to complete depletion is expected to be more regular with respect to the original distribution.

Accurate determination of a distribution function in the tail regions is not readily accomplished experimentally. A simultaneous determination of a reference base line would be extremely helpful; however, the necessary experimental components are not available for conditions employed in sedimentation velocity experiments. Although evidence is rather limited, improvements might be obtained by using higher solution concentrations for sedimentation. Other considerations are discussed in Appendix III.

Comparison of Partitioning Relationship with Recent Theoretical Developments

The probability, p , that a given segment of an adsorbed molecule is located precisely at the interface has been discussed extensively by Frisch and co-workers (85-89). Using a statistical approach, the following relationship was derived for very weak attractive forces:

$$p = 2\alpha_o(1 - \phi)/(\pi fx)^{1/2} \quad (89)$$

where

α_o = the probability of a successful contact between an active site on the surface and a segment

ϕ = fraction of adsorption sites occupied by polymer

f = segment "diffusion" coefficient which includes the effects of valence angles and bond rotation on the molecular configuration

Gilliland and Gutoff (24) combined Equation (1) on page 6 with Equation (89) to obtain the following relationship:

$$N'_x/N_x = \{(N_s x^{1/2})/(N_o q)\} \{(1 - \phi) \exp[\chi_1 - \chi_1(1 - 2\phi)]\}^x \cdot \{(j_a/j_u) \exp(H/kT)\}^{q/x} \quad (90)$$

where $q = 2\alpha_o(1 - \phi)/(\pi f)^{1/2}$.

The above equation can be used to predict the partitioning behavior with respect to x . Assuming that the variables are independent of x , Equation (90) can be written as follows:

$$N'_x/N_x = c_1 x^{1/2} (c_2)^x (c_3)^{\sqrt{x}} \quad (91)$$

where c_1 , c_2 , and c_3 are constants for a particular equilibrium condition and are given by:

$$C_1 = N_s / (N_o q) \quad (92),$$

$$C_2 = \left\{ (1 - \phi) \exp[\chi_1 - \chi_1'(1 - 2\phi)] \right\}, \text{ and} \quad (93)$$

$$C_3 = [(j_a/j_u) \exp(H/kT)]^q \quad (94).$$

The quantity, (N'_x/N_x) , represents the weight ratio and is given by Equation (78) if the polymer is assumed to be continuously distributed with respect to \underline{x} :

$$N'_x/N_x = X_A f_A(M)/X_B f_B(M) \quad (95).$$

By combining Equations (91) and (95), the following can be obtained:

$$\ln[X_A f_A(M)/X_B f_B(M)] = (1/2)[\ln(x)] + \ln(C_1) + x[\ln(C_2)] + x^{1/2}[\ln(C_3)] \quad (96).$$

Note that the above expression is considerably more complicated than that observed experimentally, i.e., Equation (81) on page 104.

Silberberg's treatment (5, 79), based on lattice statistics, has been quite successful in describing many essential features of polymer adsorption. In particular, his analysis predicts Langmuir behavior but not for the reasons usually associated with that behavior. The probability, \underline{p} , was found to be nearly independent of \underline{x} for several models considered (79). If the probability is represented by \underline{q} , the partitioning relationship of Gilliland and Gutoff (24), i.e., Equation (1) on page 6, takes the form:

$$\ln[X_A f_A(M)/X_B f_B(M)] = x[\ln(C_2 C_3)] + \ln(C_1) \quad (97)$$

where \underline{C}_1 , \underline{C}_2 , and \underline{C}_3 are defined by Equations (92), (93), and (94), respectively, with \underline{q} taken as the probability, \underline{p} (a constant). Note that the above expression has the same functional relationship as Equation (77) describing phase separation.

The applicability of Silberberg's treatment or at least his choice of lattice co-ordination numbers and restrictive parameters must be questioned for the system employed in the present study. For very low adsorption energies, his theory predicts values of \underline{p} in the vicinity of 0.3. For adsorption energies of $(1/2)kT$, the theory predicts that more than half of the segments of an adsorbed molecule will be adsorbed at the interface, restricting the adsorbed polymer film thickness to the combined length of a few mers, e.g., ~ 20 A.

The thickness of adsorbed polystyrene layers was investigated recently by Stromberg, et al. (2) using ellipsometry. These workers reported an average film thickness of 210 A. for polystyrene adsorbed from cyclohexane onto chrome ferrotype plates. The average thickness remained constant over a wide range of concentration (corresponding to the plateau region of the Langmuir isotherm) and was independent of time soon after adsorption was initiated.

The lack of agreement between experimentally measured film thicknesses and values predicted from the theory of Silberberg is believed to be the result of excessive steric hindrance. Before discussing this point more fully, a digression on the statistical theories seems in order.

In early statistical theories describing the adsorption of flexible macromolecules, Frisch, et al. (85, 87) considered the equilibrium of an isolated macromolecule at a surface and derived parameters characterizing its shape. The probability, \underline{p} , was derived from lattice models and Gaussian chain statistics. The surface was treated as a perfectly reflecting wall, and polymer segments were placed at random in the lattice, neglecting interactions from other adsorbing chains and the surface proximity. The thermodynamics of adsorption also were derived, but the shape of the polymer molecule was not allowed to vary in the

process. In subsequent treatments (86, 88), improvements were introduced by considerations for short range chain interference near the surface and by the use of attractive surface forces. Corrections to the foregoing treatments were made for overcounting the number of possible configurations at the interface (89). This approach was extended recently by Higuchi (90) to cover a wide range of adsorption energies; however, the treatment still utilized the reflecting wall statistics.

According to Silberberg (79), a real surface does not reflect the random walk placement of segments but promotes continuance of the random walk in two out of three dimensions, i.e., along the surface, with a small reduction in internal energy per segment compensating largely for the loss of entropy in the third dimension. This concept of chain behavior at the interface is much more realistic than the reflecting wall statistics, and the agreement between well-established experimental observations and Silberberg's treatment apparently bears this out. Unlike earlier statistical theories, Silberberg treated the configuration of the polymer molecule at the interface as a variable and derived pertinent equilibrium quantities from the partition function for the entire system. The treatment, employing an hexagonal lattice with a minimum of restrictive parameters, predicts short loops of unadsorbed segments extending into the bulk phase with interim short stretches of successively adsorbed segments on the surface. As indicated earlier, his choice of lattice co-ordination numbers and restrictive parameters does not predict satisfactorily the film thickness, i.e., the length of the unadsorbed loops for polystyrene. Examination of the polystyrene configuration in solution and the probable configuration at the surface is useful in explaining this difficulty.

Polystyrene exhibits a configuration in solution which is considerably extended over that which free rotation about the vinyl backbone carbon atoms would permit. Even in solvent systems at their theta temperatures, the potential energy associated with bond rotation is sufficient to extend the chain as much as 2.4 times over the free rotation length (67). The potential functions restricting rotation about the backbone atoms in polystyrene have been discussed by Outer, *et al.* (83) and Flory (67). The potential functions for polystyrene are particularly restrictive because the bulky phenyl groups exhibit large steric interactions.

The phenyl group of an adsorbed polystyrene segment probably is nearly flattened at the interface. Because of the relatively high polarizability and low dipole moment of a polystyrene mer, the van der Waals' adsorption forces should be dominated by the London dispersion effect. According to de Boer (91), the additivity of such nonpolar van der Waals' forces tends to flatten polyatomic molecules on adsorbent surfaces in spite of the anisotropy of polarizability which tends to align the axis of greatest polarizability perpendicular to the surface. Flat configurations resulting from conjugated double bonds or aromatic rings enable such structures to approach the surface more closely and to take particular advantage of this additive effect. Consequently, an adsorbed phenyl group probably is nearly flattened at the interface.

An atomic model of the polystyrene chain was constructed and examined for steric considerations. It was found that no more than two successive segments could be adsorbed with the phenyl groups essentially flattened at the interface without imposing what appeared to be unreasonable restraint on the chain configuration. The phenyl group was responsible for this behavior because of (1) the extensive area occupied by an adsorbed phenyl group, and (2) the steric

hindrance exhibited by phenyl groups belonging to unadsorbed segments. If the adsorption of additional successive segments gives rise to unfavorable chain configurations, the effective decrease in the internal energy of the system will be lessened considerably because of potential energy stored in the chain. In fact, if the rotational potentials (potential energy associated with bond rotation) are sufficiently restrictive, additional segments are likely not to be adsorbed at the expense of overcoming these rotational barriers and associated entropy losses.

For polystyrene, it is quite conceivable that not more than one or two successively adsorbed segments are possible for a single adsorbed stretch. Such a restriction corresponds closely to several situations examined by Silberberg (79). Although the complete thermodynamics of adsorption were not derived, the configuration of an isolated macromolecule at the interface was investigated for several restrictive conditions. For each of the restrictions considered, the size of unadsorbed loops and adsorbed stretches were independent of molecular weight. The restrictions tended to increase the size of the unadsorbed loops and the polymer film thickness and easily accounted for the experimental film thicknesses reported (2) for polystyrene.

Although the fraction of segments adsorbed, i.e., the probability, p , was substantially affected by structural restrictions, this quantity was, nevertheless, found to be independent of molecular weight. The dependence of p on molecular weight, derived by Frisch, et al. (85, 87), apparently resulted from the physically unrealistic condition of a perfectly reflecting wall. Consequently, with p taken as a constant independent of molecular weight, the treatment of Gilliland and Gutoff (24), i.e., Equation (97), should describe the partitioning behavior.

The failure of Equation (97) to predict the observed partitioning relationship is believed to be the result of an admittedly crude lattice treatment used by Gilliland and Gutoff in their derivation of Equation (1) on page 6. For example, no restrictions on placement of polymer in the surface lattice were included in the treatment. In fact, none of the segments of a molecule in the surface-phase lattice actually have to be in physical contact with the surface even though the molecule is considered to be adsorbed. From the treatment of Silberberg (5, 79), the absence of such restrictive conditions must be regarded as a serious oversimplification of the polymer adsorption process. It must be noted, however, that one of the conditions imposed by Gilliland and Gutoff (24) was not satisfied by the system employed in the study, namely a theta solvent.

With the probability, p , taken as a constant, i.e., independent of molecular weight, it is not surprising that the relationship derived by Gilliland and Gutoff, i.e., Equation (1), reduces to the same functional relationship derived by Flory (67) for phase separation. The only difference in these treatments is the addition of a free energy term (for the adsorption case) to account for the heat of adsorption and the additional entropy loss incurred for each of the segments actually adsorbed.

Degree of Fractionation

The degree of fractionation can be written in terms of the distribution of sedimentation coefficient by substituting Equation (36) into Equations (59) and (60), respectively, as follows:

$$DF_B = \int_0^{\infty} \left| f_O(M) - f_B(M) \right| dM / 2(X_A), \text{ and} \quad (98)$$

$$DF_A = \int_0^{\infty} \left| f_O(M) - f_A(M) \right| dM / 2(X_B) \quad (99).$$

Using Equations (98) and (99), the degree of fractionation was calculated for each of the distributions obtained in this work, and the results are compared in Fig. 22 (p. 87) with those obtained from intrinsic viscosity methods, i.e., $\frac{DF}{v}$. Note that the $\frac{DF}{A}$ and $\frac{DF}{B}$ values are considerably lower than the corresponding $\frac{DF}{v}$ values and are less dependent on the weight fraction of polymer adsorbed.

The degree of fractionation given by Equations (98) and (99) is not biased by a weighting function; each solute type is weighted in proportion to its weight fraction. Consequently, the $\frac{DF}{A}$ and $\frac{DF}{B}$ quantities can be taken as a measure of the fractionation efficiency. The results shown in Fig. 22 indicate that the efficiency of the adsorption process as a means of fractionation was not particularly high (~35%). Although the range of X_A was limited, it appears that the efficiency, i.e., $\frac{DF}{A}$ or $\frac{DF}{B}$, was not strongly dependent on X_A (at least, not nearly as dependent as the $\frac{DF}{v}$ quantities).

Summary

Distributions of sedimentation coefficient were determined for Polystyrene PB6 before and after adsorption had taken place. Assuming that no polymer degradation had occurred, the distribution of polymer in the surface phase was calculated. At equilibrium, the corresponding distributions for the bulk and surface phases were related by a partitioning equation which differed substantially from that describing phase separation. The observed partitioning relationship was not in agreement with a recent theoretical development (24); however, this discrepancy is believed to be the result of a serious oversimplification of the polymer adsorption problem in the statistical treatment.

The partitioning relationship obtained for the adsorption system failed to describe the results in the high molecular weight regions. It is not known just

how much of this difficulty can be attributed to complete depletion (adsorption) of the higher molecular weight species or to convective effects in the sedimentation velocity experiments. The $\frac{DF}{v}$ quantities obtained from intrinsic viscosity studies do indicate, however, that the higher molecular weight species were extensively if not completely depleted (adsorbed) at high levels of $\underline{X_A}$.

In the region of low $\underline{X_A}$ (see Fig. 20), the intrinsic viscosity of the surface phase, $[\eta]_{\underline{A}}$, changed very slowly. In that region, the amount of polymer removed from the original solution via adsorption was quite limited, permitting only small changes in the bulk-phase distribution. With only minor changes in the bulk-phase distribution because of its much greater weight fraction, the partitioning phenomenon probably reflected a nearly constant distribution in the surface phase. This would explain the near constancy of $[\eta]_{\underline{A}}$ when large excesses of adsorbable species were present.

Changes in the solution concentration did not significantly affect the fractionation process over a limited range of concentration.

The polymer samples were fractionated significantly by the adsorption process. Each of the molecular weight averages for corresponding bulk and surface phases differed by approximately a factor of two, the average being higher for the surface phase. Although a strong fractionation was observed, the adsorption process was not an efficient analytical tool for molecular separations. The polymer in either phase was broadly distributed with respect to molecular weight following equilibrium adsorption.

In future studies, knowledge of the slope, \underline{B} , and intercept, $\underline{I(X_A)}$, as a function of $\underline{X_A}$ should make it possible to predict the intrinsic viscosity fractionation curves.

ADSORPTION AND FRACTIONATION OF POLYSTYRENES
OF BROAD MOLECULAR WEIGHT DISTRIBUTION
DURING THE APPROACH TO EQUILIBRIUM

EXPERIMENTAL

Nonequilibrium adsorption runs, employing polystyrene samples of broad molecular weight distribution, were conducted according to the experimental conditions summarized in Table XIX. Each adsorption tube employed 25.0 ml. of solution and 3.0 g. of furnace-treated FT-D4 graphitized carbon black.

TABLE XIX

SUMMARY OF EXPERIMENTAL CONDITIONS FOR
NONEQUILIBRIUM ADSORPTION RUNS

Adsorption Run No.	Polystyrene Sample	Initial Concentration, wt. %	Shaker Angle, °	Shaker Speed, r.p.m.
4S1-TCB	PB6	0.2972	40	36
4S2-TCB	PB6	0.2972	40	36
4S3-TCB	PB6	0.2972	10	20
2S1-TCB	DRT8	0.2650	30	24
2S2-TCB	DRT8	0.2650	30	25.5

In experiments employing Polystyrene PB6, an attempt was made to vary the fluid film resistance to diffusional transport by changing the degree of agitation. This was accomplished by varying the rotational speed of the shaker and the shaker angle.

Immediately following the loading and sealing operations, the adsorption tubes were shaken vigorously by hand for a few seconds to aid the adsorbent dispersion. For runs of short duration, the adsorbent and solution were separated by filtration. For runs of 24 hours or longer, the separation was made by

centrifugation. Following the initial separation, the solutions were filtered through type AA ($0.8\ \mu$) Millipore filters. The resulting solutions were analyzed for changes in intrinsic viscosity and concentration. The time of contact between the solution and adsorbent, i.e., the adsorption time, was measured from the instant of first contact between the solution and adsorbent to completion of the initial separation.

RESULTS

The intrinsic viscosity results for the nonequilibrium runs employing Polystyrene PB6 are shown in Fig. 33. Note that the intrinsic viscosity of the bulk phase increased very rapidly with contact time, reaching a maximum in approximately two minutes. Thereafter, the intrinsic viscosity decreased nearly linearly with the logarithm of contact time until equilibrium was nearly attained.

The intrinsic viscosity results for the surface phase were calculated with Equation (43) and are shown in Fig. 34. These results indicate that the lower molecular weight species were preferentially adsorbed initially, which was anticipated because of their greater mobility. Both diffusion through the fluid film adjacent to the adsorbing surfaces and molecular adsorption rates favor the adsorption of smaller molecules.

Comparison of the intrinsic viscosity results from Adsorption Run no. 4S3-TCB with Runs no. 4S1-TCB and 4S2-TCB indicates that the degree of agitation influenced the fractionation behavior. It appears that the effective fluid-film resistance adjacent to the adsorbing surfaces was altered by the degree of agitation; however, it must be cautioned that there are many complex factors involved in such a nonequilibrium adsorption process. Note that the experimental scatter in the results is higher for Adsorption Run no. 4S3-TCB (mild agitation)

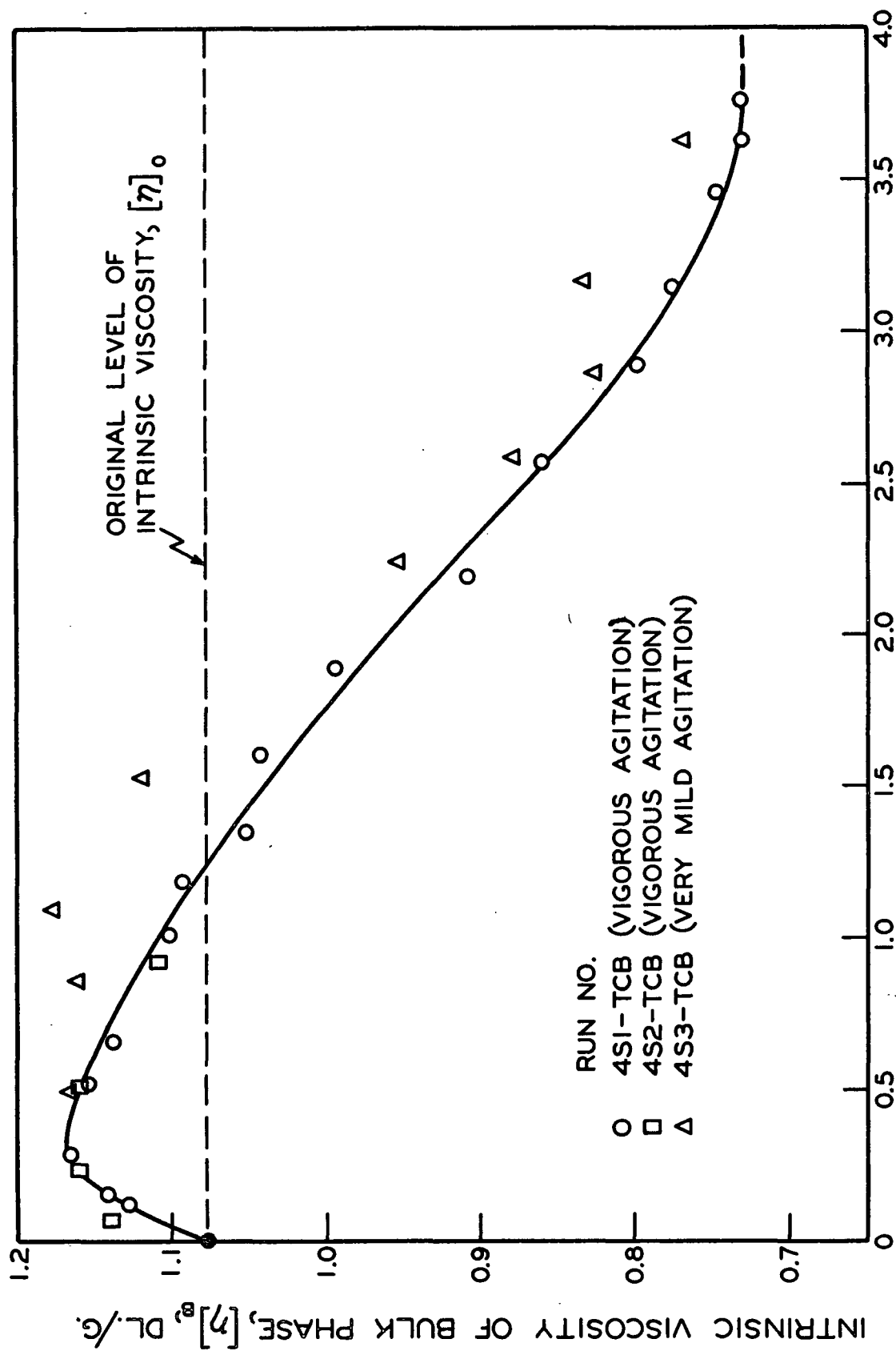


Figure 33. Effect of Contact Time on the Intrinsic Viscosity of Polystyrene PB6 in the Bulk Phase

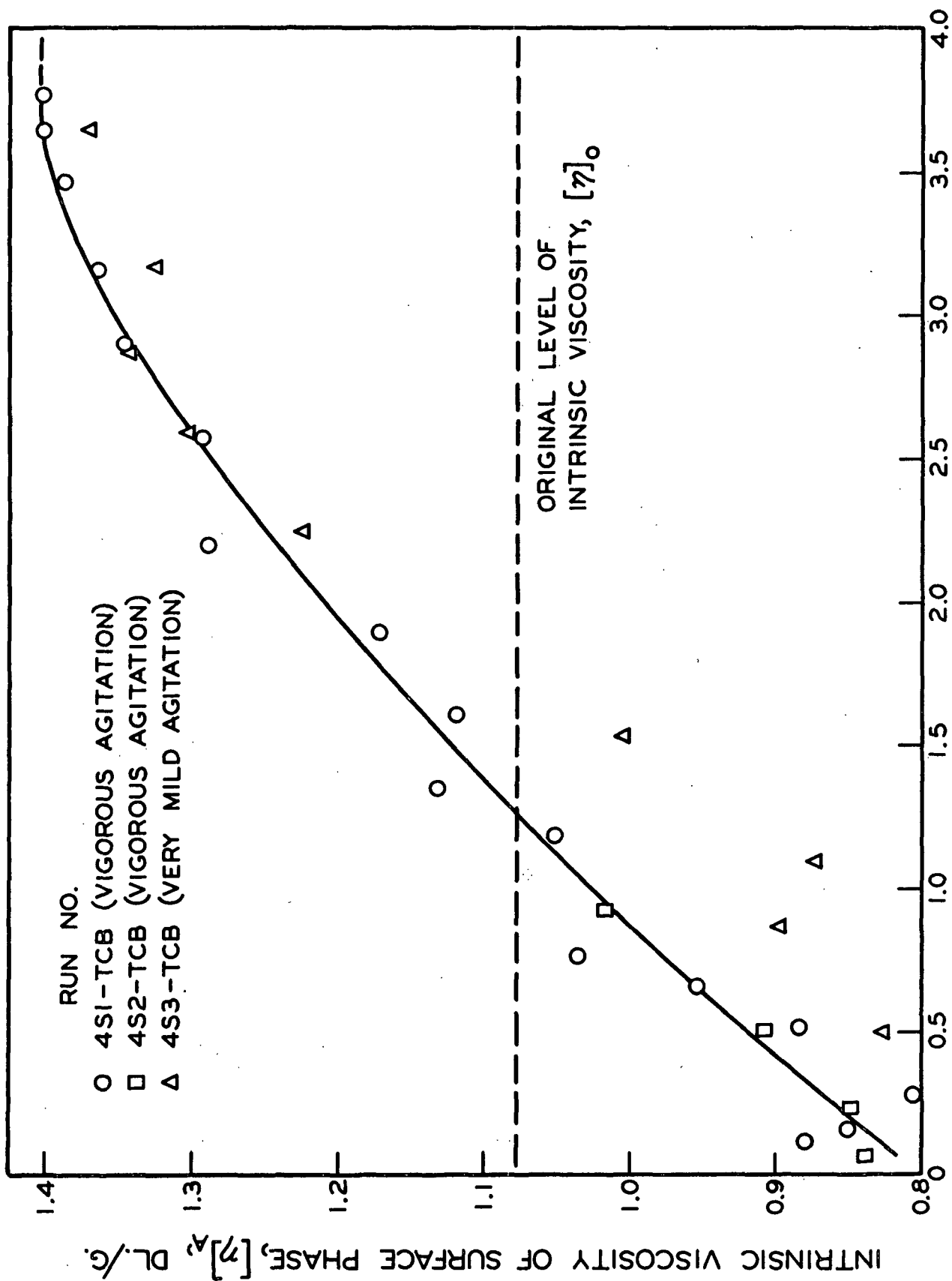


Figure 34. Effect of Contact Time on the Intrinsic Viscosity of Polystyrene PB6 in the Surface Phase

than the runs with vigorous agitation. The likely cause was the varying degree of adsorbent dispersion.

Further evidence of a dispersion effect can be found by examination of the specific adsorption as a function of time, as shown in Fig. 35. Note that the paths followed by the respective runs depended on the degree of agitation. This behavior could be attributed to differences in diffusional transport rates; however, it is demonstrated in a subsequent section that diffusion is not an important factor in the time range over which this effect was observed.

The fractionation observed for short contact times (Fig. 33 and 34) is caused by differences in the relative rates of adsorption which may result from differences in availability or concentration at the interface (as influenced by transport steps), differences in the mobilities of available molecules at the interface, or some combination of such factors.

Although the total surface area available for adsorption has a direct effect upon the over-all rate of adsorption, small changes in the effective surface area (caused by differences in adsorbent dispersion) should not affect the relative rates of adsorption for different species if diffusion is unimportant. Consequently, the fractionation behavior for short contact times should be independent of the degree of agitation when compared for similar extents of adsorption, i.e., similar weight fractions of polymer adsorbed. (At longer contact times, this may not be true because of the exchange phenomenon which will be discussed subsequently.)

The adsorption results for the bulk phase were plotted according to the above concept, i.e., against $\underline{X_A}$, and are shown in Fig. 36. As expected, the observations corresponding to the shorter contact time region are in much

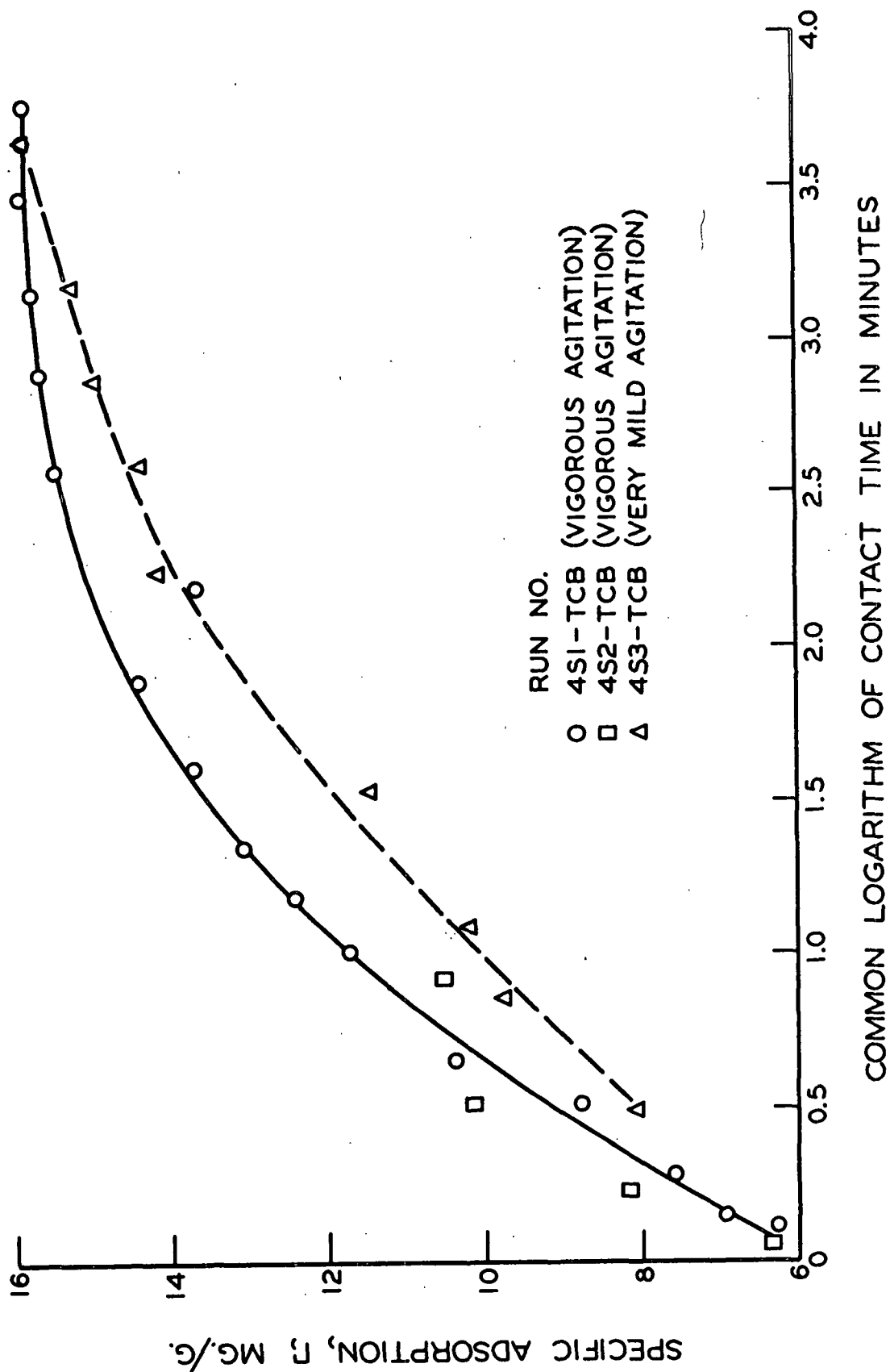


Figure 35. Effect of Contact Time on the Specific Adsorption of Polystyrene PB6

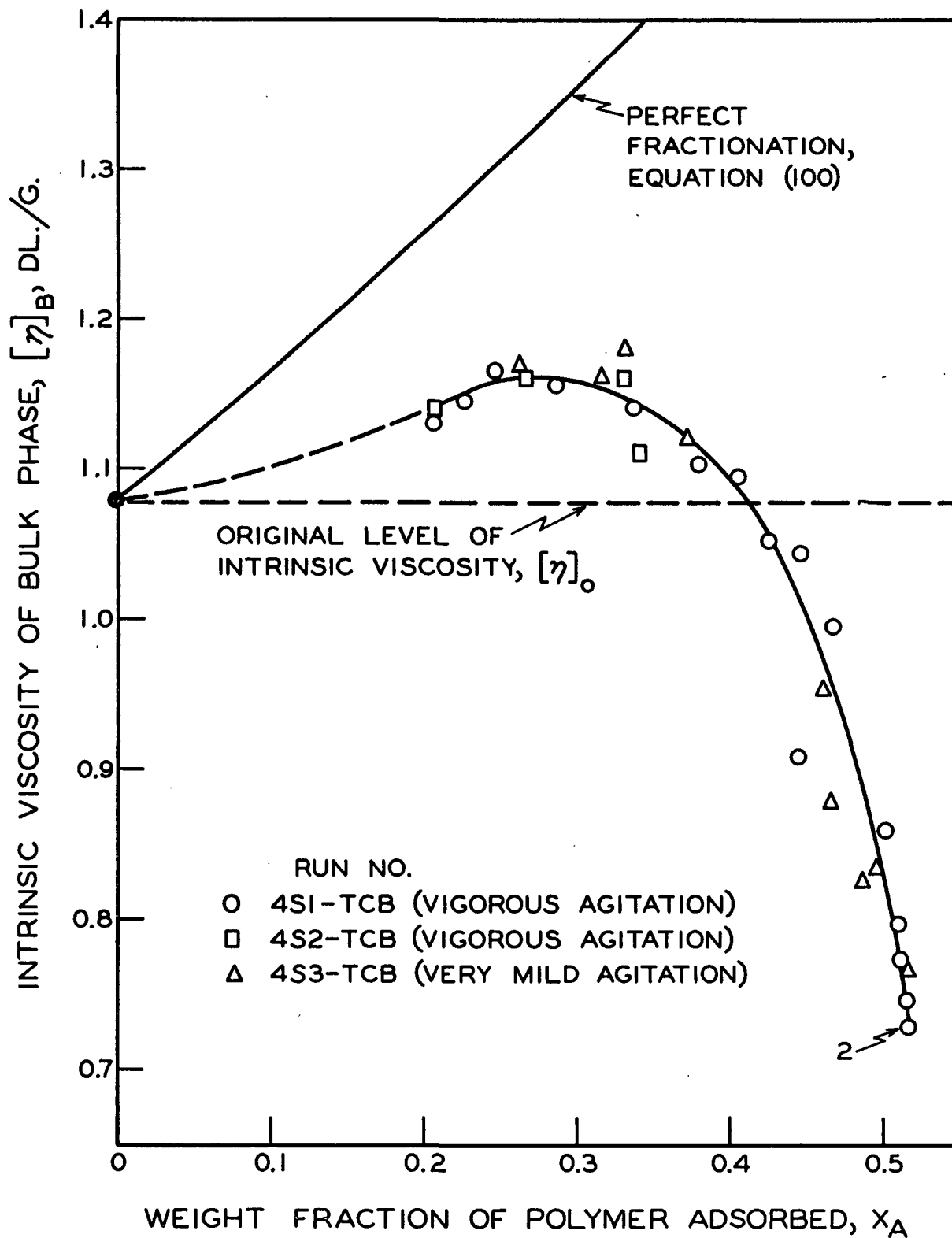


Figure 36. Fractionation Behavior of Polystyrene PB6 in Bulk Phase During Approach to Equilibrium

better agreement, i.e., independent of the degree of agitation, than they were in the previous figures.

The fractionation observed initially was well below the maximum limit given by the perfect fractionation curve as shown in Fig. 36. The perfect fractionation curve was obtained by assuming that the lowest molecular weight species present in the original sample were removed successively (via adsorption) with increases in the weight fraction of polymer adsorbed. In this case, the maximum intrinsic viscosity possible for the bulk phase, $[\eta]_{Bi}$, is given by:

$$[\eta]_{Bi} = K(k)^{-a/b} \int_{S_i}^{\infty} S^{a/b} g_o(S) dS / \int_{S_i}^{\infty} g_o(S) dS \quad (100)$$

where the lower limit of integration, S_i , corresponds to the weight fraction of polymer adsorbed, X_{Ai} , according to:

$$X_{Ai} = \int_0^{S_i} g_o(S) dS \quad (101).$$

The intrinsic viscosity results for the surface phase are shown in Fig. 37. A curvilinear regression of $[\eta]_A$ on X_A yielded the following:

$$[\eta]_A = 1.100 - 2.467(X_A) + 5.871(X_A)^2 \quad (102).$$

Similar fractionation behavior was observed for Polystyrene DRT⁸ in Adsorption Runs no. 2S1-TCB and 2S2-TCB, as shown in Fig. 38. (According to the supplier, DRT⁸ is a commercial grade of high molecular weight polystyrene having a broad, nearly Gaussian molecular weight distribution.) Although the molecular weight distribution of Polystyrene DRT⁸ is not known accurately, it is of interest to note that the fractionation behavior observed during the approach to equilibrium is of the same general nature.

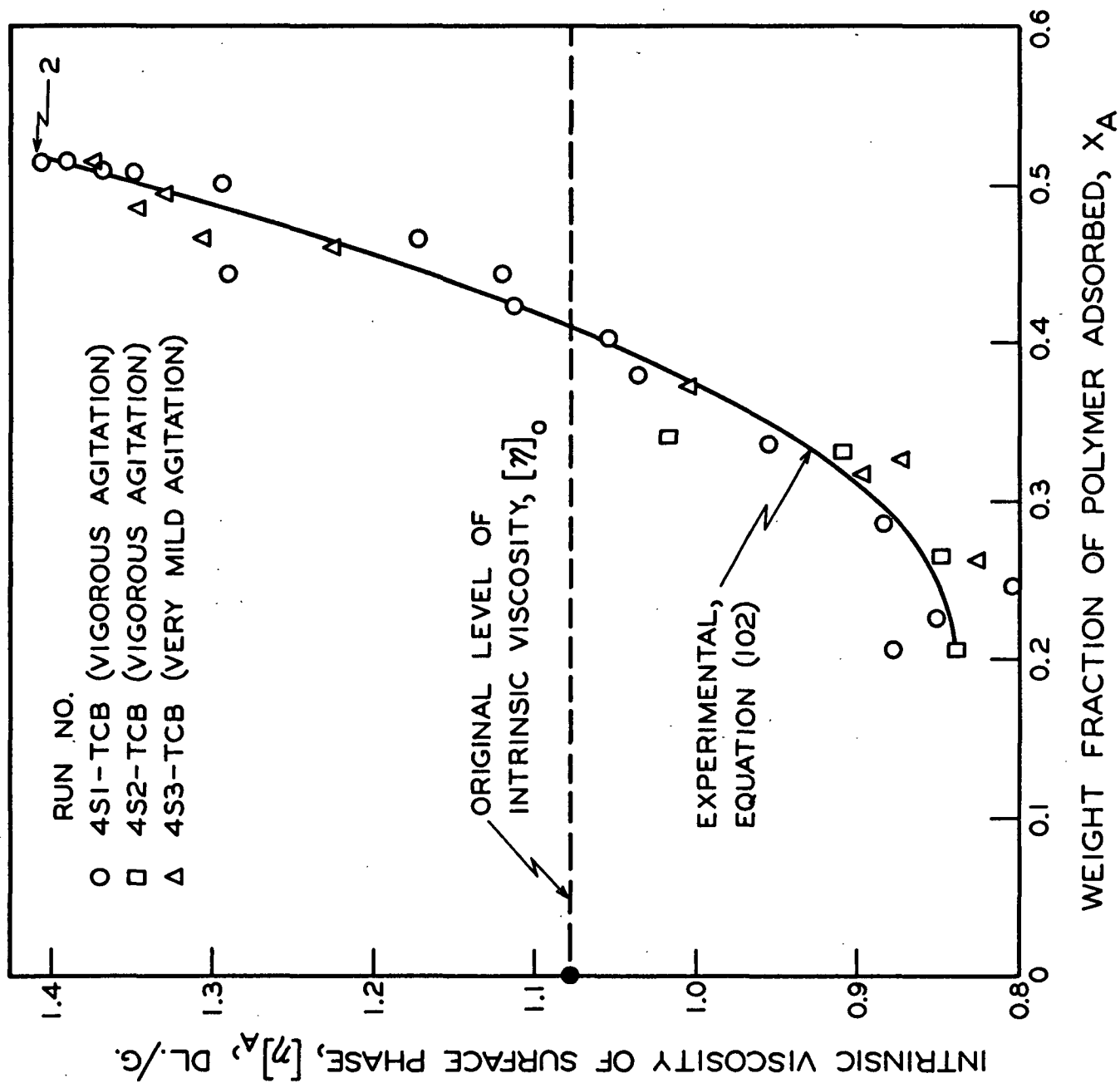


Figure 37. Fractionation Behavior of Polystyrene PB6 in Surface Phase During Approach to Equilibrium

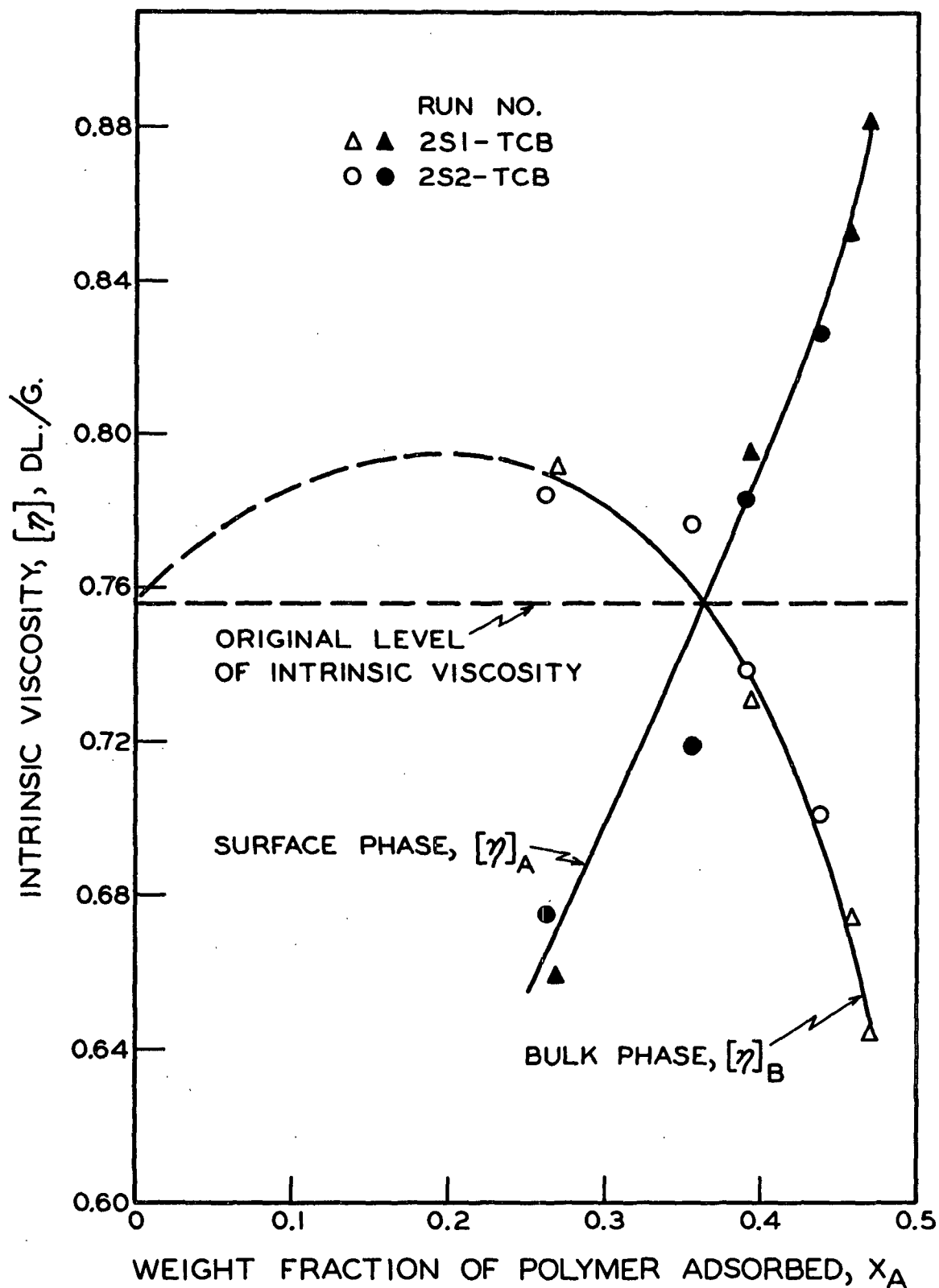


Figure 38. Fractionation Behavior of Polystyrene DRT8 During Approach to Equilibrium

EXCHANGE PHENOMENA

Kolthoff and co-workers (17-19) observed intrinsic viscosity behavior similar to that shown in Fig. 33 during the sorption of rubber on a series of carbon blacks. These investigators suggested that the low molecular weight species were preferentially adsorbed initially and were displaced gradually by larger molecules.

Other investigators (21, 22) have reported similar viscosity behavior for different systems and also have suggested that such an exchange was responsible. On the basis of viscosity behavior alone, it cannot be established that an exchange of high for low molecular weight species occurred unless the molecular weight distribution is known.

The intrinsic viscosity of the surface phase increased very rapidly with correspondingly small increases in the weight fraction of polymer adsorbed, as shown in Fig. 37. Such a sharp increase in $[\eta]_{\underline{A}}$ can occur either by (1) the adsorption of very high molecular weight species (if available) from the bulk phase, (2) the displacement of initially adsorbed small molecules by larger ones, or (3) combinations of (1) and (2). With knowledge of the molecular weight distribution, the possibility of mechanism (1) being solely responsible for the observed increase can be determined.

From the weight additivity of intrinsic viscosity quantities, the final intrinsic viscosity of the surface phase, $[\eta]_{\underline{A2}}$, can be written as follows:

$$[\eta]_{\underline{A2}} = (X_{\underline{1}}[\eta]_{\underline{A1}}) + (X_{\underline{\Delta}}[\eta]_{\underline{\Delta}}) \quad (103)$$

where $[\eta]_{\underline{A1}}$ is an earlier observation of $[\eta]_{\underline{A}}$ during the approach to equilibrium, and $X_{\underline{1}}$ is the corresponding weight fraction; $[\eta]_{\underline{\Delta}}$ is the intrinsic viscosity

necessary to raise the level of $[\eta]_{\underline{A}}$ from $[\eta]_{\underline{A1}}$ to $[\eta]_{\underline{A2}}$, and \underline{X}_{Δ} is the corresponding weight fraction. These weight fractions were defined on the basis of the weight of polymer in the surface phase, i.e., such that $\underline{X}_{\underline{1}} + \underline{X}_{\underline{\Delta}} = 1$, and can be written in terms of the total weight of polymer in the system according to:

$$\underline{X}_{\underline{1}} = \underline{X}_{\underline{A1}}/\underline{X}_{\underline{A2}}, \text{ and} \quad (104)$$

$$\underline{X}_{\underline{\Delta}} = (\underline{X}_{\underline{A2}} - \underline{X}_{\underline{A1}})/\underline{X}_{\underline{A2}} \quad (105)$$

where the subscript \underline{A} indicates that the quantities refer to the usual weight fraction of polymer adsorbed. Equations (103), (104), and (105) can be combined to obtain the following:

$$[\eta]_{\underline{\Delta}} = \left\{ (\underline{X}_{\underline{A2}}[\eta]_{\underline{A2}}) - (\underline{X}_{\underline{A1}}[\eta]_{\underline{A1}}) \right\} / (\underline{X}_{\underline{A2}} - \underline{X}_{\underline{A1}}) \quad (106).$$

Using Equations (102) and (106), it can be demonstrated that an exchange of small molecules on the surface by larger ones was in part responsible for the sharp increase of $[\eta]_{\underline{A}}$ shown in Fig. 37. For example, in order to proceed from the point $\underline{X}_{\underline{A1}} = 0.32$ to $\underline{X}_{\underline{A2}} = 0.52$ solely by additional adsorption, the minimum intrinsic viscosity, $[\eta]_{\underline{\Delta}}$, for the upper 20% of the original sample would have to be 2.193 dl./g. (The 20% value comes from the difference, $\underline{X}_{\underline{A2}} - \underline{X}_{\underline{A1}}$.) However, the upper 20% of the original sample yields an intrinsic viscosity of only 2.065 dl./g. [This information was calculated previously for the perfect fractionation curves with Equations (40) and (46).]

Because of experimental errors, the deficit in $[\eta]_{\underline{\Delta}}$ is not sufficient to conclude that an exchange of molecules must have occurred. However, the fact that the entire upper 20% of the sample would have to be adsorbed in the range $\underline{X}_{\underline{A1}} \leq \underline{X}_{\underline{A}} \leq \underline{X}_{\underline{A2}}$ to satisfy Equation (103) is too restrictive. First, this means

that only a negligible weight of the higher molecular weight species, i.e., species with molecular weights placing them in the upper 20% by weight, could be adsorbed in the range $0 < \underline{X}_A \leq \underline{X}_{A1}$. Second, this demands complete adsorption of the upper 20% of the original sample at $\underline{X}_A = \underline{X}_{A2}$. In this particular case, the observations at $\underline{X}_{A2} = 0.52$ correspond to equilibrium quantities; hence, it is possible to compare these demands with the equilibrium results from Adsorption Run No. 4S5-ECB. (All of these runs employed Polystyrene PB6.) The equilibrium distributions shown in Fig. 31 ($\underline{X}_A \approx 0.5$) should represent closely the condition of the bulk phase for $\underline{X}_{A2} = 0.52$. To satisfy the demand that the upper 20% of the original sample be adsorbed, all of the species with \underline{S} -values greater than 11.6 svedbergs must be removed (adsorbed) from the bulk phase. It is evident from Fig. 31 that this demand was not satisfied experimentally.

The argument can be continued by analysis of the situation for $\underline{X}_{A1} = 0.27$ and $\underline{X}_{A2} = 0.52$. In this case the value of $[\eta]_\Delta$ necessary to increase $[\eta]_A$ from $[\eta]_{A1}$ to $[\eta]_{A2}$, according to Equations (102) and (106), is 1.991 dl./g. and corresponds to 25% of the original sample. The maximum intrinsic viscosity for the upper 25% of the original sample is 1.956 dl./g. Although closer to satisfying the demand for $[\eta]_\Delta$, all species with \underline{S} -values greater than 10.9 svedbergs would have to be removed from the bulk phase. Consequently, it appears that the displacement of initially adsorbed small molecules by larger ones was in part responsible for the fractionation behavior observed during the approach to equilibrium.

IMPORTANCE OF DIFFUSIONAL TRANSPORT IN THE ADSORPTION PROCESS

In order to estimate the importance of diffusion in the adsorption process a simplified analysis was undertaken. It was assumed that the adsorbing surfaces

are planar and that the fluid-film resistance adjacent to the adsorbing surfaces can be approximated by a thickness, L . The term, fluid-film resistance, implies a stagnant or laminar layer of fluid adjacent to the adsorbing surfaces, and the mechanism of transport across the film is limited to diffusion. The physical situation can be schematically represented by Fig. 39.

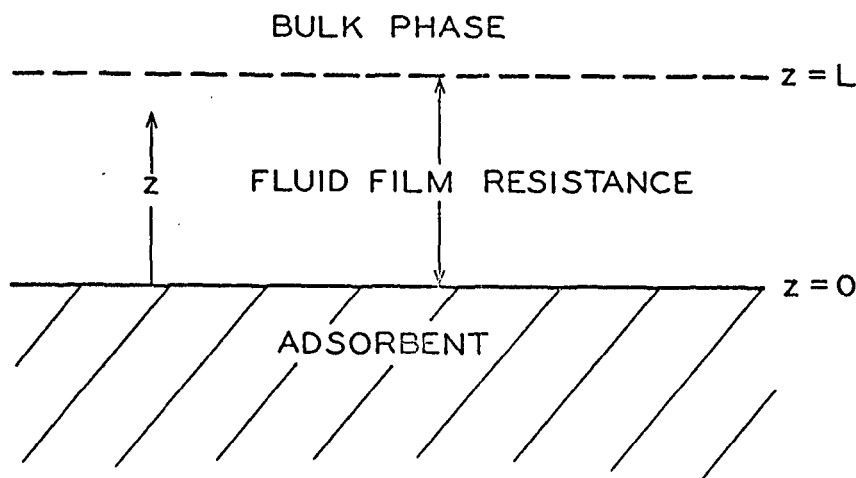


Figure 39. Schematic Representation of Fluid Film Resistance

Substitution of Fick's first law into the continuity equation yields the usual expression for one-dimensional diffusion in a two-component system (93):

$$\frac{\partial C}{\partial t} = \frac{\partial [D(\partial C / \partial z)]}{\partial z} \quad (107)$$

where C is the concentration at any position, z , and time, t , and D is the diffusion coefficient of the solute component. Equation (107) can describe the diffusional transport of a monodisperse polymer solute across a fluid film when the proper boundary conditions are employed.

The boundary condition at $z = L$ can be simplified by assuming infinite bath conditions and perfect mixing in the bulk phase. However, the boundary condition

at the adsorbing surface, i.e., at $\underline{z} = 0$, depends on the rate expression for polymer adsorption. Although there is not sufficient information available to formulate a general mathematical expression for the rate of adsorption, an estimate of the time requirements for the completely diffusion-controlled case can be made. By assuming that the polymer is adsorbed so rapidly and irreversibly at the interface that the effective concentration at $\underline{z} = 0$ is zero, the initial and boundary conditions can be described as follows:

$$\underline{C} = \underline{C}_0 \text{ at } \underline{z} > 0 \text{ for } \underline{t} = 0,$$

$$\underline{C} = 0 \text{ at } \underline{z} = 0 \text{ for } \underline{t} \geq 0, \text{ and}$$

$$\underline{C} = \underline{C}_0 \text{ at } \underline{z} \geq \underline{L} \text{ for } \underline{t} \geq 0.$$

By assuming that the diffusion coefficient is independent of concentration, Equation (107) can be written as:

$$\partial C / \partial t = D(\partial^2 C / \partial z^2) \quad (108).$$

Solving Equation (108) for the above conditions, the concentration distribution across the fluid film can be written (94) as a function of time, \underline{t} , and position, \underline{z} , according to:

$$\begin{aligned} C = & C_0 z / L \\ & + (2C_0 / \pi) \sum_{n=1}^{n=\infty} \left\{ (1/n) \cos(n\pi) \sin(n\pi z / L) \exp(-n^2 \pi^2 D t / L^2) \right\} \\ & + (4C_0 / \pi) \sum_{m=0}^{m=\infty} \left\{ [1/(2m + 1)] [\sin\{(2m + 1)\pi z / L\}] \cdot \exp[-(2m + 1)^2 \pi^2 D t / L^2] \right\} \end{aligned} \quad (109)$$

where \underline{n} and \underline{m} represent successively ascending integers in the summations.

The mass flux, \underline{J} , defined as a positive quantity when directed in the negative z -direction, i.e., toward the adsorbing surface, is given by Fick's first law as follows:

$$J = D(\partial C / \partial z) \quad (110).$$

To find the quantity of solute at the interface, the mass flux, \underline{J} , must be evaluated at $\underline{z} = 0$ and integrated over the elapsed time interval according to:

$$Q_t = \int_0^t J \Big|_{z=0} dt' \quad (111)$$

where \underline{Q}_t is the total mass of diffusing solute having arrived at unit area of the plane located at $\underline{z} = 0$ in elapsed time, \underline{t} .

Equations (109), (110), and (111) can be combined to obtain the following relationship:

$$Q_t / LC_0 = Dt / L^2 \quad (112)$$

$$+ (2/\pi^2) \sum_{n=1}^{n=\infty} \left\{ (-1)^n (1/n^2) [1 - \exp(-n^2 \pi^2 Dt / L^2)] \right\}$$

$$+ (4/\pi^2) \sum_{m=0}^{m=\infty} \left\{ [1/(2m+1)^2] [1 - \exp\{-(2m+1)^2 \pi^2 Dt / L^2\}] \right\}.$$

With the above relationship, the importance of diffusion can be assessed under the conditions for which Equation (108) was solved.

The diffusion coefficient of polystyrene in dichloroethane has been reported by Tsvetkov and Klenin (95) as follows:

$$D = (1.12 \times 10^{-4})M^{-0.51} \quad (113).$$

Using the weight-average molecular weight for the original distribution, i.e., $\overline{M}_w = 5.12 \times 10^5$, the corresponding average diffusion coefficient from Equation (113) is 1.37×10^{-7} sq. cm./sec. The surface concentration, \underline{Q}_t , is given by:

$$Q_t = \Gamma/A_s \quad (114)$$

where Γ is the specific adsorption, and \underline{A}_s is the specific surface area. Using the specific surface area obtained from nitrogen gas adsorption (12.44 sq. m./g.) and the approximate maximum specific adsorption (15.9 mg./g.), the maximum surface concentration obtained from Equation (114) is 1.28×10^{-4} mg./sq. cm. The initial concentration of solution employed in Adsorption Runs No. 4S1-TCB, 4S2-TCB, and 4S3-TCB was 7.464 mg./cc.

Using the above values for the designated quantities in Equation (112), the time requirements for maximum adsorption were determined for a wide range of fluid-film thicknesses as shown in Table XX. Assuming that the adsorbent was completely and uniformly dispersed, it can be demonstrated that the average fluid-film thickness associated with an individual particle was less than 1.0×10^{-4} cm. for the experimental conditions employed. It is evident that diffusional transport was probably not an important rate-controlling mechanism in the time range over which the experimental observations were made.

This does not imply that diffusion is unimportant in the adsorption process. On the contrary, differences in solute diffusion rates may be responsible for the initial fractionation observed. Note that the initial fractionation for the surface phase (Fig. 34) already was well established by the time the earliest measurements were made. Just how extensive the fractionation might have been

for shorter contact times is not known. (Experimental conditions made it impossible to obtain data for contact times of less than a minute.)

TABLE XX
TIME REQUIREMENTS FOR DIFFUSIONAL TRANSPORT
ACROSS A FLUID FILM

Fluid Film Thickness, cm.	$\frac{Q_t}{LC_0}$	$\frac{Dt}{L^2}$	t , sec.
1.0×10^{-2}	1.714×10^{-3}	3.48×10^{-4}	0.254
1.0×10^{-4}	0.171	4.24×10^{-2}	3.09×10^{-3}
1.0×10^{-6}	17.1	16.8	1.23×10^{-4}

Recent experimental studies have indicated that diffusion is not important at any period in adsorption systems with limited fluid-film thicknesses. Petersen and Kwei (96) studied the rate of adsorption of radioactive polyvinyl acetate from dilute benzene solutions onto surfaces of chromeplate. The rate of stirring did not affect the rate of adsorption until the solution concentration was reduced below 5×10^{-3} mg./cc. However, in a bulk system the fluid-film resistance is not readily controlled, particularly in the early stages of contact between the adsorbent and solution. Consequently, it is not known whether the initial fractionation observed in the present study was the result of relative diffusion rates, molecular adsorption rates, or some combination of these factors. On the basis of the work by Peterson and Kwei (96), it is the author's belief that differences in solute mobilities at the interface, i.e., differences in molecular adsorption rates, were more important.

SUMMARY

During the approach to equilibrium, the intrinsic viscosity of the bulk phase increased very rapidly with contact time, reaching a maximum in just a

little over two minutes. The fractionation observed initially was well below the maximum limit given by the perfect fractionation curve. Thereafter, the intrinsic viscosity of the bulk phase decreased nearly linearly with the logarithm of contact time until equilibrium was approached. The system required approximately 3 days to reach equilibrium (no further decreases in intrinsic viscosity occurred over an additional period of 24 hours).

The intrinsic viscosity results for the surface phase indicated that smaller molecules were preferentially adsorbed initially. From analysis of fractionation curves, it was found that the displacement of initially adsorbed small molecules by larger ones was in part responsible for the fractionation behavior observed during the approach to equilibrium. Similar fractionation behavior was observed for two samples of polystyrene of broad molecular weight distribution, indicating that the fractionation process was of the same general nature.

From a simplified analysis of diffusional transport across a fluid film, it was found that diffusion of the solutes was not an important rate-controlling factor in the time range over which the experimental observations were made. However, the initial fractionation obtained for the surface phase already was well established by the time the earliest measurements were made, and differential diffusion rates could have been responsible for that behavior. Whether the initial fractionation was caused by differences in solute diffusion rates, molecular adsorption rates, or some combination of these factors, is not known, but it is the author's belief that differences in solute mobilities at the interface, i.e., differences in molecular adsorption rates, were more important.

Fractionation differences which were observed for the nonequilibrium adsorption runs as a result of different degrees of agitation are believed to have

resulted from incomplete dispersion of the adsorbent and not from varying fluid film thicknesses, i.e., differences in diffusional transport.

EXCHANGE EXPERIMENTS USING POLYSTYRENES OF NARROW
MOLECULAR WEIGHT DISTRIBUTION

EXPERIMENTAL

Two polymer samples of narrow molecular weight distribution, Polystyrenes PS26 and PS34 (see Table II, p. 15), were combined in nearly equal weight ratios to prepare a stock solution for the exchange experiments. The adsorption experiments (Run No. 5S2-TCB) were similar to previous nonequilibrium runs and employed the conditions summarized in Table XXI. The volume of solution, weight of adsorbent, and solution concentration were maintained constant throughout the run whereas the contact time was varied from one minute to five days. For experiments of short duration, i.e., for contact times of less than 14 hours, the initial separation of adsorbent and solution was made by filtration. For runs of longer duration, the initial separation was made by centrifugation. The resulting solutions were filtered and analyzed for changes in intrinsic viscosity and solution concentration.

TABLE XXI

SUMMARY OF EXPERIMENTAL CONDITIONS
FOR ADSORPTION RUN NO. 5S2-TCB

Weight fraction of Polystyrene PS26 in mixture: 0.5072
Weight fraction of Polystyrene PS34 in mixture: 0.4928
Volume of solution: 15.0 ml.
Concentration of stock solution: 0.3567 weight %
Weight of adsorbent: 2.0 g.
Shaker speed: 24.0 r.p.m.
Shaker angle: 15°

The intrinsic viscosity of the original stock solution, $[\eta]_o$, was calculated with the following relationship:

$$[\eta]_o = (X_{26}[\eta]_{26}) + (X_{34}[\eta]_{34}) \quad (115)$$

where X_{26} and X_{34} are the weight fractions of Polystyrenes PS26 and PS34, respectively, and $[\eta]_{26}$ (0.501 dl./g.) and $[\eta]_{34}$ (0.892 dl./g.) are the corresponding intrinsic viscosities for the individual polymer samples. (Plots of the intrinsic viscosity data for Samples PS26 and PS34 are shown in Appendix I.) An approximate check of the intrinsic viscosity was made directly on the stock solution mixture, yielding 0.687 dl./g. which compares favorably with 0.693 dl./g. obtained from Equation (115).

RESULTS AND DISCUSSION

The fractionation behavior shown in Fig. 40 was observed for the mixture of narrow polymer fractions. The intrinsic viscosity of the polymer mixture in the surface phase, $[\eta]_A$, was calculated with Equation (43). The fractionation behavior was similar to that found for samples of broad molecular weight distribution during the approach to equilibrium except that no preferential adsorption of the low molecular weight species was observed in the early stages. This was probably the result of two factors: (1) the average molecular weights of the narrow polymer fractions differed only by a factor of two, restricting the ultimate preferential adsorption, and (2) the exchange process may have been extremely rapid because of the low molecular weights involved.

The weight of each of the narrow polymer fractions in the surface phase can be calculated by assuming that no fractionation occurred within the narrow fractions during adsorption. For this purpose, the intrinsic viscosity of the

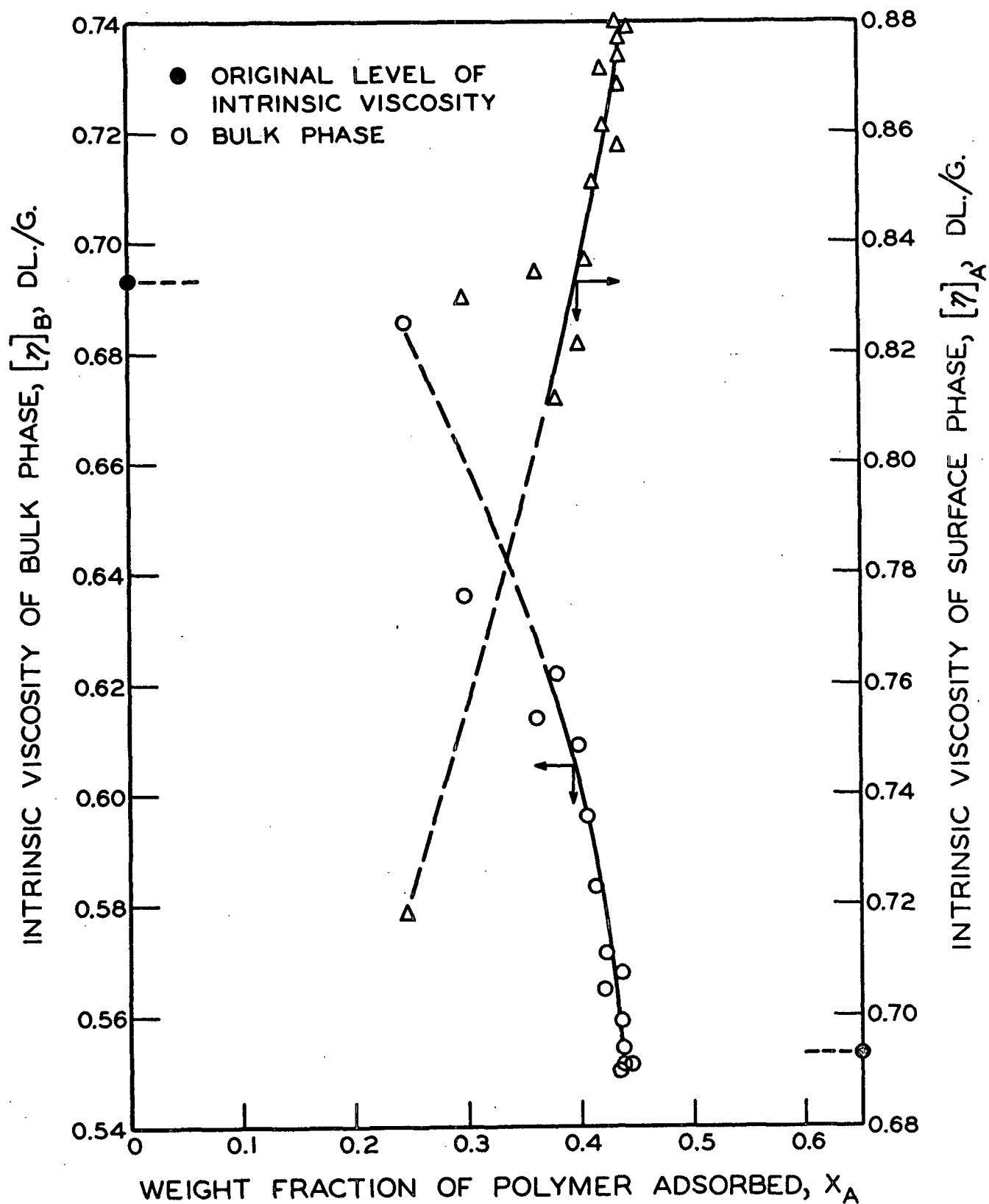


Figure 40. Fractionation Behavior of Polystyrene PS26 and PS34 Mixture During Approach to Equilibrium

surface phase, $[\eta]_{\underline{A}}$, can be written as:

$$[\eta]_{\underline{A}} = (X_{\underline{A26}}[\eta]_{26}) + (X_{\underline{A34}}[\eta]_{34}) \quad (116)$$

where $X_{\underline{A26}}$ and $X_{\underline{A34}}$ are the weight fractions of adsorbed polymer made up of Polystyrenes PS26 and PS34, respectively. The sum of these weight fractions obviously is given by:

$$X_{\underline{A26}} + X_{\underline{A34}} = 1 \quad (117).$$

By combining Equations (116) and (117), the following relationships can be obtained:

$$X_{\underline{A26}} = ([\eta]_{34} - [\eta]_{\underline{A}})/([\eta]_{34} - [\eta]_{26}), \text{ and} \quad (118)$$

$$X_{\underline{A34}} = ([\eta]_{\underline{A}} - [\eta]_{26})/([\eta]_{34} - [\eta]_{26}) \quad (119)$$

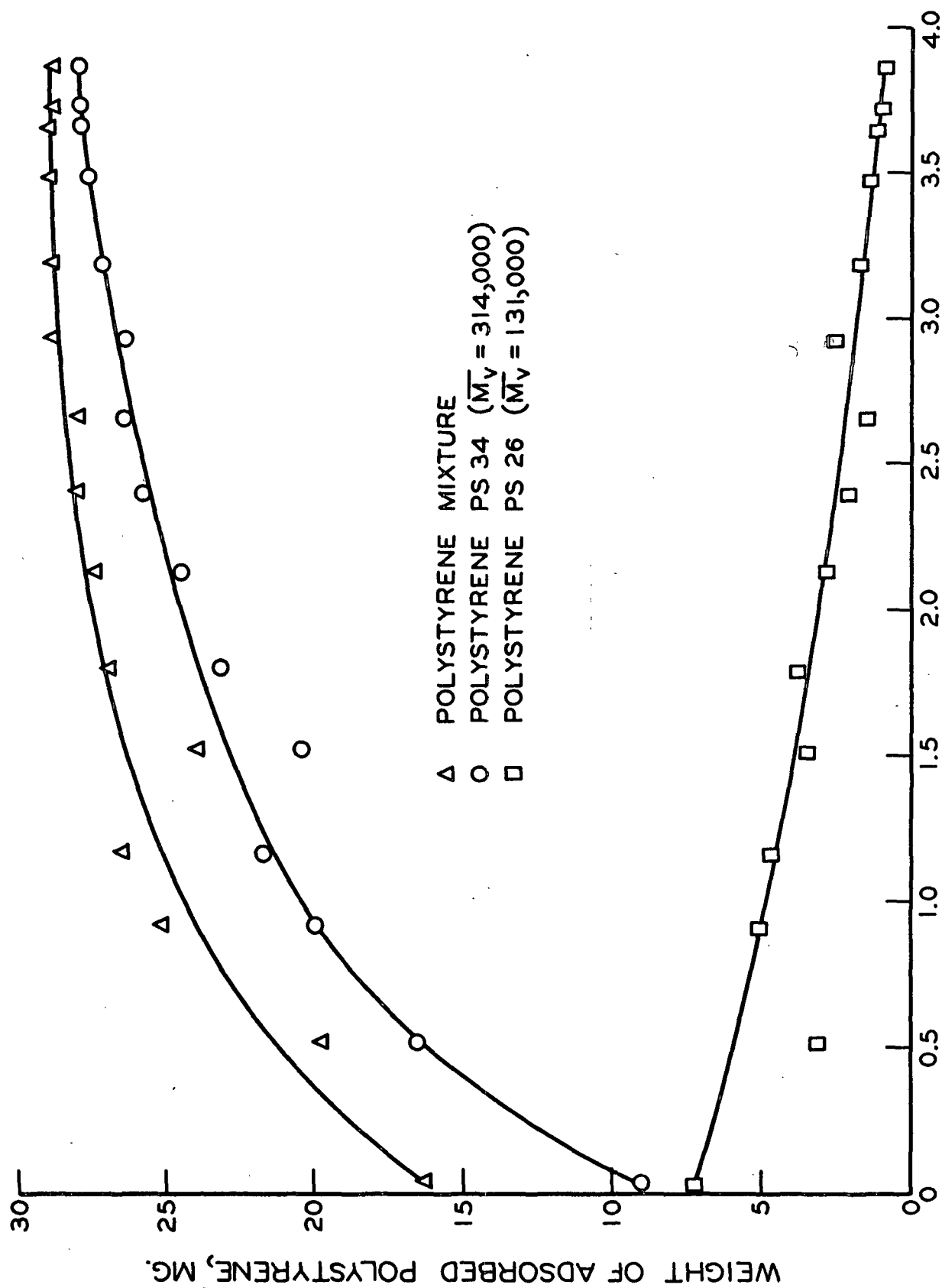
The weights of Polystyrenes PS26 and PS34 in the surface phase, $\underline{W}_{\underline{A26}}$ and $\underline{W}_{\underline{A34}}$, respectively, are given by:

$$\underline{W}_{\underline{A26}} = X_{\underline{A26}}\underline{W}_p, \text{ and} \quad (120)$$

$$\underline{W}_{\underline{A34}} = X_{\underline{A34}}\underline{W}_p \quad (121).$$

where \underline{W}_p is the total weight of adsorbed polymer.

The weights of each of the narrow polymer fractions in the surface phase were calculated with Equations (118), (119), (120), and (121) and are shown in Fig. 41. According to these results, the weight of the lower molecular weight fraction, i.e., Polystyrene PS26, in the surface phase decreased with time (following an initially rapid adsorption) even though the total weight of adsorbed polymer continued to increase sharply. This appears to be direct



COMMON LOGARITHM OF CONTACT TIME IN MINUTES

Figure 41. Effect of Contact Time on Weight of Polystyrene Adsorbed in Surface Phase

evidence of an exchange phenomenon, the lower molecular weight material having been displaced by the higher molecular weight species.

The results shown in Fig. 41 indicate that the exchange process was important even in the early stages where the rate of adsorption was quite high. It is now evident that the fractionation behavior of a polymolecular sample during the approach to equilibrium is the result of several complex rate phenomena which may include differential diffusion rates, differential rates of adsorption, and exchange phenomena.

The continued increase in total weight of adsorbed polymer over long periods of time as shown in Fig. 41 should not be associated necessarily with the rate of adsorption. Part of the increase probably resulted from the exchange phenomenon. Increases in specific adsorption with increasing molecular weight have been reported (7, 20, 80, 97-100) for a variety of systems. This behavior also was observed in the present study, obtaining specific adsorption values of 12.90 and 15.75 mg./g. for Polystyrenes PS26 and PS34, respectively. These determinations were made at sufficiently high equilibrium concentrations, i.e., $C > 2.5$ mg./cc., to be regarded as approximations to the limiting values, i.e., Γ_m .

The results shown in Fig. 41 for long contact times, i.e., greater than 3 days, correspond to equilibrium quantities and indicate that a partitioning of the species was obtained. Species from each of the narrow polymer fractions were present in both of the phases at equilibrium with species from the higher molecular weight fraction being adsorbed preferentially. Both the partitioning behavior and preferential adsorption at equilibrium were in agreement with behavior observed earlier for samples of broad molecular weight distribution.

Although the original polystyrene samples (S26 and S34) were of narrow molecular weight distribution as indicated by their ratios of weight- to number-average molecular weights (see Table I, p. 13), the purified samples (PS26 and PS34) were fractionated significantly when employed individually in adsorption experiments, as shown in Table XXII. Note that the intrinsic viscosity of the bulk phase, $[\eta]_{\underline{B}}$, exhibited a substantial decrease from the original level, $[\eta]_{\underline{O}}$, after four days of contact with the adsorbent.

TABLE XXII
FRACTIONATION WITHIN NARROW
POLYMER FRACTIONS

Polystyrene Sample	$[\eta]_{\underline{O}}$, dl./g.	$[\eta]_{\underline{B}}$, dl./g.	\underline{X}_A	Equilibrium Concentration, mg./cc.
PS26	0.501	0.467	0.381	2.794
PS34	0.892	0.783	0.454	2.526

From the low fractionation efficiency found for polystyrenes of broad molecular weight distribution, no significant fractionation within the narrow polymer fractions was anticipated. The results in Table XXII suggest that the partitioning parameters, i.e., \underline{B} and $\underline{I}(\underline{X}_A)$, varied with the molecular weight distribution (as well as \underline{X}_A), which is not surprising. Flory (67) has demonstrated by thermodynamic considerations that the partitioning parameter in phase separation, i.e., σ in Equation (76), varies with the number-average D.P. for each phase along with several other variables. Whether the fractionation within these narrow polymer fractions was as great when the samples were combined is not known. Consequently, these results must be regarded as qualitative.

Since fractionation within the individual samples favored the adsorption of higher molecular weight species, at least in the longer contact time region, the

effective intrinsic viscosities to be used in place of $[\eta]_{26}$ and $[\eta]_{34}$ in Equations (118) and (119) would have to be larger (and would vary with time). This would decrease the differences between \underline{W}_{A26} and \underline{W}_{A34} (Fig. 41), making the actual weight of Polystyrene PS26 greater and that for PS34 smaller than those calculated.

The exchange experiments were helpful in assessing the conditions needed for a quantitative study of the exchange process. In principle, the exchange experiments make it possible to follow the concentration of each solute type in the bulk phase and the weight of each type in the surface phase. It is evident that the molecular weight distributions of the samples must be extremely narrow. The rate of adsorption of each solute type, needed for a quantitative study of the exchange phenomenon, can be obtained (in the absence of diffusion effects) from the method of Peterson and Kwei (96). By accounting for the rate of concentration decrease for each solute type in the bulk phase due to adsorption, the rate of accumulation or depletion from the exchange phenomenon can be assessed. In this way, the exchange kinetics for two narrow polymer fractions can be studied.

SUMMARY

The fractionation behavior observed for a mixture of two narrow polymer fractions during the approach to equilibrium was similar to that found earlier for samples of broad molecular weight distribution except that no preferential adsorption of the low molecular weight material was obtained initially. The weight of each of the narrow polymer fractions in the surface phase was calculated by assuming that no fractionation occurred within the polymer fractions. The results indicated that the weight of the lower molecular weight fraction,

i.e., Polystyrene PS26, in the surface phase decreased (following an initially rapid adsorption) even though the total weight of adsorbed polymer continued to increase sharply. This behavior appeared to be direct evidence of an exchange phenomenon and suggested that the exchange process was important even in the early stages where the rate of adsorption was high.

The results for long contact times, i.e., greater than 3 days, indicated that the solutes were partitioned between the phases at equilibrium with species from each of the narrow polymer fractions present in both of the phases. A strong preferential adsorption of species from the higher molecular weight fraction was obtained. Both the partitioning behavior and preferential adsorption at equilibrium were in agreement with the behavior observed for samples of broad molecular weight distribution.

Although the polymer fractions employed in this work were of narrow molecular weight distribution, a significant decrease in intrinsic viscosity was obtained when the samples were employed individually in adsorption experiments. Since earlier results indicated that polymer degradation was not significant, the decrease was attributed to fractionation of the narrow polymer fractions. It is not known if the fractionation within the narrow polymer fractions was as great when the samples were combined. Consequently, the results obtained from the exchange experiments must be regarded as qualitative.

In principle, the exchange experiments provide a quantitative method for studying the exchange kinetics.

REPLACEMENT EXPERIMENTS USING POLYSTYRENES
OF NARROW MOLECULAR WEIGHT DISTRIBUTION

EXPERIMENTAL

Replacement experiments were conducted to verify the existence of an exchange phenomenon and to investigate the reversibility of the molecular weight effects.

In the replacement experiments, a narrow fraction of polystyrene in solution was equilibrated with adsorbent. The equilibrium solution was decanted, and the adsorbent was rinsed with pure solvent. Another narrow fraction of polystyrene (of different average molecular weight) in solution was equilibrated with the rinsed adsorbent. The resulting solutions were isolated and analyzed for changes in intrinsic viscosity and concentration.

Six adsorption tubes, each containing 2.0 g. of furnace-treated adsorbent, were employed (Adsorption Run No. 5S1-ECB). Using 15-ml. aliquots, Polystyrene PS26 solution was added to three of the adsorption tubes and Polystyrene PS34 solution to the remaining three. The shaker speed and angle were maintained at 24.0 r.p.m. and 15°, respectively. A minimum of 4 days was permitted for equilibration, after which the solution and adsorbent were separated by centrifugation.

Following decantation of the initial solution, a solvent wash was provided to remove any undecanted solution (containing unadsorbed polystyrene) from the bulk of the adsorbent. After the addition of approximately 20 ml. of pure solvent, the adsorption tubes were resealed and mounted on the shaker for a minimum of 12 hours. The adsorbent, nearly saturated with polystyrene, was redispersed with no difficulty. At the conclusion of the wash period, the

tubes were centrifuged and the wash solvent was decanted and analyzed for polystyrene content.

At that point, the solution additions were interchanged, i.e., Polystyrene PS₃₄ solution was added to the tubes which had initially contained PS₂₆ solution and vice versa. The solution volumes were maintained at 15.0 ml. From the schedule of initial and replacement solutions summarized in Table XXIII, note that the initial solution concentrations were held constant whereas the replacement concentrations were varied.

Following addition of the replacement solutions, the tubes were resealed and mounted on the shaker. A minimum of 4 days was allowed for equilibration before the solution and adsorbent were separated by centrifugation.

The solutions which resulted from equilibrium adsorption of the initial and replacement solutions were isolated and analyzed for changes in intrinsic viscosity and concentration.

RESULTS AND DISCUSSION

The fractionation results for the initial solutions (following equilibrium adsorption) were shown previously in Table XXII (p. 146) to demonstrate the fractionation obtained within the narrow polymer fractions. Note that the intrinsic viscosities of the equilibrium solutions, $[\eta]_{\underline{B}}$, were substantially lower than the original levels, $[\eta]_{\underline{O}}$. Since polymer degradation was not significant, the decreases in intrinsic viscosity were attributed to fractionation of the narrow polymer fractions. Using Equation (43), the intrinsic viscosities for the surface phase were found to be 0.554 and 1.022 dl./g. following equilibration with initial solutions of Polystyrene PS₂₆ and PS₃₄, respectively.

TABLE XXIII
SOLUTIONS USED IN THE REPLACEMENT EXPERIMENTS

Adsorption Tube No.	Initial Solutions			Replacement Solutions		
	Polystyrene Sample	Initial Concentration, mg./cc.	Intrinsic Viscosity, dl./g.	Polystyrene Sample	Initial Concentration, mg./cc.	Intrinsic Viscosity, dl./g.
45	PS34	4.626	0.892	PS26	2.350	0.501
40	PS34	4.626	0.892	PS26	4.514	0.501
42	PS34	4.626	0.892	PS26	7.156	0.501
44	PS26	4.514	0.501	PS34	2.561	0.892
7	PS26	4.514	0.501	PS34	4.626	0.892
16	PS26	4.514	0.501	PS34	7.368	0.892

Since decantation of the initial solution (following equilibration) was unavoidably incomplete, an estimate of the unadsorbed polymer remaining in the bulk of the adsorbent was made from the weight of solution that was decanted. In each case, the weight of polymer subsequently obtained from the wash solvent was less than the corresponding estimate of unadsorbed polymer available, indicating that no significant desorption occurred as a result of the solvent wash.

Several investigators (2, 3, 21, 96, 97, 99, 101) have reported that adsorbed polymer could not be removed by washing (or dilution) with pure solvent. It is believed that the desorption encountered in the present work was negligible.

The final results for the replacement experiments (following equilibrium adsorption of the replacement solutions) are shown in Table XXIV. The "original" values refer to the intrinsic viscosity and concentration of the original replacement solutions, and the "equilibrium" values refer to the same quantities for the bulk phase following equilibration.

TABLE XXIV

RESULTS FROM REPLACEMENT EXPERIMENTS

Adsorption Tube No.	Intrinsic Viscosity, dl./g.		Concentration, mg./cc.		$\frac{X}{A}$
	Original	Equilibrium ^c	Original	Equilibrium ^c	
45 ^a	0.501	0.527	2.350	2.294	0.484
40 ^a	0.501	0.529	4.514	4.258	0.356
42 ^a	0.501	0.528	7.156	6.694	0.277
44 ^b	0.892	0.656	2.561	2.118	0.505
7 ^b	0.892	0.721	4.626	3.917	0.383
16 ^b	0.892	0.773	7.368	6.455	0.290

^a Displacement of previously adsorbed high molecular weight species by lower ones.

^b Displacement of previously adsorbed low molecular weight species by higher ones.

^c Refers to bulk phase.

Although the adsorbent surfaces were nearly saturated with polymer from the initial solution, the concentration of the replacement solution decreased significantly as seen in Table XXIV. Part of the decrease in concentration probably resulted from small quantities of solvent remaining in the bulk of the adsorbent following the solvent wash. (The decantations purposely were not exhaustive in order to prevent losing or drying any of the adsorbent.)

The intrinsic viscosity changes in the replacement solutions (Table XXIV) indicate that an exchange of molecules occurred in both cases, i.e., that the low molecular weight species displaced previously adsorbed higher molecular weight species and vice versa; however, these results must be interpreted with caution. In the case of low molecular weight species displacing higher ones (Tubes No. 45, 40, and 42), the intrinsic viscosity increase was small. Although fractionation of species within the replacement solution (by additional adsorption) would tend to decrease the final equilibrium intrinsic viscosity, any high molecular weight species (from the initial solution) remaining in the bulk of the adsorbent as a result of incomplete decantations, would tend to increase the intrinsic viscosity.

From knowledge of the bulk phase condition following equilibration of initial solutions (Table XXII) and the intrinsic viscosity increase of replacement solutions (Table XXIV), it can be demonstrated that at least 10% of the species in the equilibrium replacement solutions must have come from the initial solutions if no exchange of species occurred. Since this large quantity of species could not have escaped in the initial decantation and the solvent wash, it is concluded that the low molecular weight species probably did replace previously adsorbed higher ones.

In the case of high molecular weight species displacing previously adsorbed lower ones (Tubes No. 44, 7, and 16), the intrinsic viscosity decreases (Table XXIV) were far too large to be accounted for on any basis other than an exchange of solutes. Although the concentration decreases were large, the additional adsorption possible was far too limited to account for the observed decreases in intrinsic viscosity on the basis of fractionation within the replacement solution (see Table XXII). Note that the concentration decreases were significantly larger for experiments involving the displacement of low molecular weight species by higher ones, as expected from the usual increase in Γ_m with increasing molecular weight (see page 146).

Since an exchange of solutes occurred after the initially adsorbed layer had been in contact with the adsorbent for several days, it is believed that the adsorptive forces in the system were only physical in nature.

The total weight and weight fraction of polymer adsorbed, shown in Tables XXV and XXIV, respectively, were calculated on the basis that no polymer losses (no desorption by pure solvent) and no residue losses occurred and that solvent decantation was complete following the solvent wash.

Kolthoff and Gutmacher (19) conducted replacement experiments which differed from the present work only in the lack of a solvent wash. Using a rubber - heptane - carbon black adsorption system, these investigators obtained results similar to those in the present study. Because the final values of intrinsic viscosity in member pairs of experiments were quite different, they stated that incomplete reversibility of adsorption was indicated. (The term, member pair, refers to two replacement experiments with only the addition of the initial and replacement solutions reversed.)

TABLE XXV
COMPOSITION OF THE SURFACE PHASE

Adsorption Tube No.	X_{A26}	X_{A34}	Original Concentration, ^c mg./cc.	Total Weight Adsorbed Polymer, mg.
45 ^a	0.08	0.92	2.350	32.3
40 ^a	0.21	0.79	4.514	35.3
42 ^a	0.32	0.68	7.156	38.4
44 ^b	0.32	0.68	2.561	32.4
7 ^b	0.18	0.82	4.626	36.4
16 ^b	0.11	0.89	7.368	39.5

^a Displacement of previously adsorbed high molecular weight species by lower ones.

^b Displacement of previously adsorbed low molecular weight species by higher ones.

^c Refers to replacement solution.

It should be pointed out that only under the most exact conditions would the final molecular weight distributions of polymer in the supernatant solutions be identical for any member pair in a replacement experiment. In fact, if fractionation occurred within the polymer samples, it would be virtually impossible to obtain such a situation, [Kolthoff and Gutmacher (19) also observed fractionation within their samples.] From the partitioning behavior discussed earlier, one would not expect to obtain similar values of intrinsic viscosity for the final equilibrium solutions unless the molecular weight distributions (of all the polymer present in each system) were nearly identical.

With the following assumptions, an estimate of the surface phase composition, i.e., the weight fraction of surface-phase polymer contributed by each of the narrow polymer fractions, was made: (1) No fractionation occurred within the narrow polymer fractions after the initial solution equilibration. (2) No polymer desorption occurred during the solvent wash. (3) Unadsorbed polymer,

remaining in the bulk of the adsorbent after the initial decantation, was removed completely by the solvent wash. (4) Complete decantation was obtained at the conclusion of the solvent wash. (5) No losses of adsorbent were incurred throughout the experiment. With the above assumptions and the information shown in Tables XXII and XXIV, Equations (118) and (119) were used to calculate the surface-phase weight fractions shown in Table XXV. Although these values are only approximations, the order of magnitude of the weight fractions is similar for both types of displacement, i.e., for low molecular weight species displacing higher ones and high molecular weight species displacing lower ones. Furthermore, these findings are in agreement with earlier results, namely that adsorption of the higher molecular weight fraction was strongly preferred.

The results obtained from the replacement experiments suggest that the molecular weight effects were reversible.

SUMMARY

Replacement experiments, designed to investigate the exchange of different molecular weight species between the bulk and surface phases, were conducted with polystyrene samples of narrow molecular weight distribution.

In the replacement experiments, solution containing a narrow polymer fraction was equilibrated with adsorbent and decanted. The resulting adsorbent was rinsed with pure solvent and equilibrated with another solution of a narrow polymer fraction (of different average molecular weight).

Following decantation of the initial solution, a solvent wash was provided to remove undecanted solution (containing unadsorbed polystyrene) from the bulk of the adsorbent. From the limited quantities of polymer found in the wash

solvents, it was concluded that no significant desorption of polymer was caused by prolonged washing (12 hours) with pure solvent.

The intrinsic viscosity of the replacement solutions increased when the adsorbent had been equilibrated previously with solution containing a higher molecular weight fraction and decreased when equilibrated previously with solution containing a lower molecular weight fraction. It was concluded that the low molecular weight species probably did replace previously adsorbed higher ones. The displacement of previously adsorbed low molecular weight species by higher ones was firmly established - in agreement with the nonequilibrium runs with polystyrene of broad molecular weight distribution and the exchange experiments.

An exchange of polymer molecules occurred between the bulk and surface phases even after the initially adsorbed layer had been in contact with the adsorbent for several days, indicating that the adsorptive forces in the system were only physical in nature.

From the intrinsic viscosity changes in the replacement solutions, an estimate was made of the weight fraction of surface-phase polymer contributed by each of the narrow polymer fractions. The order of magnitude of these weight fractions was similar for both types of displacement, i.e., for the displacement of previously adsorbed low molecular weight species by higher ones and vice versa, and demonstrated that adsorption of the higher molecular weight fraction was preferred strongly.

The results obtained from the replacement experiments suggested that the molecular weight effects were reversible, but this could not be established because of such qualitative factors as fractionation within the narrow polymer fractions.

GENERAL DISCUSSION

POLYMER DEGRADATION

It has been suggested in the literature that prolonged contact between polymer molecules and adsorbent may cause extensive degradation of the polymer. It is believed that no significant degradation was encountered in the present work. In each case, the intrinsic viscosity approached a constant value (at the end of 3 days) and did not change significantly, thereafter, upon continued exposure to the adsorbent for periods up to 5 days. There is no reason to believe that polymer degradation would cease after a certain period of time and that the partitioning relationships subsequently observed were coincidental. Furthermore, the equilibrium fractionation curves (see Fig. 18) closely extrapolate back to the original level of intrinsic viscosity.

STRUCTURE OF THE SURFACE LAYER

Recent studies of a theoretical and experimental nature have investigated the structure of the surface layer. Silberberg (5, 79) and Higuchi (90) demonstrated by diverse statistical treatments, that strong surface interactions can cause a nearly complete collapse of polymeric adsorbates on solid substrates.

Using infrared spectrometry, Fontana and Thomas (1) studied the configuration of alkyl methacrylate polymers adsorbed from solution onto a nonporous silica. From the infrared shift of the normal carbonyl vibration frequency, caused by hydrogen bonding to the surface hydroxyl groups, these investigators determined the fraction of adsorbed carbonyl groups, i.e., \bar{p} . On the average, about 36% of the segments were attached to the substrate, indicating that the polymer was essentially flattened at the interface. In confirmation, sedimentation velocity studies indicated that the effective hydrodynamic thickness of the adsorbed layer was 25 ± 10 Å.

Using a vibrating electrode apparatus, Gottlieb (3) studied the adsorption of polyvinyl acetate from various solvents onto metal substrates. Surface potential measurements for octadecyl and polyvinyl acetates were compared as a function of the surface coverage. It was concluded that the surface was covered first by a layer of tightly bound polymer with most of the acetate groups oriented and in contact with the surface; subsequent polymer deposition was believed to occur as a random overfilm on top of the first layer of oriented molecules. (Gottlieb admitted that the surface potential data may not represent the structure of the surface layer as adsorbed from solution but may represent structures which result from rearrangements following removal from solution.)

From their experimental results, Jenckel and Rumbach (102) postulated that the adsorbed layer consisted of sparsely adsorbed segments bridged by loops of unadsorbed segments extending into the solution — a concept which corresponds closely to the models analyzed by Silberberg (79). Stromberg, et al. (2) suggested that the extensive thicknesses observed for adsorbed polystyrene layers could correspond to either the extended loops postulated by Jenckel and Rumbach (102) or the random overfilm advanced by Gottlieb (3). From earlier discussions regarding the restrictive nature of the phenyl group, it seems unlikely that the adsorption of polystyrene would correspond to Gottlieb's proposal.

It is of interest to compare the quantity of adsorbed polymer with the area occupied by small molecules of similar chemical make-up. Van der Waarden (103) found that xylene was adsorbed in a flattened configuration and occupied a cross-sectional area of approximately 0.63 A.^2 . Harris and Emmett (104) compared the adsorption of toluene (75°C.) with nitrogen (-195°C.) on a variety of surfaces. For toluene, the cross-sectional area calculated from the density

of the liquified adsorbate (32.9 A.^2) was not sufficient to account for the area actually occupied ($\approx 61 \text{ A.}^2$), indicating that the molecule was adsorbed in a flat position.

The maximum surface concentration, calculated with Equation (114) on page 137, was $1.28 \times 10^{-4} \text{ mg./sq. cm.}$ for the system employed in the present study. This concentration of polymer is about 4.4 times greater than that which the surface would accommodate by assuming that the adsorbate was flattened at the interface and that each segment occupied a cross-sectional area of 60 A.^2 (in accordance with the areas found for similar small molecules).

From the adsorbate structure advanced by Jenckel and Rumbach (102), it is of interest to compare the area occupied by the adsorbate with the molecular dimensions exhibited in solution. The dimensions of polystyrene in dichloroethane at 25°C. have been investigated by Outer, *et al.* (83). For a polystyrene fraction ($\overline{M}_w = 5.62 \times 10^5$) having an intrinsic viscosity (1.42 dl./g.) similar to the $[\eta]_A$ values obtained in the present work (see Fig. 19 and 20), a weight-average root-mean-square radius of gyration of 310 A. was obtained. Using that dimension for the adsorbate radius and assuming an hexagonal packing on the substrate, the area required by this hypothetical structure was found to be 4.6 times greater than that available experimentally - indicating that the polymer coil undergoes considerable compression upon adsorption.

BEHAVIOR OF THE SURFACE LAYER

Several observations indicate that the surface layer possesses a dynamic character - at least in adsorption systems where adsorbate-substrate interactions are limited to attractive forces of the van der Waals type. Irrespective of the exact structure of the surface layer, it is quite certain that the

polymer molecule is adsorbed at multiple points of attachment along the chain. It is envisioned that the individual segments of an adsorbed molecule are continually being adsorbed and desorbed with no substantial net changes in the total number of adsorbed segments in the system (at equilibrium).

As noted earlier, adsorbed polymer generally is not removed by washing (or dilution) with pure solvent. Silberberg (5) has stated that this inability of the solvent to desorb the polymer is merely an expression of the fact that the surface is still in equilibrium with the solvent. In this case, the solvent is unable to compete for additional adsorption sites.

It has been demonstrated (19, 80, 97) that solvent with a greater affinity for the polymer or the substrate (greater than the solvent from which adsorption occurred) can remove previously adsorbed molecules. As the individual segments of an adsorbed molecule undergo adsorption and desorption, it is envisioned that the new solvent molecules (which are not in equilibrium with the substrate) are able to compete for the occupancy of vacated sites. Ultimately, the polymer molecule is released from the substrate.

A similar mechanism is believed to be responsible for the exchange of adsorbate species. When new polymeric species are introduced into the adsorption system (solutes which have not previously been in equilibrium with the surface), they conceivably compete for desorbed sites, eventually resulting in the displacement of previously adsorbed species. Apparently, the process continues until an equilibrium partitioning of all the species is obtained. From the excessive size and low mobility of polymeric adsorbates, it is not surprising that the exchange process is relatively slow (nearly 3 days required for equilibration).

It is believed that the exchange phenomenon made it possible for the system to attain a distinct partitioning condition at equilibrium. The existence of a partitioning relationship indicates that the adsorbed molecules are accessible to molecules in the bulk phase, making it difficult to envision an adsorbed structure composed of a tightly bound two-dimensional layer covered with a random overfilm as advanced by Gottlieb (3). Rearrangement of the surface layer from a two- to a three-dimensional structure with increasing surface coverage, as postulated by Peterson and Kwei (96) from kinetic studies, would explain this difficulty.

It is of interest to note that Ellerstein (8) did not observe a substantial exchange of polymeric species during the adsorption of polymethyl methacrylate ($\frac{M_w}{M_n} > 2$) from benzene onto iron powder. The intrinsic viscosity of the polymer solutions decreased approximately 14% in the first 10 min. of adsorption followed by an additional 6% in the next 72 hours. It was noted that urea or a similar compound was tightly bound to the adsorbent surfaces (desorbed only with acetonitrile); this may have promoted hydrogen bonding (of the type O...H-N) or some other strong interaction which can retard the exchange process.

SUMMARY AND CONCLUSIONS

The role of adsorbate polymolecularity in the adsorption of high polymers at liquid-solid interfaces was investigated with the polystyrene - dichloroethane - carbon black system. Polystyrene samples of broad and narrow molecular weight distribution were employed. The adsorbent (Sterling-FT graphitized carbon black) had a specific surface area of 12.4 sq. m./g., determined by nitrogen gas adsorption.

Solutions of polystyrene were mixed with the adsorbent for specified periods of time, and the resulting supernatant solutions were isolated and analyzed for changes in intrinsic viscosity and concentration. The weight of adsorbed polymer was determined from the change in solution concentration. Fractionation and preferential adsorption of the polymer were adjudged by changes in intrinsic viscosity.

For adsorption experiments employing polystyrene of broad molecular weight distribution and a mixture of narrow polystyrene fractions, no additional changes in either intrinsic viscosity or the weight of adsorbed polymer occurred after 3 days of adsorption, indicating that the system required approximately 3 days for equilibration and that polymer degradation was negligible.

Whenever distribution functions of polymer were required, distributions of sedimentation coefficient were determined with an ultracentrifugal technique. Corrections were applied to the distributions for the effects of diffusion and solution concentration.

The following is a summary of the main experiments conducted, the results obtained, and the conclusions drawn therefrom.

Employing polystyrenes of broad molecular weight distribution, equilibrium adsorption experiments were conducted for different ratios of adsorbent to solution over a wide range of solution concentration. The adsorption data were described by the Langmuir isotherm over nearly four decades of concentration and for a wide range of surface coverage, confirming Langmuir behavior as predicted by Silberberg (5) and reported (1, 80, 99) in previous investigations. The polymers were strongly adsorbed in the system, nearly saturating the adsorbent surfaces at equilibrium concentrations as low as 0.05% by weight.

The intrinsic viscosity of supernatant solutions (bulk phase) was lower in all cases than the original level and depended only on the weight fraction of polymer adsorbed. From the weight additivity of viscometric quantities, the intrinsic viscosity of polymer in the surface phase was calculated and found to be higher in all cases than that of the original polymer, showing that the polymer samples were fractionated significantly by the adsorption process and that the higher molecular weight species were adsorbed preferentially for all the equilibrium conditions investigated. Fractionation appeared to depend only on the weight fraction of polymer adsorbed, irrespective of the ratio of adsorbent to solution or equilibrium concentration.

Knowing the distribution functions for the original polymer samples, perfect fractionation curves were calculated and compared with the intrinsic viscosity results. It was apparent that the observed fractionation was not perfect or complete and that the adsorption process could not be used to predict the molecular weight distribution or its equivalent by the methods employed.

The intrinsic viscosity, i.e., fractionation, apparently depended only on the weight fraction of polymer adsorbed. However, the strong affinity of polymer

for the adsorbent surfaces limited the viscometric data to the region of nearly complete surface coverage, thereby limiting the validity of the experimental relationships to that region.

The fact that the adsorption and fractionation results were independent of the ratio of adsorbent to solution indicated that the adsorbent was dispersed readily in the solutions and that a consistent fraction of the surface area was available for adsorption.

For selected equilibrium adsorption experiments with polystyrene of broad molecular weight distribution, the distribution of sedimentation coefficient was determined for the polymer in each of the supernatant solutions. Knowing the polymer distributions (for the bulk phase) before and after adsorption, the distribution of polymer in the surface phase was calculated. In each case, the distributions for the bulk and surface phases were related by a partitioning expression which differed substantially from that describing phase separation. The experimental relationship did not agree with the three-dimensional case derived by Gilliland and Gutoff (24); this discrepancy probably resulted from an oversimplification of the polymer adsorption problem in their statistical treatment.

By comparing distributions for corresponding bulk and surface phases, it was evident that the polymer was fractionated significantly by the adsorption process. The molecular weight averages for the surface phase were approximately twice as high as those for the bulk phase. Although a strong fractionation was observed, the equilibrium adsorption process was not an efficient analytical tool for molecular separations — the polymer in either phase following adsorption was distributed broadly with respect to molecular weight.

The surface-phase distributions from two experiments involving different equilibrium concentrations and similar extents of adsorption were nearly identical, indicating that solution concentration did not affect the fractionation process significantly.

To investigate the adsorption process during the approach to equilibrium, adsorption experiments were conducted with polystyrene of broad molecular weight distribution, varying only the contact time, i.e., the adsorption time, and the degree of agitation. In these experiments, the intrinsic viscosity of the solution (bulk phase) increased very rapidly with contact time, reaching a maximum in approximately two minutes. Thereafter, the viscosity decreased nearly linearly with the logarithm of contact time until equilibrium was approached at which time the intrinsic viscosity was well below that of the original solution. No further decreases occurred after 3 days, indicating that equilibrium had been established.

The intrinsic viscosity of the surface phase was calculated from the weight additivity of viscometric quantities. Initially, the intrinsic viscosity of the surface phase was well below the level of the original solution; thereafter, it increased nearly linearly with the logarithm of contact time until equilibrium was approached and was well above the level of the original solution at equilibrium.

The intrinsic viscosity results for each of the runs were compared for similar extents of adsorption, i.e., vs. the weight fraction of polymer adsorbed. The data for different degrees of agitation fell on a single curve, indicating that differences in fluid-film thickness, i.e., differences in diffusional transport, during the period of agitation did not affect the fractionation observed.

The intrinsic viscosity results for the surface phase demonstrated that the smaller molecules were preferentially adsorbed initially, the initial fractionation being well below the maximum limit given by the perfect fractionation curve. From analysis of experimental fractionation curves, i.e., plots of intrinsic viscosity vs. the weight fraction of polymer adsorbed, it was concluded that the displacement of initially adsorbed small molecules by larger ones was in part responsible for the fractionation behavior observed during the approach to equilibrium - confirming the displacement behavior suggested by previous investigators (17-19, 21, 92).

Similar intrinsic viscosity behavior was observed for different polymer samples of broad molecular weight distribution, indicating that the fractionation process during the approach to equilibrium was of a rather general nature.

In agreement with the fractionation results, an analysis of diffusional transport across a fluid film indicated that diffusion of solutes was not an important rate-controlling factor in the time range over which the experimental observations were made. However, the initial fractionation already was well established by the time the earliest measurements were made, and differential diffusion rates could have been responsible for this behavior. Whether the initial fractionation was caused by differences in solute diffusion rates, molecular adsorption rates, or a combination of these factors was not known, but the work of Peterson and Kwei (96) indicated that differences in solute mobilities at the interface, i.e., differences in molecular adsorption rates, were probably more important.

To verify the existence of a displacement or exchange process during the approach to equilibrium, adsorption experiments were conducted with a mixture

of two narrow polymer fractions. Only the contact time, i.e., adsorption time, was varied in these exchange experiments. The intrinsic viscosity behavior of the polymer mixture was similar to that observed for samples of broad molecular weight distribution except that no increase in intrinsic viscosity was observed initially, indicating that low molecular weight species were not preferentially adsorbed initially. This was probably the result of two factors: (1) the average molecular weights of the narrow polymer fractions differed only by a factor of two, restricting the ultimate preferential adsorption, and (2) the exchange process may have been extremely rapid because of the low molecular weights involved.

From the viscometric data, the weight of each of the narrow polymer fractions in the surface phase was calculated by assuming that no fractionation occurred within the individual polymer fractions. The weight of adsorbed polymer constituted by the lower molecular weight fraction decreased with adsorption time (following an initially rapid adsorption) even though the total weight of adsorbed polymer increased sharply. This behavior appeared to be direct evidence of an exchange phenomenon (the lower molecular weight material having been displaced by the higher molecular weight species) and suggested that the exchange process was important even in the early stages where the rate of adsorption was high.

Although the polymer samples employed in the exchange experiments were of narrow molecular weight distribution, a significant decrease in the intrinsic viscosity of the bulk phase was obtained when the samples were adsorbed individually. Since polymer degradation was negligible, the decrease was attributed to fractionation within the narrow polymer fractions. It is not known if fractionation within the narrow polymer fractions was as great when they were combined.

Consequently, the results obtained from the exchange experiments were regarded as qualitative.

In spite of their qualitative nature, the fractionation results for long contact times, i.e., greater than 3 days, indicated that the solutes were partitioned between the phases at equilibrium (with species from each of the narrow polymer fractions present in both phases) and that a strong preferential adsorption of the higher molecular weight fraction was obtained - in agreement with the equilibrium behavior observed for samples of broad molecular weight distribution.

In principle, exchange experiments employing samples of very narrow molecular weight distribution provide a quantitative method for studying the exchange kinetics.

In order to confirm the existence of a displacement or exchange process and to investigate the displacement ability of different molecular weight species, replacement experiments were conducted with polystyrene samples of narrow molecular weight distribution. In these experiments, solution containing a narrow polymer fraction was equilibrated with adsorbent and decanted. The resulting adsorbent was rinsed with pure solvent and equilibrated with another solution of a narrow polymer fraction (of different average molecular weight).

After rinsing the adsorbent, the solvent contained only limited quantities of polymer, indicating that no significant desorption of polymer was caused by prolonged exposure (12 hours) to pure solvent.

The intrinsic viscosity of the replacement solutions increased when the adsorbent had been equilibrated previously with solution containing a higher

molecular weight fraction and decreased when equilibrated previously with solution containing a lower molecular weight fraction. It was concluded that low molecular weight species probably did displace previously adsorbed higher ones. The displacement of previously adsorbed low molecular weight species by higher ones was firmly established - in agreement with experiments employing polystyrene of broad molecular weight distribution and the exchange experiments.

An exchange of polymer molecules occurred between the bulk and surface phases even after the initially adsorbed layer had been in contact with the adsorbent for several days, indicating that the adsorptive forces in the system were only physical in nature.

From intrinsic viscosity changes in the replacement solutions, an estimate was made of the weight fraction of surface-phase polymer contributed by each of the narrow polymer fractions. The order of magnitude of these weight fractions was similar for both types of displacement, i.e., for the displacement of previously adsorbed low molecular weight species by higher ones and vice versa, and demonstrated that the higher molecular weight fraction was adsorbed preferentially.

The results obtained from the replacement experiments suggested that the molecular weight effects were reversible, but this could not be established because of such qualitative factors as fractionation within the narrow polymer fractions.

In conclusion, it is believed from the exchange and partitioning phenomena encountered in the present study that the exchange process made it possible for the adsorption system to attain a distinct partitioning condition at equilibrium - one which conceivably minimized the Gibbs free energy of the system.

SUGGESTIONS FOR FUTURE RESEARCH

It was noted in the text that recent attempts to apply more powerful methods to the investigation of polymer adsorption have been successful. Techniques such as infrared spectrometry, ellipsometry, and surface potential studies hold promise for further research.

From the present study, there appear to be several logical extensions which warrant further investigation.

The equilibrium partitioning behavior needs to be studied more extensively than was undertaken in the present work. The existence of such a phenomenon implies that a thermodynamic equilibrium can be attained. This is particularly important from a theoretical standpoint. Investigation along this line can be pursued by extending the present study to include a variety of molecular weight distributions. Improvements in the ultracentrifugal technique would be desirable, particularly with regard to the "tail" region.

Of interest to the paper industry is the possible existence of an exchange phenomenon in hydrogen-bonded systems. A study similar to the present one should be made with an adsorbate-adsorbent combination which can form hydrogen bonds at the interface. (Any adsorbate which tends to form hydrogen bonds with itself should be avoided.) The system employed by Fontana and Thomas (1), i.e., methacrylate polymers and nonporous silica, should be satisfactory and could be compared directly with one involving only weak interactions, by an appropriate change of adsorbent. The value of radioactive adsorbate in such investigations should not be overlooked.

The investigation of rate phenomena is a challenge experimentally but may be very rewarding. Using the method of Peterson and Kwei (96), it should be

possible to evaluate the dependence of adsorption rate on the molecular weight of the adsorbate. At present, there is no conclusive evidence of such an effect although it is well established that a very rapid fractionation can be obtained initially in adsorption systems (usually attributed to diffusion).

A kinetic study of the exchange phenomenon, as outlined in the text, may reveal the nature of the exchange process. Also, a quantitative study of the reversibility of molecular weight effects with replacement experiments might be helpful in establishing the existence of a thermodynamic equilibrium.

ACKNOWLEDGMENTS

The author would like to express his sincere appreciation to the numerous members of the faculty and staff at The Institute of Paper Chemistry who have contributed on countless occasions to the completion of this thesis.

The aid of a number of individuals is sincerely appreciated and worthy of special mention. Grateful acknowledgments are made to the following: J. W. Swanson, chairman of the thesis advisory committee, S. F. Kurath and W. P. Riemen, committee members, for their continued guidance, patience, and encouragement throughout the course of this work; J. A. Carlson and E. O. Dillingham for their aid and guidance in securing the sedimentation velocity data; Miss. O. A. Smith for obtaining the electron micrographs; J. D. Hultman for securing the nitrogen gas adsorption data; L. O. Sell for operating the Beckman model DK-2 spectrophotometer; H. Marx and M. C. Filz, Jr. for their aid in the design and construction of apparatus; H. A. Swenson for many helpful discussions and his criticism of the manuscript; Mrs. S. M. Emery for typing and proofreading the manuscript.

Finally, the author would like to express his deepest appreciation to Mr. John W. Swanson, Mr. Edgar E. Dickey, and Mrs. Sylvia M. Emery for their outstanding support and encouragement which made the completion of this thesis a reality.

LITERATURE CITED

1. Fontana, B. J., and Thomas, J. R., J. Phys. Chem. 65:480-7(1961).
2. Stromberg, R. R., Passaglia, E., and Tutas, D. J., J. Res. Natl. Bur. Std. 67A, no. 5:431-40(1963).
3. Gottlieb, M. H., J. Phys. Chem. 64:427-32(1960).
4. Hughes, R. E., and von Frankenberg, C. A. High Polymers. In Annual review of physical chemistry. Vol. 14. p. 291. Palo Alto, Calif., Annual Reviews, Inc., 1963.
5. Silberberg, A., J. Phys. Chem. 66:1884-907(1962).
6. Koral, J. The adsorption of polyvinyl acetate from solution on to solid surfaces. Doctor's Dissertation. Brooklyn, N. Y., Polytechnic Institute of Brooklyn, 1957. 105 p.
7. Perkel, R. J. The adsorption of polydimethyl siloxanes from solution on solid surfaces. Doctor's Dissertation. Brooklyn, N. Y., Polytechnic Institute of Brooklyn, 1959. 189 p.
8. Ellerstein, S. The adsorption of poly-(methyl methacrylate) from solution. Doctor's Dissertation. Brooklyn, N. Y., Polytechnic Institute of Brooklyn, 1960. 138 p.
9. Mark, H., and Saito, G., Monatsh. 68:237-43(1936); C.A. 31:252.
10. Levi, G. R., and Giera, A., Gazz. chim. ital. 67:719-23(1937); C.A. 32:4327.
11. Goldfinger, G., Rubber Chem. and Technol. 18:286-91(1945).
12. Goldfinger, G., J. Polymer Sci. 1:58-62(1946).
13. Amborski, L. E., Black, C. E., and Goldfinger, G., Rubber Chem. and Technol. 23:417-24(1950).
14. Iandler, I., Rubber Chem. and Technol. 21:682-3(1948).
15. Claesson, I., and Claesson, S., Phys. Rev. 73:1221(1948).
16. Claesson, S., Discn. Faraday Soc. 7:321-5(1949).
17. Kolthoff, I. M., and Kahn, A., J. Phys. Colloid Chem. 54:251-6(1950).
18. Kolthoff, I. M., Gutmacher, R. G., and Kahn, A., J. Phys. Colloid Chem. 55:1240-6(1951).
19. Kolthoff, I. M., and Gutmacher, R. G., J. Phys. Chem. 56:740-5(1952).
20. Gilliland, E. R., and Gutoff, E. B., J. Appl. Polymer Sci. 3, no. 7:26-42 (1960).

21. Frisch, H. L., Hellman, M. Y., and Lundberg, J. L., J. Polymer Sci. 38:441-9 (1959).
22. Swenson, H. A., Acta Chem. Scand. 9:572-82(1955).
23. Miller, B., and Pacsu, E., J. Polymer Sci. 41:97-117(1959).
24. Gilliland, E. R., and Gutoff, E. B., J. Phys. Chem. 64:407-10(1960).
25. Fox, T. G., Jr., and Flory, P. J., J. Am. Chem. Soc. 73:1915-20(1951).
26. Rudd, J. F., J. Polymer Sci. 44:459-74(1960).
27. McCormick, H. W., J. Polymer Sci. 36:341-9(1959).
28. McCormick, H. W., Brower, F. M., and Kin, L., J. Polymer Sci. 39:87-100(1959).
29. Taylor, D. L. An evaluation of column thermal diffusion as a means of polymer characterization. Doctor's Dissertation. Appleton, Wis., The Institute of Paper Chemistry, 1962. 123 p.
30. Barton, D. H. R., and Howlett, K. E., J. Chem. Soc. 1949:155-64.
31. Maclean, M. E., Jencks, P. J., and Acree, S. F., J. Res. Natl. Bur. Std. 34:271-80(1945).
32. Committee on Emission Spectroscopy of the American Society for Testing Materials. Methods for emission spectrochemical analysis. 3rd ed. Philadelphia, Pa., American Society for Testing Materials, 1960. 685 p.
33. Timmermans, J., and Martin, F., J. chim. phys. 25:411-51(1928); C.A. 22:4024.
34. Trice, W. H. The effect of autoxidation on the wettability of a linoleic acid monolayer. Doctor's Dissertation. Appleton, Wis., The Institute of Paper Chemistry, 1963. 168 p.
35. Schaeffer, W. D., Smith, W. R., and Polley, M. H., Ind. Eng. Chem. 45, no. 8:1721-5(1953).
36. Biscoe, J., and Warren, B. E., J. Appl. Phys. 13:364-71(1942).
37. Beebe, R. A., Biscoe, J., Smith, W. R., and Wendell, C. B., J. Am. Chem. Soc. 69:95-101(1947).
38. Polley, M. H., Schaeffer, W. D., and Smith, W. R., J. Phys. Chem. 57:469-71 (1953).
39. Smith, W. R., and Polley, M. H., J. Phys. Chem. 60:689-91(1956).
40. Graham, D., J. Phys. Chem. 61:1310-13(1957).
41. Singleton, J. H., and Halsey, G. D., Jr., J. Phys. Chem. 58:330-5(1954).

42. Beebe, R. A., Millard, B., and Cynarski, J., J. Am. Chem. Soc. 75:839-45 (1953).
43. Joyner, L. G., and Emmett, P. H., J. Am. Chem. Soc. 70:2353-9(1948).
44. Pierce, C., and Smith, R. N., J. Am. Chem. Soc. 75:846-8(1953).
45. Hall, C. E., J. Appl. Phys. 19:271-7(1948).
46. Walker, P. L., Jr., McKinstry, H. A., and Wright, C. C., Ind. Eng. Chem. 45, no. 8:1711-15(1953).
47. Brunauer, S., Emmett, P. H., and Teller, E., J. Am. Chem. Soc. 60:309-19 (1938).
48. Emmett, P. H., and Brunauer, S., J. Am. Chem. Soc. 59:1553-64(1937).
49. Corrin, M. L., J. Am. Chem. Soc. 73:4061-5(1951).
50. Smith, R. N., Pierce, C., and Joel, C. D., J. Phys. Chem. 58:298-302(1954).
51. Healey, F. H., Yu, Y.-f., and Chessick, J. J., J. Phys. Chem. 59:399-402 (1955).
52. Cannon, M. R., Manning, R. E., and Bell, J. D., Anal. Chem. 32, no. 3:355-8 (1960).
53. Fox, T. G., Jr., Fox, J. C., and Flory, P. J., J. Am. Chem. Soc. 73:1901-4 (1951).
54. Fox, T. G., Jr., and Flory, P. J., J. Am. Chem. Soc. 73:1909-15(1951).
55. Huggins, M. L., J. Am. Chem. Soc. 64:2716-18(1942).
56. McCormick, H. W., J. Colloid Sci. 16:635-7(1961).
57. Maron, S. H., J. Appl. Polymer Sci. 5:282-4(1961).
58. Heller, W., and Thompson, A. C., J. Colloid Sci. 6:57-74(1951).
59. Griffel, M., Jessup, R. S., Cogliano, J. A., and Park, R. P., J. Res. Natl. Bur. Std. 52, no. 4:217-22(1954).
60. Rosen, B., J. Polymer Sci. 17:559-81(1955).
61. Schulz, G. V., and Hoffmann, M., Makromol. Chem. 23:220-32(1957).
62. Williams, J. W., Van Holde, K. E., Baldwin, R. L., and Fujita, H., Chem. Rev. 58:715-806(1958).
63. Baldwin, R. L., and Van Holde, K. E., Fortschr. Hochpolymer-Forsch. 1, no. 4:451-511(1960).

64. Fujita, H. Mathematical theory of sedimentation analysis. New York, Academic Press, 1962. 315 p.
65. Schachman, H. K. Ultracentrifugation in biochemistry. New York, Academic Press, 1959. 272 p.
66. Baldwin, R. L., and Williams, J. W., J. Am. Chem. Soc. 72:4325(1950).
67. Flory, P. J. Principles of polymer chemistry. Ithaca, Cornell Univ. Press, 1953. 672 p.
68. Cantow, H.-J., Makromol. Chem. 30:169-88(1959).
69. Krigbaum, W. R., J. Am. Chem. Soc. 76:3758-64(1954).
70. Schultz, A. R., and Flory, P. J., J. Polymer Sci. 11:37-51(1953).
71. Krigbaum, W. R., and Carpenter, D. K., J. Phys. Chem. 59:1166-72(1955).
72. Trautman, R., and Schumaker, V., J. Chem. Phys. 22:551-4(1954).
73. Baldwin, R. L., Gosting, L. J., Williams, J. W., and Alberty, R. A., Disc. Faraday Soc. 20:13-24(1955).
74. Williams, J. W., Baldwin, R. L., Saunders, W. M., and Squire, P. G., J. Am. Chem. Soc. 74:1542-8(1952).
75. Baldwin, R. L., J. Phys. Chem. 58:1081-6(1954).
76. Baldwin, R. L., J. Phys. Chem. 63:1570-3(1959).
77. Eriksson, A. F. V., Acta Chem. Scand. 10:360-77(1956).
78. Baldwin, R. L., J. Am. Chem. Soc. 76:402-7(1954).
79. Silberberg, A., J. Phys. Chem. 66:1872-83(1962).
80. Koral, J., Ullman, R., and Eirich, F. R., J. Phys. Chem. 62:541-50(1958).
81. Davies, O. L. Statistical methods in research and production. New York, Hafner Publishing Co., 1958. 396 p.
82. Flory, P. J., J. Am. Chem. Soc. 65:372-82(1943).
83. Outer, P., Carr, C. I., and Zimm, B. H., J. Chem. Phys. 18:830-9(1950).
84. McCormick, H. W., J. Polymer Sci. 1A:103-10(1963).
85. Frisch, H. L., Simha, R., and Eirich, F. R., J. Chem. Phys. 21:365-6(1953).
86. Frisch, H. L., and Simha, R., J. Phys. Chem. 58:507-12(1954).
87. Simha, R., Frisch, H. L., and Eirich, F. R., J. Phys. Chem. 57:584-9(1953).

88. Frisch, H. L., J. Phys. Chem. 59:633-6(1955).
89. Frisch, H. L., and Simha, R., J. Chem. Phys. 27:702-6(1957).
90. Higuchi, W. I., J. Phys. Chem. 65:487-91(1961).
91. de Boer, J. H. Atomic forces and adsorption. In Advances in colloid science. Vol. 3. p. 27. New York, Interscience, 1950.
92. Skolnik, L. The adsorption of polystyrene from solution by carbon black. Doctor's Dissertation. Cleveland, Ohio, Case Institute of Technology, 1952. 69 p.
93. Gosting, L. J. Measurement and interpretation of diffusion coefficients of proteins. In Advances in protein chemistry. Vol. XI. New York, Academic Press Inc., 1956. 665 p.
94. Crank, J. The mathematics of diffusion. Oxford, Oxford Univ. Press, 1957. 347 p.
95. Tsvetkov, V. N., and Klenin, S. I., Doklady Akad. Nauk S.S.S.R. 88:49-52 (1953); C.A. 47:5765.
96. Peterson, C., and Kwei, T. K., J. Phys. Chem. 65:1330-3(1961).
97. Ellerstein, S., and Ullman, R., J. Polymer Sci. 55:123-35(1961).
98. Ullman, R., Trans. N. Y. Acad. Sci. 20, no. 6:483-92(1958).
99. Binford, J. S., and Gessler, A. M., J. Phys. Chem. 63:1376-8(1959).
100. Heller, W., and Tanaka, W., Phys. Rev. 82:302(1951).
101. Stromberg, R. R., Quasius, A. R., Toner, S. D., and Parker, M. S., J. Res. Natl. Bur. Std. 62, no. 2:71-7(1959).
102. Jenckel, E., and Rumbach, B., Z. Electrochem. 55:612-18(1951).
103. Van der Waarden, M. J., J. Colloid Sci. 6:443-9(1951).
104. Harris, B. L., and Emmett, P. H., J. Phys. Colloid Chem. 53:811-25(1949).
105. Billick, I. H., J. Phys. Chem. 66:1941-4(1962).

APPENDIX I

INTRINSIC VISCOSITY DETERMINATIONS AND
RELATED PARAMETERS

TABLE XXVI

SUMMARY OF INTRINSIC VISCOSITY RESULTS

Polystyrene Sample	Temperature, °C.	$[\eta]$, dl./g.	$\frac{k}{\alpha}$	$\frac{k}{\beta}$	$(\frac{k}{\alpha} + \frac{k}{\beta})$
B6	30.0	1.090	0.330	0.157	0.487
PB6	30.0	1.078	0.339	0.152	0.491
	25.0	1.078	0.332	0.154	0.486
PS34	30.0	0.892	0.319	0.166	0.485
	25.0	0.885	0.329	0.161	0.490
PS26	30.0	0.501	0.355	0.146	0.501
	25.0	0.498	0.364	0.143	0.507
DRT8	30.0	0.760	--	--	--

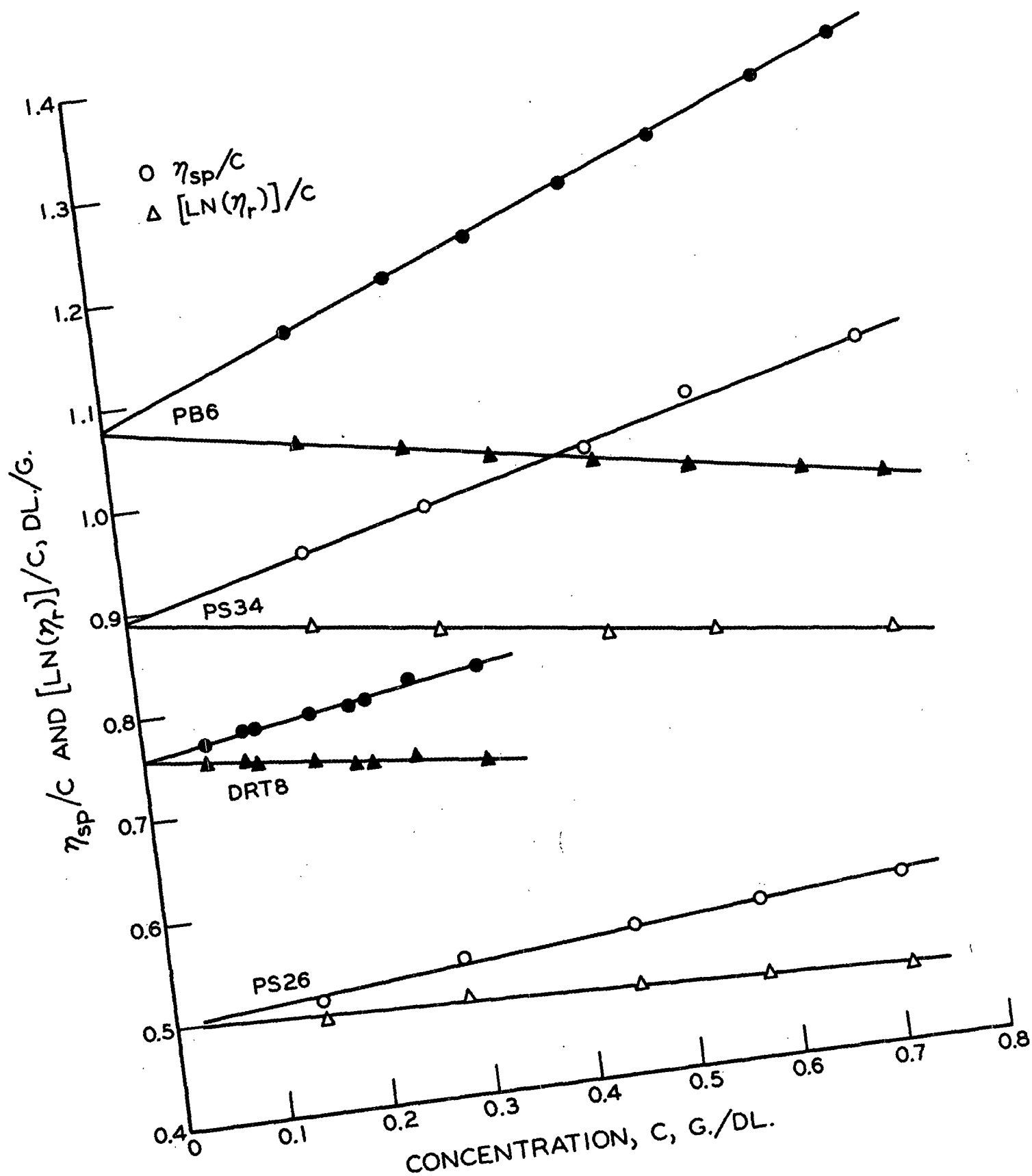


Figure 42. Intrinsic Viscosity Determinations of Polystyrene Samples in 1,2-Dichloroethane at 30.0°C.

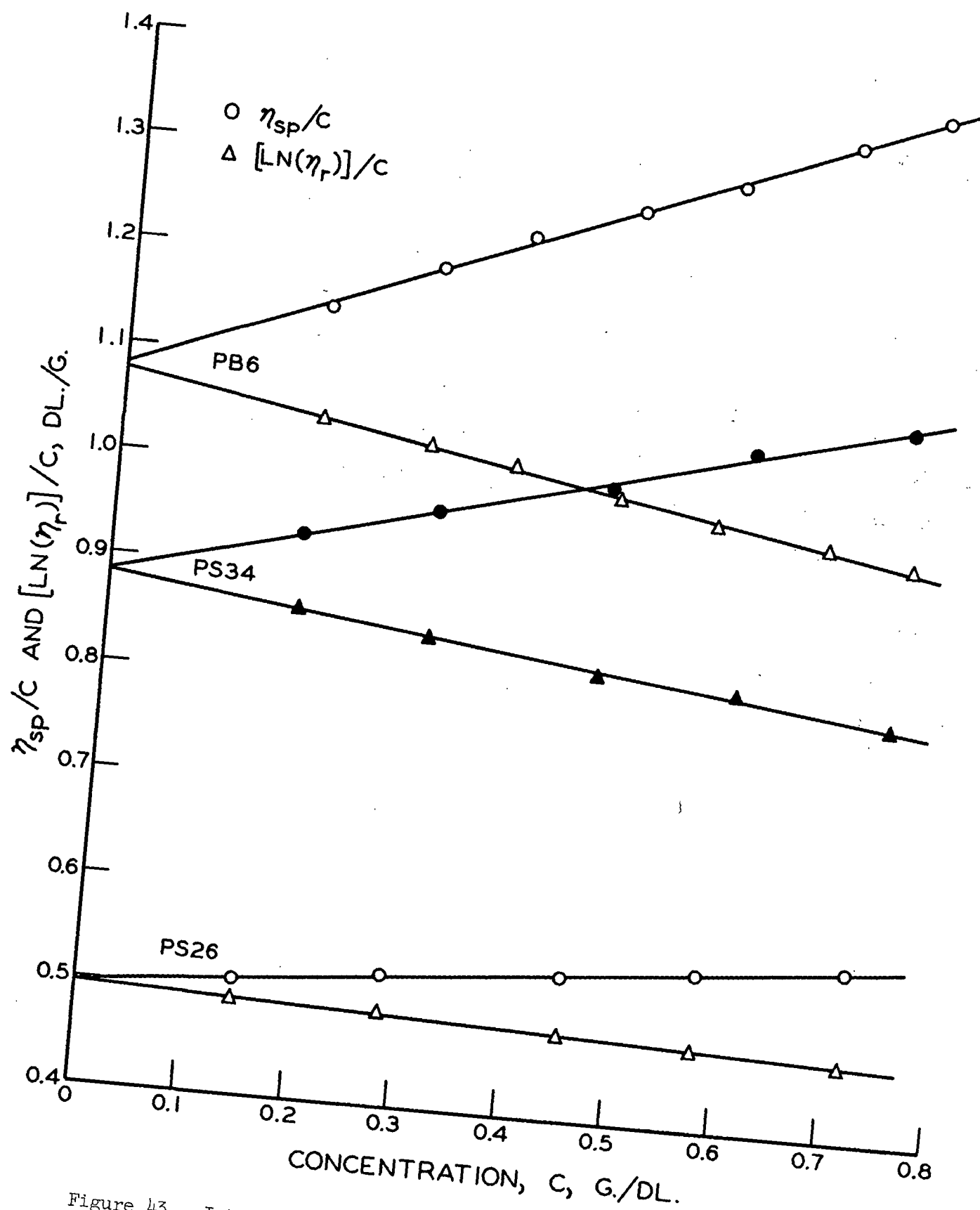


Figure 43. Intrinsic Viscosity Determinations of Polystyrene Samples in 1,2-Dichloroethane at 25°C.

APPENDIX II

CLEANING PROCEDURES

The glassware which came into direct contact with the adsorption system components was cleaned prior to use by the following procedure. First, residual polymer from previous experiments was removed by boiling the glassware in technical-grade toluene for approximately one hour. This was followed by boiling the glassware in a nearly saturated solution of potassium hydroxide in 95% ethanol for approximately one-half hour. After rinsing with distilled water, the glassware was soaked overnight in a 1:1 volume mixture of 6% hydrogen peroxide and 6N hydrochloric acid. Finally, the glassware was rinsed thoroughly with distilled water, dried in an oven at 110°C., and stored in a desiccator over anhydrous calcium chloride until needed.

Teflon film was cleaned by scrubbing with detergent, followed by a distilled-water rinse. The teflon then was soaked overnight in the same peroxide-acid mixture used for glassware, followed by rinsing and drying as described above.

APPENDIX III

EMPIRICAL CONSTANTS USED IN CONVERSION OF SEDIMENTATION COEFFICIENT DISTRIBUTIONS TO INTRINSIC VISCOSITY QUANTITIES

It is demonstrated in the text that the intrinsic viscosity can be calculated from the distribution of sedimentation coefficient with Equation (38) as follows:

$$[\eta] = K(k)^{-a/b} \int_0^{\infty} S^{a/b} g(S) dS / \int_0^{\infty} g(S) dS.$$

The constants, K and a, pertain to the solvent system for which the intrinsic viscosity calculation is desired and are given by Equation (42) for the present system. The constants, k and b, relate to the solvent system in which the distribution, S-g(S), was determined, i.e., cyclohexane at 35°C., and are given by Equation (41).

Using Equation (38), the intrinsic viscosities were calculated for the distributions obtained in the present work and are compared with the experimental values in Table XXVIII. Although the agreement is not bad, a consistent deviation does exist between the experimental and calculated values. Examination of Equation (38) revealed that the calculated value of $[\eta]$ is particularly dependent on small changes in the exponential quantities. Consequently, errors in the empirical constants can have a substantial effect on subsequent computations. It should be pointed out that some of this deviation may be the result of difficulty with the ultracentrifugal determinations.

Because of the dependence of Equation (38) on the exponential quantities, it is desirable to obtain a direct relationship between the intrinsic viscosity and distribution function. The following method is recommended for future studies.

TABLE XXVIII

COMPARISON OF EXPERIMENTAL AND CALCULATED
VALUES OF INTRINSIC VISCOSITY

Sample	Distribution Description	Intrinsic Viscosity, dl./g.	
		Experimental	Equation (38)
3	Bulk phase	0.624	0.759
4	Bulk phase	0.769	0.891
5	Bulk phase	0.776	0.849
100	Original	1.078	1.125
101	Original	1.078	1.138
3	Surface phase	1.318 ^a	1.337
5	Surface phase	1.376 ^a	1.417
4	Surface phase	1.397 ^a	1.408

^aCalculated with Equation (43).

Using Equation (37), the viscosity-average sedimentation coefficient, \overline{S}_V , can be defined as follows:

$$\overline{S}_V = k(\overline{M}_V)^b \quad (122)$$

where \overline{M}_V is the viscosity-average molecular weight of the distribution in question. By combining Equations (32), (36), and (37), the viscosity-average molecular weight can be written as follows:

$$\overline{M}_V = \left\{ k^{-a/b} \int_0^\infty s^{a/b} g(s) ds / \int_0^\infty g(s) ds \right\}^{1/a} \quad (123).$$

By combining Equations (122) and (123), the viscosity-average sedimentation coefficient can be defined directly in terms of the distribution function as follows:

$$\overline{S}_v = \left\{ \int_0^\infty S^{a/b} g(S) dS / \int_0^\infty g(S) dS \right\}^{b/a} \quad (124).$$

By combining Equations (31) and (122), one finds that

$$[\eta] = K(\overline{S}_v)^\beta \quad (125)$$

where K and β are given by $K(k)^{-a/b}$ and a/b , respectively. Equations (124) and (125) establish a direct correlation between the distribution function and intrinsic viscosity.

In order to evaluate the constants, K and β , the distribution function and intrinsic viscosity are required for samples of narrow molecular weight distribution (covering the intrinsic viscosity range over which the correlation is to be employed). Using an initial estimate of β , the value of \overline{S}_v can be calculated with Equation (124) for each of the samples employed. Calculated values of \overline{S}_v and experimental determinations of $[\eta]$ then are correlated with the linear form of Equation (125) as follows:

$$\ln[\eta] = \beta[\ln(\overline{S}_v)] + \ln(K) \quad (126).$$

The constants can be evaluated readily by the method of least squares. At this point, the calculations are repeated with the new estimate of β . This procedure is continued until the value of β remains constant within the desired precision.

It has been pointed out that the ultracentrifugal technique may be responsible for part of the deviation between the experimental and calculated values of intrinsic viscosity shown in Table XXVIII. Evidence was presented in the text which suggested that higher solution concentrations in the sedimentation velocity runs might improve the determinations, particularly in the "tail" region. Another

factor which should be considered in future studies is the possibility of making corrections to the sedimentation coefficient for the effects of pressure. Fujita (64) has discussed various approaches to this problem although none of them are completely general. The experimental information in the literature was too limited to undertake any such corrections in the present study. From estimates based on the investigation of Billick (105), it is believed that the error in \bar{S} as a result of pressure effects was well below 10% in all cases for the distributions obtained in the present work.